2010

Development of stable microencapsulated astaxanthin powders using extracted astaxanthin from crawfish and shrimp byproducts

Jianing Pu
Louisiana State University and Agricultural and Mechanical College

DEVELOPMENT OF STABLE MICROENCAPSULATED ASTAXANTHIN POWDERS USING EXTRACTED ASTAXANTHIN FROM CRAWFISH AND SHRIMP BYPRODUCTS

A Thesis
Submitted to the Graduate Faculty of the
Louisiana State University and
Agricultural and Mechanical College
in partial fulfillment of the
requirements for the degree of
Master of Science

in

The Department of Food Science

by
Jianing Pu
B.E., Jiangnan University, 2008

December 2010

ACKNOWLEDGEMENTS

I would like to express my sincere gratitude to my major professor Dr. Subramaniam Sathivel for his expertise, patience, guidance, motivation and continuous support throughout my study and research. My appreciation is also extended to the committee members Dr. Joan M. King, Dr. Paul W. Wilson, Dr. J. David Bankston for their thoughtful help and guidelines in my research. Special thanks go to Dr. Peter J. Bechtel in University of Alaska Fairbanks within USDA/ARS Subarctic Agricultural Research Unit for his help for determination of fatty acid profiles. I also would like to thank Dr. Robert P. Romaire from the Aquaculture Research Station for his kind help to provide crawfish byproducts. Appreciation also goes to Dr. Bob Xiang who helped me to order the chemical reagents and help me operate spray dryer.

Many thanks to my labmates: Huaixia Yin, Yuting Wan, Jose Daniel Estrada, Jenny Sundararajan, Kevin Mis, Ahalya Kosal Ram, Fathima Waheeda Mohideen, Luis Alfaro, Luis Espinoza for their kind assistance and suggestions in my research.

Without the support of my family nothing would be possible. I thank my parents for their endless love and support throughout my study. Without their support I could not have achieved the goal of my life. I would like to thank my sister and my wife for their consideration and encouragement that keeps pushing me forward.

TABLE OF CONTENTS

LIST OF TABLES

LIST OF FIGURES

ABSTRACT

Crawfish and shrimp byproducts are an excellent source of astaxanthin. The antioxidant-rich natural astaxanthin dispersed in alpha linolenic acid-rich flaxseed oil (FO) may provide healthier functional food options for US consumers. The goals of this study were to extract astaxanthin from crawfish and shrimp byproducts and to develop astaxanthin dry powders using microencapsulation technology. Astaxanthin extracted with FO from crawfish (FOCA) and shrimp (FOSA) byproducts were stable at 30 and 40 ^{o}C, but had substantial degradation at 50 and 60 ^{o}C during four 4 h heating. The astaxathin degradation of FOCA and FOSA fitted with zero and first orders kinetics showed that the rate constant for astaxanthin degradation of FOCA and FOSA increased with increased temperature and first order kinetics could be used to describe the degradation of astaxanthin in FOCA and FOSA between 30 to 60 ^{o}C, while zero order kinetics might describe the astaxanthin degradation in FOCA and FOSA at 60 ^{o}C. The emulsions prepared with FOCA (ECA) and FOSA (ESA) were spray dried to produce microencapsulated powders containing FOCA (MCA) and FOSA (MSA) using a pilot scale spray dryer. The energy required to spray dry 0.433 kg ECA and 0.428 kg ESA was 1.022×10^{4} and 1.028×10^{4} kJ, respectively. The astaxanthin concentration of MCA and MSA was 13.76±0.37 and 16.08±0.24 μg/g powder, respectively. Alpha-linolenic acid (ALA) was the predominant fatty acid in MCA and MSA, which accounted for 56.32 % and 55.47 % for MCA and MSA, respectively. The lipid oxidation of MCA and MSA was lower at 5 ^{o}C storage than those at 25 ^{o}C and 40 ^{o}C during 26 days storage. Degradation of astaxanthin in MCA and MSA fitted with first order reaction kinetics model showed that the degradation

rate constants for MCA and MSA increased with increased storage temperature. This which indicated that astaxanthin degraded faster at higher temperature than that at lower temperature. This study demonstrated that astaxanthin extracted from crawfish and shrimp byproducts using flaxseed oil can be microencapsulated using spray drying technology.

CHAPTER 1 LITERATURE REVIEW

1.1 General Information on Astaxanthin

Astaxanthin is a red orange color pigment which belongs to the family of carotenoids (Miki 1991). Astaxanthin is one of the main pigments found in aquaculture animals including salmon, trout, shrimp, crawfish, and crabs. It is widely used as a pigment in aquaculture feed. Many recent studies have shown that astaxanthin also has many functional properties and excellent antioxidant activity (Tanaka and others 1995a; Kritchevsky 1999; Tracy 1999).

1.1.1 Chemical Structure

The carotenoids family comprising more than 600 pigments, is a class of hydrocarbons (carotenes) and their oxygenated derivatives (xanthophylls). Carotenes are only composed of carbon and hydrogen, while the xanthophylls are oxygenated derivatives. Astaxanthin [(3S,3′S)-3,3′-dihydroxy-β,β-carotene-4,4′-dione)] contains 11 conjugated double bonds and two hydroxyl groups (Figure 1.1). The long chain of conjugated double bonds and two terminal ring systems determine its chemical characteristics and light absorption properties. In nature, most astaxanthin is found in its isomer forms (Figure 1.2). Due to the different chirality at C-3, 3′, astaxanthin has R/S (optical) isomers including two enantiomers (3S,3′S) and (3R,3′R) and the *meso* form (3R,3′S) (Figure 1.2).

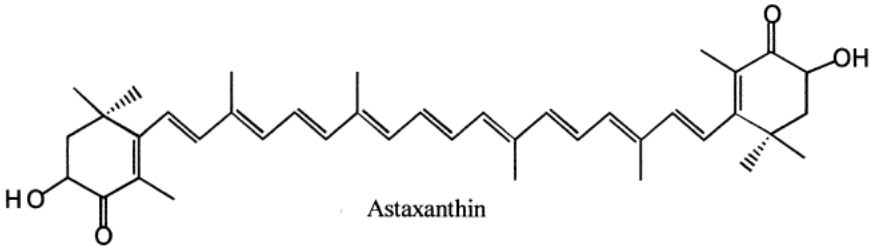

Figure 1.1 Chemical structure of astaxanthin

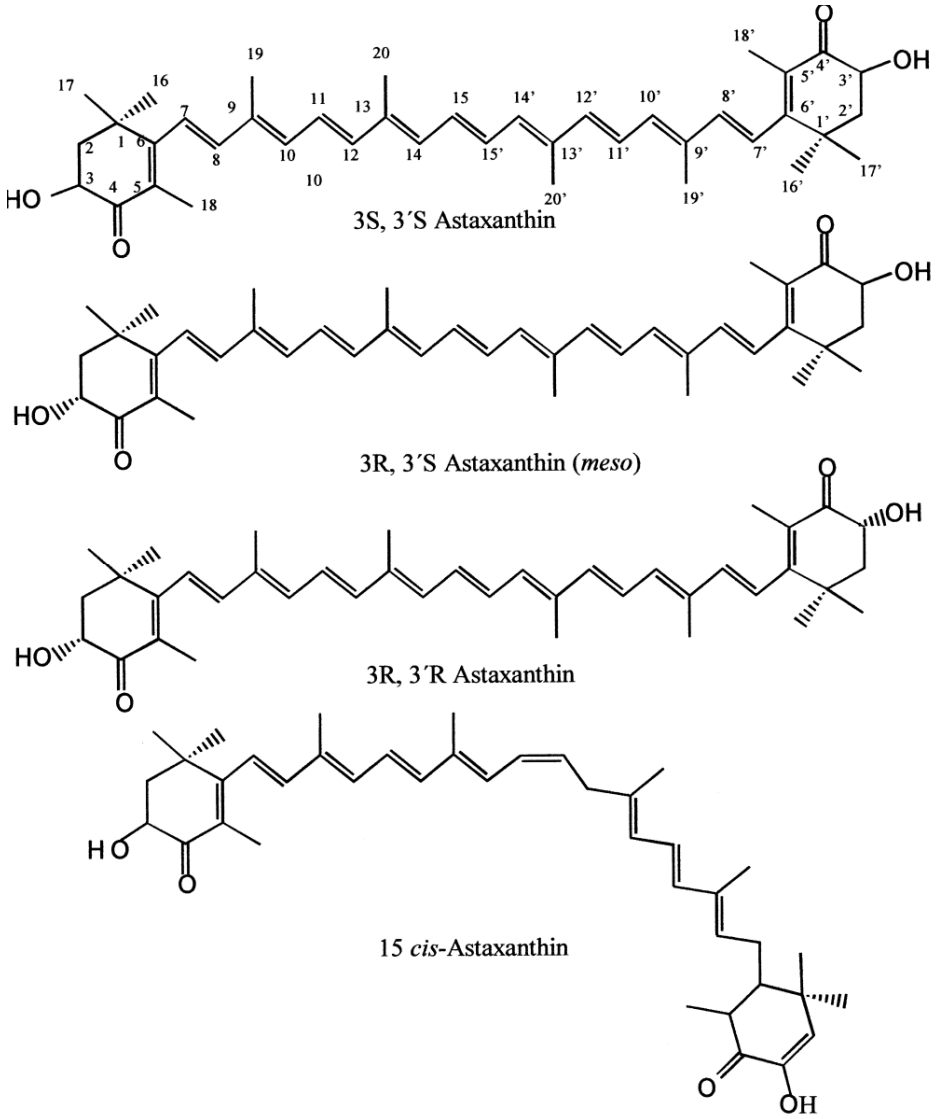

Figure 1.2 Chemical structure of astaxanthin isomers

1.1.2 Sources of Astaxanthin

1.1.2.1 Crustacean Byproducts

Crustacean byproducts are generated from peeling and processing operations of crawfish, shrimp, crabs, and lobsters. Normally, these byproducts are discarded as waste, which is not only a loss of potentially valuable byproducts and can also cause environmental problems. Crustacean byproducts have been reported to be an excellent source of protein, chitin, and astaxanthin (De Holanda and Netto 2006). The amount of carotenoid pigments in these

byproducts has been well documented by many previous studies (Guillou and others 1995; Meyers and Bligh 1981; Shahidi and Synowiecki 1991; Torrissen and others 1981) (Table 1.1). The amount of total astaxanthin in these byproducts depends on the species, development stage, and storage conditions. The major carotenoid pigment is astaxanthin and its esters (Sachindra and others 2005). Numerous studies have reported the recovery of astaxanthin from crustacean byproducts such as snow crab (Shahidi and Synowiecki 1991), shrimp (De Holanda and Netto 2006; Handayani and others 2008; Sachindra and others 2005; Sachindra and others 2006), and crawfish (Chen and Meyers 1982; Meyers and Bligh 1981). In their study, different methods were used to extract astaxanthin such as fermentation (Sachindra and others 2007), enzymatic (De Holanda and Netto 2006), and organic solvent (Sachindra and others 2006) processes. Organic solvents such as acetone, methanol, isopropyl alcohol, and petroleum ether have been used to extract astaxanthin from crustacean byproducts (Sachindra and others 2006; Sachindra and Mahendrakar 2005). Chen and Meyers (1982) developed a soy oil process to extract astaxanthin from crawfish byproducts and Sachindra and Mahendrakar (2005) used a number of different oils to extract carotenoids from shrimp byproducts.

1.1.2.2 Microorganisms

Astaxanthin has been found in several microorganisms, including algae (Gong and Chen 1998), yeast (Liu and Wu 2007), and bacteria (Gu and others 2008). Numerous previous studies have been conducted to isolate astaxanthin from natural resources such as microalgae *Haematococcus pluvialis* (Zhang and others 2009) and *Chlorella zofingiensis* (Ip and Chen

2005); yeast *Xanthophyllomyces dendrorhous* (Liu and Wu 2007), *Phaffia rhodozyma* (Ramirez and others 2001), and *Rhodotorula rubra* (Shih and Hang 1996); and bacteria *Rhodobacter sphaeroides* (Gu and others 2008; Chen and others 2006). Many studies investigated the effects of medium components and culture conditions on the growth of microalgae and yield of astaxanthin, and the reported astaxanthin content varied from 1% up to 5% of the dry weight (Choi and others 2002; Orosa and others 2001; Fabregas and others 2000). Physical factors (pH, temperature) and nutritional factors (carbon and nitrogen sources) affecting astaxanthin production by yeast and bacteria have been studied (Ramirez and others 2001; Johnson and Lewis 1979; Fang and Cheng 1993; Meyer and others 1993; Kesava and others 1998; Parajo and others 1998). Moreover, some researchers used genetically-improved strains of the yeasts and bacteria to increase astaxanthin yield (Fang and Chiou 1996; Calo and others 1995).

Table 1.1 Carotenoids content in various sources of crustacean byproducts

Source	Astaxanthin (mg/100g byproducts)	Other carotenoids	References
Shrimp (*Parapenaeopsis stylifera*)	8.36	β-carotene, zeaxanthin	Shahidi and others 1998
Shrimp (*Metapenaeus dobsonii*)	8.41	β-carotene,zeaxanthin	Shahidi and others 1998
Shrimp (*Penaeus indicus*)	8.27	β-carotene,zeaxanthin	Shahidi and others 1998
Shrimp (*Penaeus monodon*)	7.47	β-carotene,zeaxanthin	Shahidi and others 1998
Shrimp (*Penaeus.borealis*)	14.77	β-carotene,zeaxanthin	Shahidi and Synowiecki, 1991
Shrimp (*Penaeus.borealis*)	4.97	-	Torrisen and others1981
Shrimp(*Penaeus.borealis*)	3.09	-	Guilou and others 1995
Crawfish (*P.clarkii*)	12.3	Astacene	Meyers and Bligh 1981
Backs snow crab (*Ch.Opilio*)	11.96	Lutein, zeaxanthin, astacene	Shahidi and Synowiecki, 1991

1.1.3 Applications of Astaxanthin

1.1.3.1 Pigmentation

The red orange color astaxanthin is responsible for many animal colors such as salmon, shrimp, crawfish, and rainbow trout (Shahidi and Synowiecki 1991). In the environment, astaxanthin is biosynthesized by plants and some bacteria and fungi, which are absorbed and metabolized by fish (Chen and Meyers 1982). Astaxanthin then accumulates in their skin, muscle, and exoskeleton, thereby producing the red orange color of these animals. Fish and crustaceans are unable to biosynthesize astaxanthin in their bodies and must uptake this pigment from their diet. Hence, astaxanthin is widely used as a colorant incorporated into aquaculture feed to enhance natural color. The use of astaxanthin as a pigmentation agent in aquaculture feed has been well documented by many previous studies (Chen and Meyers 1982; Gentles and Haard 1991; Saito and Regier 1971; Sigurgisladottir and others 1994). Moreover, astaxanthin is also widely used in the poultry industry (Perez-Galvez and others 2008). Natural astaxanthin, isolated from microalgae *Haematococcus*, has been successfully incorporated into poultry feed to change the egg yolk color from original yellow to red hues which may be more appealing to consumers (Lorenz and Cysewski 2000). It was also found that the addition of algae in the meal increased astaxanthin concentrations in chicken liver, adipose tissue, and breast muscle (Lorenz and Cysewski 2000).

1.1.3.2 Antioxidant Activity

Free radicals (e.g. hydroxyl and peroxyl radicals) and activated forms of oxygen (e.g. singlet oxygen) are produced in the body during normal metabolic reactions and processes,

which could cause oxidative damage *in vivo* (Di Mascio and others 1991). An antioxidant is defined as a molecule that is able to remove free radicals from a system by reacting with them or by disrupting the oxidation reactions (Britton and others 1995).

Astaxanthin contains a long chain of conjugated double bond and ketonic and hydroxilic groups which are attributed to its high antioxidant properties by removing free radicals and quenching singlet oxygen. It has been reported that the antioxidant activity of astaxanthin is 10 times higher than other carotenoids such as zeaxanthin, lutein, canthaxantin, and β-carotene (Miki 1991). Numerous studies have identified astaxanthin antioxidant mechanisms that quench active oxygen species and free radicals *in vitro* and *in vivo* (Edge and others 1997; Palozza and Krinsky 1992; Rengel and others 2000).

Singlet oxygen is generated by energy transfer from the excited state of a sensitizer (^3S) to oxygen (reactions 1 and 2). The sensitizer absorbs energy and transfers to its excited form (^3S). Then, the excited sensitizer reacts with triplet oxygen ($^3O_2$) to transfer its energy to singlet oxygen ($^1O_2$) followed by return to its ground state (S) (Piette 1991; Girotti 1990).

$$S \xrightarrow{h\nu} {}^3S \qquad (1)$$

$${}^3S + {}^3O_2 \rightarrow S + {}^1O_2 \qquad (2)$$

Carotenoids have the ability to inhibit photo-sensitized oxidation by quenching singlet oxygen ($^1O_2$) or triplet sensitizer (^3S) (reactions 3 and 4). Carotenoids could react with singlet oxygen or triplet sensitizer to bring them back to their ground state by transferring energy with electron exchange (Farmilo and Wilkinso.F 1973). The ability to quench singlet oxygen increases with increasing number of conjugated double bonds (Conn and others 1991). As the

product of these reactions, triplet state carotenoid (^3CAR) could return to its ground state with release of energy (e.g., heat) to the environment (reaction 5).

$$^3S + CAR \rightarrow S + {}^3CAR \quad (3)$$

$$^1O_2 + CAR \rightarrow {}^3O_2 + {}^3CAR \quad (4)$$

$$^3CAR \rightarrow CAR + heat \quad (5)$$

In addition to reacting with singlet oxygen, carotenoids can also quench free radicals (reactions 6, 7, and 8). It was reported that carotenoids are able to limit the oxidative damage caused by oxygen radicals (Edge and others 1997).

The mechanism of quenching peroxyl radicals by carotenoids has not yet been defined. However, researchers proposed a hypothesis that carotenoids could react with peroxyl radical to form a carotenoid radical (reactions 6 and 7). Then, the carotenoid peroxyl complex could react with another peroxyl radical, leading to a termination reaction (reaction 8) (Burton and Ingold 1984).

$$CAR + ROO^{\bullet} \rightarrow CAR^{\bullet} + ROOH \quad (6)$$

$$CAR^{\bullet} + O_2 \Leftrightarrow CAR - OO^{\bullet} \quad (7)$$

$$CAR - OO^{\bullet} + ROO^{\bullet} \rightarrow inactive \quad products \quad (8)$$

Due to its antioxidant properties, astaxanthin has a role in the treatment of chronic diseases such as cardiovascular diseases, cataract development, macular degeneration, and some types of cancer (Mayne 1996).

1.1.3.3 Other Functional Properties

Apart from antioxidant activity, astaxanthin has been reported to have many other

functional properties such as anti-cancer activity (Tanaka and others 1995a; Tanaka and others 1995b), prevention of cardiovascular diseases and inflammation (Kritchevsky 1999; Tracy 1999), and benefit to heart disease and eye health (Jacques 1999; Seddon and others 1994). It was reported that the high daily supplementation of carotenoids could reduce the risk for both nuclear cataracts and AMD (age-related macular degeneration) which are two main causes of visual impairment and blindness. Also, supplementation of astaxanthin effectively suppresses carcinogenesis in mice urinary bladder tissue and inhibits tumor growth in breast cancer (Chew and others 1999; Jyonouchi and others 2000; Tanaka and others 1994).

1.2 Recovery of Astaxanthin

Numerous studies have reported the recovery of astaxanthin from crustacean byproducts such as snow crab (Shahidi and Synowiecki 1991), shrimp (De Holanda and Netto 2006; Handayani and others 2008; Sachindra and others 2006; Sachindra and Mahendrakar 2005), and crawfish (Chen and Meyers 1982; Chen and Meyers 1984; Meyers and Bligh 1981). In their study, different methods were used to extract astaxanthin such as fermentation (Sachindra and others 2007), enzymatic (De Holanda and Netto 2006), and organic solvent process (Sachindra and others 2006).

1.2.1 Organic Solvent

A large number of studies have been conducted to extract astaxanthin from crustacean byproducts using organic solvents. Sachindra and others (2007) extracted astaxanthin from ensilaged shrimp waste using a solvent mixture of hexane and isopropanol (60:40 v/v). Another study reported that the extraction of astaxanthin was carried out using mixtures of

chloroform: methanol: water (1: 2: 4), petroleum ether: acetone: water (15: 75: 10) (Meyers and Bligh 1981), and ethanol: water (40: 60) (Armenta and Guerrero-Legarreta 2009). Sachindra and others (2006) compared the yield of carotenoids from shrimp waste using different organic solvents and their mixtures (e.g. acetone, methanol, ethyl methyl ketone, isopropyl alcohol, ethyl acetate, ethanol, petroleum ether, hexane). It was found that the highest carotenoid yield was obtained when the mixture of isopropyl alcohol and hexane was used as the extraction medium, while the lowest carotenoid yield was obtained with two non-polar solvents, petroleum ether and hexane.

1.2.2 Edible Oils

In addition to organic solvents, edible oils are widely used as the media to extract astaxanthin from crustacean byproducts due to lipid solubility of astaxanthin. Chen and Meyers (1982) developed a soy oil process to extract astaxanthin from crawfish byproducts with assistance of enzyme hydrolysis. Sachindra and Mahendrakar (2005) used a number of different vegetable oils such as sunflower oil, groundnut oil, gingelly oil, mustard oil, coconut oil, and rice bran oil to extract carotenoids from shrimp byproducts and compared the carotenoids yield. The results showed that the highest yield was obtained using sunflower oil. Handayani and others (2008) studied extraction of astaxanthin from shrimp waste using palm oil and evaluated the kinetics and thermodynamics of the extraction process. The experimental data could be well described by both mass transfer kinetics model and reaction kinetics model.

1.3 Flaxseed Oil

Flaxseed oil is derived from flaxseeds which grow in Western Canada traditionally and has a high content of polyunsaturated fatty acids, dietary fiber and lignans (Cunnane and others 1993). In recent years, flaxseed oil has gained plenty of attention due to its unique nutrient profile and protective effects to cardiovascular disease, inflammation, and some cancers (Bloedon and Szapary 2004; Harper and others 2006; Tzang and others 2009). It was reported that flaxseed oil contains a high content of polyunsaturated fatty acids (73 % of total fatty acids), a moderate content of monounsaturated fatty acids (18 %), and a low content of saturated fatty acids (9 %). It contains 16 % linoleic acid (LA) and about 57% alpha-linolenic acid (ALA), yielding the highest n-3/n-6 fatty acid ratio amongst plant sources (Tzang and others 2009). ALA and LA are precursors to long-chain (n-3) fatty acids such as eicosapentaenoic acid (EPA) and docosahexaenoic acid (DHA) (Harper and others 2007; Tzang and others 2009). Both ALA and LA are considered to be essential fatty acids and numerous studies have shown that ALA can protect against cardiovascular disease and inflammation (Bloedon and Szapary 2004).

1.4 Lipid Oxidation

Lipid oxidation is the main deteriorative reaction that affects the quality and acceptability of lipid containing food products. In lipid oxidation process, hydroperoxides are formed which then degrade to secondary oxidation products such as aldehydes, ketones, acids and alcohols, which make food products less acceptable or unacceptable to consumers. These compounds not only affect flavor, aroma, taste, nutritional value and overall quality of food

products, but also produce toxic compounds which cause safety problems to food products. The extent of lipid oxidation depends on chemical properties of foods (fatty acids composition, number of conjugated double bonds, prooxidants, chelators and antioxidants) and environmental factors (oxygen, moisture, heat, light) during processing, packaging and storage (Colakoglu 2007; McDonald and Min 1996; St. Angelo and others 1992).

Oxygen and unsaturated fatty acids are two major components involved in the oxidative process. Oxidative processes may be evoked by initiators such as heat, light, metal ions, enzyme systems, or non-radical and radical oxygen species ($^1O_2$, O_3, H_2O_2, ROOH, $\cdot O_2^-$, $\cdot$OH, RO$\cdot$, ROO$\cdot$) (St. Angelo and others 1992). It has been well documented that the oxidative process occurs by three reaction pathways: (1) free radical chain autoxidation; (2) photooxidation; (3) enzymatic oxidation. The two types of oxidation that are involved in autooxidation and photooxidation are triplet oxygen ($^3O_2$) and singlet oxygen ($^1O_2$) oxidations. Triplet oxygen is the ground state which has low energy and is stable. However, singlet oxygen is formed in the presence of sensitizer, light and triplet oxygen with an energy transfer process (reaction 9) (St. Angelo and others 1992). Due to its high energy, the singlet oxygen which is the excited state of oxygen has a higher oxidation rate than triplet oxygen. It was reported that singlet oxygen reacts with oleic, linolenic acids about 1000-30000 times faster than triplet oxygen (Shahidi and Weenen 2006).

$$^3sens \xrightarrow{h\nu} {}^1sens + {}^3O_2 \longrightarrow {}^1O_2 \qquad (9)$$

Although enzymatic and photo oxidation may play a role, autoxidation seems to be a key mechanism in lipid oxidation which is illustrated through a three phase process (initiation,

propagation and termination).

Initiation $RH \xrightarrow{Initiator} R\cdot + H\cdot$ (10)

Propagation $R\cdot + O_2 \longrightarrow ROO$ (11)

$ROO\cdot + RH \longrightarrow ROOH + R\cdot$ (12)

Termination $R\cdot + R\cdot \longrightarrow RR$ (13)

$ROO\cdot + ROO\cdot \longrightarrow O_2 + RO_2R$ (14)

$ROO\cdot + R\cdot \longrightarrow RO_2R$ (15)

In the initiation phase, it is improbable that direct reaction occurs between a lipid molecule and an oxygen molecule because of the high activation energy between triplet ground state oxygen and singlet electronic state lipid molecule. However, the reaction could be initiated by external agents such as metal ions, free radicals, heat, radiation or light which could help formation of singlet oxygen or activated oxygen species. The activated oxygen is more likely to be involved in the reaction. The hydrogen is abstracted from an unsaturated fatty acid, resulting in the formation of lipid free radical (R·) (reaction 10) (Frankel 1984; Halliwell and Chirico 1993; Ladikos and Lougovois 1990).

In the propagation period, the lipid free radical (R·) formed in the initiation phase reacts with oxygen molecule to form a lipid peroxyl radical (ROO·). Then, the peroxyl radical abstracts a hydrogen from another unsaturated fatty acid to form hydroperoxide (ROOH) and another lipid free radical (R·) (reactions 11 and 12). This reaction occurs at a high rate, resulting in the accumulation of hydroperoxide isomers during this phase (Frankel 1984; Halliwell and Chirico 1993; Ladikos and Lougovois 1990).

The termination process involves the decomposition of hydroperoxides into secondary nonradical compounds. The mechanism of decomposition was well documented as cleavage of the fatty acid chain adjacent to the hydroperoxyl group with formation of low molecular weight volatile compounds such as hydrocarbons, aldehydes, alcohols and volatile ketones. These breakdown compounds cause rancidity (Frankel 1984; Halliwell and Chirico 1993; Ladikos and Lougovois 1990).

1.5 Microencapsulation

Over the last decade, microencapsulation technology has gained much of attention by researchers due to its wide applications in the medical, pharmaceutical, cosmetics, chemical, agricultural and food industries (Gharsallaoui and others 2007; Dai and others 2005; Krishnan and others 2005; Magdassi 1997). Microencapsulation has been defined as 'the technology of packaging solid, liquid and gaseous materials in small capsules that release their contents at controlled rates over prolonged periods of time' (Champagne and Fustier 2007). Microencapsulation forms a coating layer around the core compound in order to protect its biological activity and enhance its stability (Figure 1.3). The core compound is defined as the particular material to be coated and the coating material should be able to form a film that is cohesive with the core compound (Augustin and Hemar 2009). The core compounds are usually some sensitive compounds such as flavors, polyunsaturated fatty acids, carotenoids, vitamins, phytosterols which need to be protected against oxygen, heat, moisture and pH during processing and storage (Augustin and Hemar 2009; McClements and others 2007).

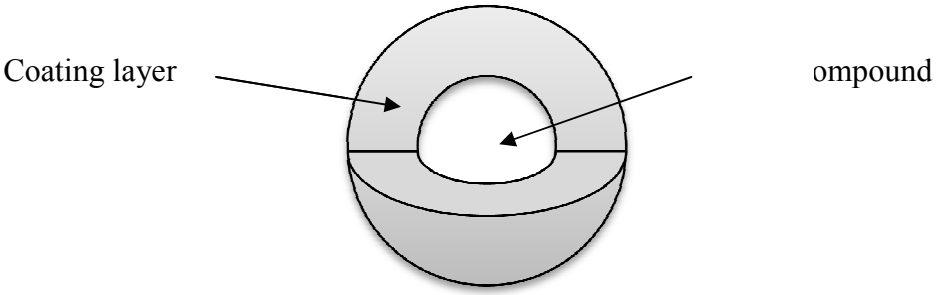

Figure 1.3 Schematic of microcapsule

Microencapsulation can reduce the reaction between core compound and environmental factors to enhance its stability and prolong its shelf life. For some strong flavored foods such as fish oil, microencapsulation can mask the core taste for the purpose of food fortification. Microencapsulation can also control the release of the core material. For example, flavoring agents in chewing gums are controlled to release during chewing and microencapsulated leavening agents are released during baking. In dairy products, some probiotic bacteria which are protected from the gastric environment are released in the small intestine (Gharsallaoui and others 2007; Homayouni and others 2008; Shahidi and Han 1993).

1.5.1 Structure of Microencapsulated Particles

A conventional microencapsulated particle consists of a core compound which could be solid, liquid or gaseous material and a thin interfacial coating layer consisting of emulsifier molecules surrounding the core (Drusch 2007; Gharsallaoui and others 2007; Krishnan and others 2005). Normally, the coating layer is formed by food grade ingredients including food proteins or carbohydrates. The structure of encapsulated ingredients can broadly be classified into capsules with: (a) a core that is surrounded by a shell of the matrix material; (b) a core that is entrapped within a continuous network of the matrix material; (c) a core that is surrounded by multi-layers; (d) multiple cores (Augustin and Hemar 2009).

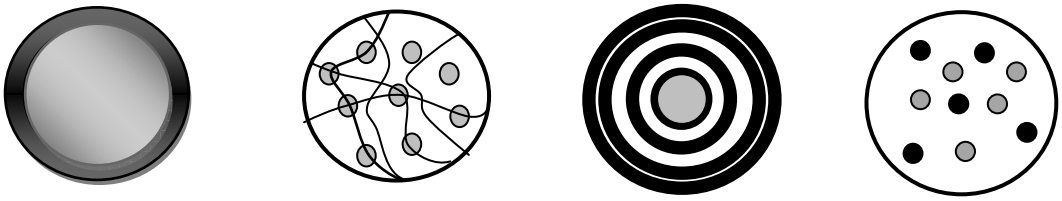

(a) (b) (c) (d)

Figure 1.4 Morphologies of microcapsules (a) single-core capsule, (b) dispersed core in polymer gel, (c) multi-layer capsule, (d) dual-core capsule

1.5.2 Wall Materials

The selection of a wall material is a very important step in microencapsulation process due to its effect on microencapsulation efficiency, microcapsule stability, and protection efficiency of the core compound (Perez-Alonso and others 2003). The choice of a particular wall material mainly depends on its physical and chemical properties such as solubility, viscosity, glass or melting transition, forming and emulsifying properties (Gharsallaoui and others 2007). A variety of different natural and synthetic polymers are available to be used as wall material including proteins (milk or whey proteins, gelatin, etc.), and carbohydrates (starches, corn syrup solids, maltodextrins, etc.).

1.5.2.1 Carbohydrates

Sugars (e.g. glucose, sucrose) and polysaccharides (e.g. starch, maltodextrins, pectin, alginate, chitosan) have been widely used as wall materials (Risch 1995b; Kenyon 1995). Sugars are considered to be good microencapsulating agents because they are able to be the carrier medium for active compound prior to dehydration and they can form glassy solids where the active core is surrounded upon dehydration. In addition, sugars can also stabilize proteins during dehydration through hydrogen bonding. However, high concentrations of low

molecular weight sugars were reported to not be suitable for spray drying due to the formation of sticky powders and caramelization reaction (Bayrarn and others 2005). Maltodextrins were reported to be good wall materials due to their low viscosity at high solids contents and good solubility. Kenyon (1995) reported that oil encapsulated with maltodextrins exhibited good oxidative stability but poor emulsifying capacity. In order to improve the poor emulsifying properties of carbohydrates, proteins are usually used in combination with carbohydrates to increase their surface-activity.

1.5.2.2 Proteins

Food proteins including milk proteins, whey proteins, and gelatin are commonly used as coating materials due to their excellent functional properties (Vega and others 2005; Sliwinski and others 2003; Bruschi and others 2003). Their properties mainly depend on their amino acid composition, conformation and charge as well as their denaturation temperature. Proteins have the ability to assemble at interfaces due to their amphiphilic nature. In addition, proteins are good wall materials for flavor compounds because of their high binding activity with flavor (Landy and others 1995). Whey proteins have been reported to be effective coating materials for milk fat by spray drying, resulting in high yield. Furthermore, the combination of whey protein with lactose significantly limits the diffusion of core material through the wall thereby leading to high microencapsulation efficiency. Sodium caseinate is also a very good wall material for encapsulation of oils (Hogan and others 2001). It was reported that sodium caseinate has strong amphiphilic characteristics and high diffusivity, which provides a better distribution around the surrounded oil surface. However, the high

protein content can significantly increase the viscosity of the emulsion, which may result in bad atomization during spray-drying, leading to the formation of irregular particles with a large particle size distribution.

1.5.3 Spray Drying

Spray drying is a common method of encapsulation of food ingredients in the food industry (Augustin and Hemar 2009; Gharsallaoui and others 2007). Numerous studies have been conducted to use spray drying technology to encapsulate food ingredients such as carotenoids, vitamins, minerals, flavors, polyunsaturated oils, enzymes and probiotic microorganisms (Augustin and Hemar 2009; Drusch 2007; Gharsallaoui and others 2007; Risch 1995a; Bayrarn and others 2005; Bruschi and others 2003; Carolina and others 2007; Kittikalwan and others 2007; Laos and others 2007; Nunes and Mercadante 2007). The basic steps in the microencapsulation process involves preparation of emulsion to be processed; homogenization of the emulsion; atomization of the emulsion; and dehydration of the atomized particles (Dziezak 1988; Shahidi and Han 1993).

In the emulsion preparation stage, the core material is dispersed into the wall solution and homogenized, leading to the formation of a fine and stable emulsion. Owing to the atomization process, the wall material should have good solubility in water and the ability to form high solids content at low viscosity. It was reported that the viscosity properties of the emulsion is important in the spray drying process. High emulsion viscosity causes the formation of large droplets which affect the drying rate (Drusch 2007; Rosenberg and Sheu 1996). The emulsion then is fed into the atomizer where the emulsion is atomized by pressure

or centrifugal energy. The hot air stream flows in either a co-current or counter-current direction. The temperature of hot air is usually 150-220 ^{o}C. Thus, the evaporation occurs rapidly, which keeps the core temperature below 100 ^{o}C (typically 50-80 ^{o}C). The contact between emulsion droplets and hot air causes the rapid evaporation of water, producing the dried microcapsules where the core is surrounded by the coating layer. The dried particles fall to the bottom of the drying chamber and are collected in a collection vessel. However, the finest ones go to the cyclone separator where they are separated from the humid air and are collected.

It is notable that spray drying can be used for heat sensitive and volatile ingredients due to the short heat exposure time (a few seconds at most) and rapid evaporation which keeps the temperature inside the powder low. The small size particles produced by spray drying makes them highly soluble and dispersible in water. However, the disadvantage of this technology is that the fine powder needs further processing such as agglomeration in which they are treated with steam to induce their cohesion and form larger particles to make them more readily soluble and to reduce segregation tendency (Augustin and Hemar 2009; Gharsallaoui and others 2007; Risch 1995a; Risch and others 1995).

CHAPTER 2 EXTRACTION OF CRAWFISH AND SHRIMP ASTAXANTHIN WITH FLAXSEED OIL: EFFECTS ON LIPID OXIDATION AND ASTAXANTHIN DEGRADATION RATES

2.1 Introduction

Louisiana produces about 100 million pounds of shrimp annually and is also the world's fourth largest crawfish producer. The state harvests between 75 to 105 million pounds of crawfish each year. Millions of pounds of byproducts generated from crawfish and shrimp peeling operations in Louisiana annually and these byproducts are discarded or used as aquaculture feed but with low economic value (Louisiana AgCenter Website).

Crawfish byproducts generated from the peeling process containing cephalothorax, abdominal exoskeleton, and viscera accounts for approximately 85% of the whole crawfish (Chen and Meyers 1982), while shrimp byproducts in the form of head and body carapace, comprise 45-60% of the whole shrimp (Sachindra and others 2007). The byproducts from crawfish and shrimp are a good source of high quality astaxanthin (Chen and Meyers 1982) and there are opportunities to use crawfish and shrimp processing byproducts to extract astaxanthin, which can be used as natural colorants and antioxidant ingredients in foods, feeds, and industrial applications. Astaxanthin, the main pigment found in crustacean and salmonids provides the desirable reddish-orange color in these organisms (Gentles and Haard 1991; Higuera-Ciapara and others 2006; Shahidi and Synowiecki 1991). In addition to its pigmentation function, antioxidant activity is one of the most important properties of astaxanthin. It has been reported that the antioxidant activity of astaxanthin is 10 times higher than other carotenoids such as zeaxanthin, lutein, canthaxantin, and β-carotene (Miki 1991).

Several studies have identified astaxanthin antioxidant mechanisms that quench active oxygen species and free radicals *in vitro* and *in vivo* (Edge and others 1997; Palozza and Krinsky 1992; Rengel and others 2000). Due to its antioxidant properties, astaxanthin may have a role in the treatment of chronic diseases such as cardiovascular diseases, cataract development, macular degeneration, and cancer (Mayne 1996).

Astaxanthin is widely used in aquaculture, cosmetic, and functional foods (Guerin and others 2003; Higuera-Ciapara and others 2006). The use of astaxanthin as a pigmentation agent in aquaculture feed has been well documented by many previous studies (Chen and Meyers 1982; Gentles and Haard 1991; Saito and Regier 1971; Sigurgisladottir and others 1994). There are also potential markets for natural carotenoids in soft drinks, ice cream, desserts, candies, meat products and pet and aquaculture feeds (Delgado-Vargas and others 2000; Delgado-Vargas and Paredes-Lopez 2003). Astaxanthin is insoluble in water and soluble in oil with increasing temperature. Astaxanthin can be extracted from crawfish and shrimp byproducts using solvent and edible oil. Chen and Meyers (1982) have extracted astaxanthin from crawfish byproducts using soybean oil. Although an established extraction method exist for extracting astaxanthin from crustacean byproducts, flaxseed oil containing astaxanthin has not been produced. The antioxidant-rich natural astaxanthin dispersed in alpha linolenic acid-rich flaxseed oil may provide healthier functional food options for US consumers.

Flaxseed oil has high content of alpha-linolenic acid (ALA) and linoleic acid (LA) which are precursors to long-chain (n-3) fatty acids such as eicosapentaenoic acid (EPA) and

docosahexaenoic acid (DHA) (Harper and others 2007; Tzang and others 2009). Both ALA and LA are considered to be essential fatty acids and studies have shown that ALA can protect against cardiovascular disease and inflammation (Bloedon and Szapary 2004). It is well documented that lipid oxidation of oils mostly depends on the storage temperature and storage period (Aidos and others 2002; Tan and others 2001). Chen and Meyers (1982) have reported that the stability of astaxanthin is affected by heat, the length of exposure to oxygen, and the intensity of exposure to light. Therefore, it is important to evaluate the lipid oxidation and astaxanthin degradation rates of flaxseed oil containing astaxanthin. The objectives of this study were to extract astaxanthin from crawfish (*Procambarus clarkii*) and shrimp (*Litopenaeus setiferus*) byproducts using flaxseed oil and to study the oxidation rates and the astaxanthin degradation rates in the flaxseed oil.

2.2 Materials and Methods

2.2.1 Determining Total Astaxanthin and Proximate of Crawfish and Shrimp Byproducts

Three batches of fresh crawfish and shrimp peeling byproducts containing cephalothorax, abdominal exoskeleton, and viscera were obtained from a local Louisiana seafood processor and stored at -20 ^{o}C. The thawed crawfish or shrimp byproducts were ground in a Hobart grinder (K5SS, Hobart Corporation, Troy, OH). The ground byproducts were analyzed for total astaxanthin content, moisture, ash, protein, and fat contents. Total astaxanthin content in crawfish and shrimp byproducts was determined using the method described by Niamnuy and others (2008) with slight modification. A 10 g sample of crawfish or shrimp byproducts was extracted three times with 40 mL of acetone using a stirrer (IKA® Works, Inc., RW20,

Wilmington, NC) at 800 rpm for 2 min. Then, 40 mL of petroleum ether and 100 mL of distilled water containing 0.5 % (w/v) sodium chloride were added to the acetone extracts. The absorbance for petroleum ether layer containing astaxanthin was measured at 472 nm using a spectrophotometer (Thermo Fisher Scientific, Vernon Hills, IL). Astaxanthin content was calculated using the astaxanthin standard curve.

Moisture content was determined according to AOAC method 934.01 (AOAC 1995). The samples were dried to a constant weight in an oven at 105 ^{o}C. Ash content was determined by ashing 2 g of samples in a muffler furnace at 550 ^{o}C for 4 h according to AOAC method 942.05 (AOAC 1995). Total nitrogen was determined by AOAC method 993.13 (AOAC 1995). The protein was calculated by multiplying nitrogen content by 6.25. Fat content was determined using a Soxhlet extraction method according to AOAC method 920.39 (AOAC 1995).

2.2.2 Extraction of Astaxanthin from Crawfish and Shrimp Byproducts

Flaxseed oil (FO) containing crawfish (FOCA) and shrimp astaxanthin (FOSA) were prepared using a modified method of Sachindra and Mahendrakar (2005) as described in Figure 2.1. Two batches of FO were purchased from iHerb (iHerb, Irwindale, CA) and the FO purchased to extract astaxanthin from crawfish was referred to as FO-1 and FO-2 for extracting shrimp astaxathin throughout the study. A 100 g sample of ground crawfish or shrimp byproducts was mixed with 100 mL of FO-1 or FO-2, stirred for 60 min at 60 ^{o}C. The mixture was centrifuged at 8630 × g using a centrifuge (Beckman J2-HC, GMI, Inc., Ramsey, MN) for 15 min at 4 ^{o}C to separate FOCA or FOSA and water phase from the solid phase. FOCA or

FOSA was separated from the water phase using a separatory funnel. The solid phase was also analyzed for total astaxanthin content, moisture, ash, protein, and fat contents as described in section 2.2.1.

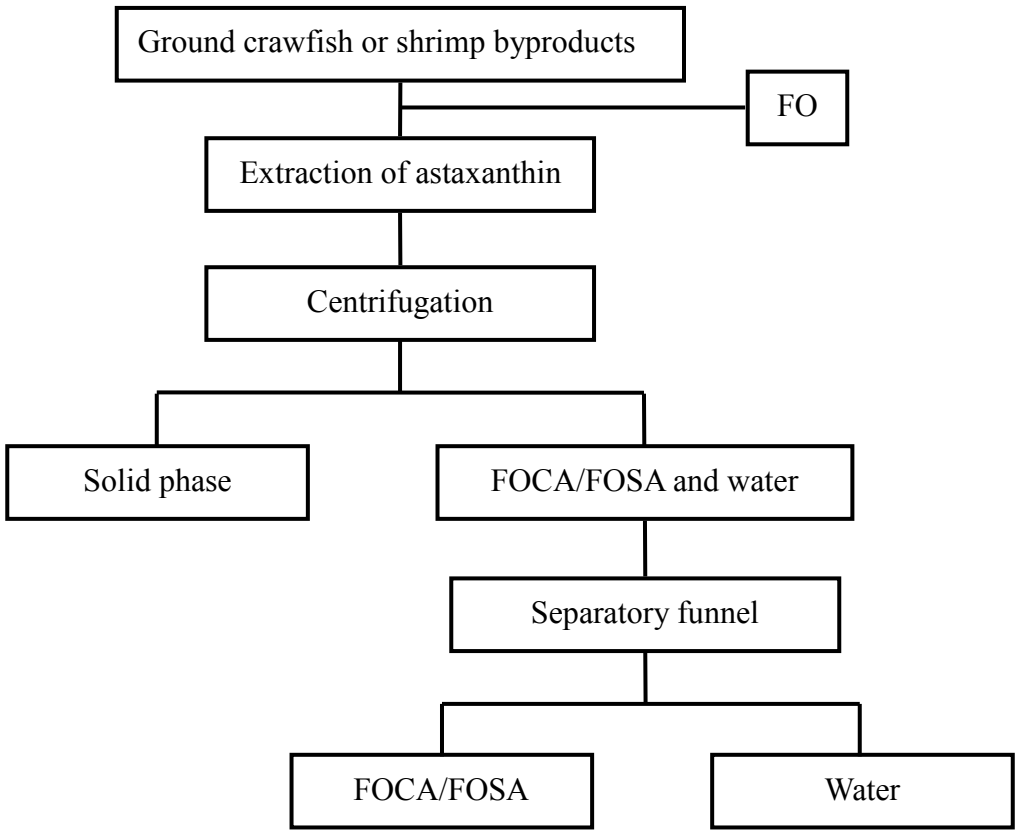

Figure 2.1 Extraction of astaxanthin from crawfish or shrimp byproducts using flaxseed oil. FO = Flaxseed oil; FOCA = Flaxseed oil containing crawfish astaxanthin; FOSA = Flaxseed oil containing shrimp astaxanthin.

2.2.3 Characterization of FO, FOCA, and FOSA

2.2.3.1 Extractable Astaxanthin Content of Crawfish and Shrimp Byproducts

The amount of extractable astaxanthin in the crawfish or shrimp byproducts was determined spectrophotometrically at 500 nm wavelength as described by Chen and Meyers (1984). The astaxanthin content was reported as mg astaxanthin/100 g waste using Equation 2.1:

$$Astaxanthin\ (mg/100g\quad waste) = \frac{A \times D \times 10^6}{1000 \times W \times E_{1cm}^{\%}} \tag{2.1}$$

where A is absorbance at 500 nm; V is volume of FOA recovered (mL); D is dilution factor; W is weight of waste (g); $E_{1cm}^{\%}$ is extinction coeffcient (1827); FOA is flaxseed oil containing astaxanthin.

The amount of astaxanthin in 100 g of oil was calculated using Equation 2.2:

$$Astaxanthin\ (mg/100g\quad FOA) = \frac{A \times D \times 10^5}{100 \times d \times S \times E_{1cm}^{\%}} \tag{2.2}$$

where A is absorbance at 500 nm; D is dilution factor, d is the cell width (1 cm); S is specific gravity of FOA; $E_{1cm}^{\%}$ is extinction coefficient (1827); FOA is flaxseed oil containing astaxanthin.

2.2.3.2 Color of FO, FOCA, and FOSA

Color of FO, FOCA, and FOSA was measured in triplicate using a LabScan® XE spectrophotometer (Hunter Associates Laboratory, INC. Resbon, VA) and was reported in CIELAB color scales (L^*, a^* and b^* values). The instrument was standardized using the calibrated black and white standards that come with the instrument. Chroma and hue angle value were calculated using Equations 2.3 and 2.4, respectively.

$$\text{Chroma} = [a^{*2} + b^{*2}]^{1/2} \tag{2.3}$$

$$\text{Hue angle} = \tan^{-1}(b^*/a^*) \tag{2.4}$$

2.2.3.3 Peroxide Value of FO, FOCA, and FOSA

The peroxide value (PV) was measured according to the AOAC method 965.33 (AOAC 1995). A 5 g sample of FO, FOCA or FOSA was dissolved in 30 mL acetic acid-chloroform (3:2 v:v) solution. Saturated KI solution (0.5 mL) was added and the mixture was shaken for 1 min and 30 mL of distilled water was added. The mixture was titrated with 0.1 N $Na_2S_2O_3$

until the yellowish color disappeared and then 0.5 mL of a 1% starch solution was added to the mixture. The mixture was titrated with 0.1 N $Na_2S_2O_3$ until blue color just disappeared. The results were expressed in terms of milliequivalents of peroxides per kg of oil.

2.2.3.4 Free Fatty Acids of FO, FOCA, and FOSA

Free fatty acids (FFA) content was determined according to AOAC procedure 940.28 (AOAC 1995). A 7.05 g sample of FO, FOCA or FOSA was added in 50 mL alcohol, previously neutralized by adding 2 mL phenolphthalein solution and enough 0.1 N NaOH to produce faint permanent pink. The oil and alcohol mixture was titrated with 0.25 N NaOH until as just permanent pink appeared. The percentage of FFA was expressed as oleic acid equivalents.

2.2.3.5 Fatty Acid Methyl Ester Profiles of FO, FOCA, and FOSA

Fatty acid methyl ester profiles of FO, FOCA, and FOSA determination were conducted in two laboratories as described below. Fatty acid methyl esters (FAMEs) were prepared at the USDA-ARS Laboratory, University of Alaska Fairbanks, AK using a modified method of Maxwell and Marmer (1983). A 20 mg sample of FO or FOA was dissolved in 4.5 mL isooctane and 500 µL internal standard (10 mg methyl tricosanoate (23:0)/mL isooctane and 500 µL 2 N KOH (1.12 g/10mL MeOH) was added to the mixture. The mixture was vortexed for 60 seconds and centrifuged to the separate upper layer. The separated upper layer was mixed with 1 mL saturated ammonium acetate solution and aqueous layer was removed and discarded. The mixture was centrifuged separated the upper layer of the mixture was removed. Then 1 mL of distilled water was added to the separated upper layer and centrifuged separated the upper layer and then 2-3 g anhydrous sodium sulfate was added,

vortexed, and kept for 20-30 min. The mixture was centrifuged and the liquid containing methyl ester was separated. A 0.5 mL of isooctane containing methyl ester and 0.5 mL isooctane were added to the amber GC vial. Gas chromatographic (GC) analysis was used with a GC model 7890A (Agilent) fitted with a HP-88 (100m x 0.25 mm ID x 0.25μm film) column. The oven program used was 90 °C for 8 min, followed by 10 °C/min to 175 °C for 10 min, 4 °C/min to 190 °C for 10 min, 5 °C/min to 210 °C for 5 min and then 20 °C/min to 250 °C for 8 min. ChemStation software was used to integrate peaks. Peaks were identified by comparing to reference standards obtained from Sigma: Supelco 37 mix. Data are expressed as percent of total integrated area.

Fatty acid methyl esters (FAMEs) were prepared at the laboratory of the W. A. Callegari Environmental Center, Louisiana State University, LA using the method described by Paquot and others (1987) with slight modification. A 25 mg sample of FO, FOCA or FOSA was dissolved in 10 mL hexane. Then 10 μL of 2 N KOH (1.12 g/10 mL MeOH) was added to the mixture followed by vortexing for 1 min and this step was repeated for four times. Then 10 μL of 1 N H_2SO_4 was added to the mixture followed by vortexing for 1 min and centrifuged for 2 min at 3400 rpm to separate the upper layer. Then 5 μL of clear supernatant containing methyl esters was transferred to an auto sampler vial. Then 5 μL of internal standard (Hexadecanoic acid, 2-hydroxy-methyles dissolved in palmitate at 4 ppm concentration) and 1 mL of hexane was added to the vial. Gas chromatographic (GC) analysis was used with a GC model 450-GC (Varian, Inc., Palo Alto, CA) fitted with a MF-28-12-1 (30 m x 0.25 mm ID x 0.25 μm film) column. The oven program used was

100 °C for 2 min, followed by 12 °C/min ramp to 255 °C and hold for 8 min. MS WorkStation software was used to integrate peaks. Data are expressed as percent of total integrated area. The results obtained by both laboratories for FO, FOCA, and FOSA of fatty acid methyl esters profiles were averaged and reported.

2.2.4 Oxidation of FO, FOCA, and FOSA

Three batches of the opened amber bottles containing 20 g of FO, FOCA and/or FOSA samples were placed in a water bath and heated at 30, 40, 50, and/or 60 ^{o}C. An oil sample was drawn from the amber bottles using a pipette every hour from 0 to 4 hours for PV and astaxanthin concentration analysis. A plot of PV versus time was constructed for 30, 40, 50, and/or 60 ^{o}C. The resulting straight line yielded the magnitude of oxidation rate (mequiv·kg oil^{-1}·h^{-1}) for the corresponding temperature. The effect of temperature on the oxidation rate was described using the Arrhenius relationship as shown in Equation 2.5:

$$k = k_{\infty} \exp(-E_a / RT) \tag{2.5}$$

The logarithms were taken on both sides of Equation 2.5.

$$\ln k = \frac{-E_a}{RT} + \ln k_{\infty} \tag{2.6}$$

where k is the reaction rate constant; k_{∞} is the frequency factor; R is the universal gas constant (8.3145 J/mol K); T is the absolute temperature (K); Ea is activation energy (J/mol). A plot of *ln* oxidation rate constant versus $1/T$ (i.e., 1/absolute temperature) was constructed for FO, FOCA, and FOSA oil. The slope of the straight line was obtained from the trend line of the plot. The magnitude of Ea was calculated as the slope of the trend line multiply by the

universal gas constant.

2.2.5 Kinetic Parameters of Astaxanthin Degradation

Zero order (Equation 2.7) and first order (Equation 2.8) models were used to describe the astaxanthin degradation kinetics according to Avila and Silva (1999) and Niamnuy and others (2008).

$$C = C' - kt \tag{2.7}$$

where C' is the initial concentration (mg·100 g oil^{-1}) of astaxanthin; C is the concentration (mg·100 g oil^{-1}) of astaxanthin at time t; k is the degradation rate constant (mg·100 g oil^{-1}·h^{-1}); t is the oxidation time (h).

A plot of astaxanthin concentration (C-C') versus time was constructed for 30, 40, 50, and/or 60 ^{o}C to obtain k by zero order model (Equation 2.7). The slope of the straight line and the correlation coefficient were obtained from the trend line of the plot. The k values for the oil heated at 30, 40, 50, and/or 60 ^{o}C were obtained from the resulted slope of the plot.

$$C = C'\exp(-kt) \tag{2.8}$$

The logarithms were taken on both sides of Equation (2.8).

$$\ln C = \ln C' - kt \tag{2.9}$$

The Equation (2.9) was rearranged as Equation (2.10).

$$\ln\left(\frac{C}{C'}\right) = -kt \tag{2.10}$$

A plot of $\ln\left(\frac{C}{C'}\right)$ versus t was constructed to determine k values and correlation coefficients. The resulted k values from zero and first order models ($ln\ k$) versus $1/T$ were

plotted and obtained activation energy for astaxanthin degradation using the Arrhenius model (Equation 2.6). The magnitude of *Ea* was calculated as the slope of the plot multiplied by the gas constant.

2.2.6 Statistical Analysis

Mean values and standard deviations of triplicate determinations were reported. Analysis of variance (ANOVA) was carried out to determine the difference among treatments means (SAS Version 8.2, SAS Institute Inc., Cary, NC) using the *post hoc* Tukey's studentized range test.

2.3 Results and Discussion

2.3.1 Proximate Compositions of Crawfish and Shrimp Byproducts

Moisture content (wet weight basis) of crawfish and shrimp byproducts was 66.95 % and 74.5 %, respectively, while the generated solid waste from extraction of astaxathin from crawfish and shrimp byproducts contained 54.68 % and 62.82 % moisture, respectively, crawfish and shrimp solid waste. Dry weight basis of ash, fat, and protein contents of crawfish byproducts before extraction of astaxanthin were 42.97 % , 1.37 %, and 38.1 %, respectively (Table 2.1) and the protein content of crawfish byproducts was similar to the value (36.7%) reported by Meyers and Bligh (1981). The ash content of crawfish was slightly higher than the reported value of 35.7 % by Meyers and Bligh (1981), while the same author reported a higher fat content (6.7 %) than that found in this study. Meyers and Bligh (1981) have also reported that crawfish byproducts contained 14.1 % chitin. The total ash, fat, and protein contents of crawfish byproducts accounted for was 82.44 %, which indicated

that the crawfish byproducts might contain 17.56% chitin.

Ash, fat, and protein contents (dry weight basis) of shrimp byproducts were 17.41 %, 7.22 %, and 60.2 %, respectively. The previously reported ash, fat, and protein contents for shrimp byproducts were 22.2%, 22.7%, and 51.3%, respectively (Lee and others, 1999). The proximate composition of shrimp byproducts depends on the age of shrimp, seasons and species of shrimp (Sachindra and others 2007). Total ash, fat, and protein contents for the shrimp byproducts accounted for 84.83 %, indicating that the byproducts might contain about 15.17 % chitin. The expected chitin amount in the shrimp byproducts was similar to reported amount of 14.2% for shrimp byproducts by Lee and others (1999).

The solid waste, liquid containing soluble proteins, and oil containing astaxathin phases were generated during the astaxathin extraction from crawfish and shrimp byproducts. The ash content of wastes generated from astaxanthin extraction was similar to both crawfish and shrimp byproducts, while the wastes had higher fat and lower protein contents (Table 2.1). This indicated that some FO used for extracting astaxanthin from the byproducts might be retained in the wastes, while some soluble protein might have been removed from the byproducts when solid and oil phases separated from the liquid phase during the separation of oil containing astaxathin.

Table 2.1 Proximate compositions of crawfish and shrimp byproducts and waste (dry weight basis)

	CB	CWA	SB	SWA
Ash %	42.97±0.07	40.25±1.53	17.41±0.73	16.74±0.61
Fat %	1.37±0.07	2.61±0.04	7.22±0.11	18.89±0.16
Protein %	38.1±0.4	30.4±0.3	60.2±0.46	43.2±0.4

Values are means and SD of three determinations. CB = Crawfish byproducts; SB = Shrimp byproducts; CWA = Crawfish waste after extraction; SWA = Shrimp waste after extraction.

2.3.2 Astaxanthin Content, Color, PV, and FFA of FO, FOCA, and FOSA

The total astaxanthin content in crawfish and shrimp byproducts was 8.84 mg/100 g wet crawfish byproducts and 6.47 mg/100 g wet shrimp byproducts, respectively. After extraction, the remaining astaxanthin in crawfish and shrimp byproducts was 3.38 mg/100 g wet crawfish waste and 0.7 mg/100 g wet shrimp waste, respectively. The amount of extractable astaxanthin in the crawfish byproducts was 3.02 mg/100 g of wet crawfish byproducts (Table 2.2), which was lower than previously reported value by Meyers and Bligh (1981). In their study, petroleum ether-acetone-water mixture was used to extract astaxanthin from crawfish waste with a concentration of 15.3 mg of astaxanthin / 100 g of crawfish peeling waste. The amount of extractable astaxanthin in the shrimp byproducts was 4.83 mg/100 g of wet shrimp waste (Table 2.3), which is similar to those reported in the previous literature for shrimp waste (De Holanda and Netto 2006; Handayani and others 2008). De Holanda and Netto (2006) used an enzymatic method to extract astaxanthin from shrimp (*Xiphopenaeus kroyeri*) waste using soy oil and extracted 4.90 mg astaxanthin/100 g waste. The extraction of astaxanthin in FOSA was higher than that in other vegetable oils such as sunflower oil, groundnut oil, coconut oil, and rice bran oil (Sachindra and Mahendrakar 2005). A number of studies have demonstrated that the yield of astaxanthin depends upon the extraction methods, solvents or media and other factors such as particle size of the waste and ratio of waste to oil used for extracting astaxanthin from seafood processing byproducts (Chen and Meyers 1982b; Meyers and Bligh 1981; Sachindra and others 2005; Sachindra and others 2006). In addition, the variation of extractable astaxanthin in the waste and different species may also affect the

extraction yield of astaxanthin. In their study, however, either proteolytic enzymes or solvents were used to extract the astaxanthin, which might explain why they obtained a higher concentration of astaxanthin. Although, our astaxanthin concentration in FOCA was lower than previously reported astaxanthin extraction concentrations, the process presently used could significantly reduce the processing time and lower the chemical waste generation during extraction of astaxanthin from crawfish byproducts. Thus, our process might reduce overall processing cost.

Table 2.2 Astaxanthin, color, PV, and FFA of FO-1 and FOCA

	FO-1	FOCA
Astaxanthin(mg/100 g wet waste)	—	3.02±0.02
Astaxanthin (mg/100 g FOCA)	—	3.90±0.34
Color L*	50.42±0.22^{a}	35.63±0.26^{b}
Color a*	4.04±0.07^{b}	35.27±0.12^{a}
Color b*	81.30±0.35^{a}	61.78±0.25^{b}
PV(mequiv /kg oil)	3.97±0.08^{b}	4.59±0.16^{a}
Chroma	81.4±0.35^{a}	71.14±0.17^{b}
Hue angle	87.16±0.04^{a}	60.28±0.17^{b}
FFA(%)	0.31±0.00^{a}	0.30±0.00^{a}

Values are means and SD of three determinations. ^{ab}means with different letters in each row are significantly different ($p < 0.05$). FO-1 = Flaxseed oil; FOCA = Flaxseed oil containing crawfish astaxanthin; FFA= Free fatty acids; PV= Peroxide value.

After extraction, significant differences of color values were observed either between FO-1 and FOCA or between FO-2 and FOSA. The FOCA and FOSA had higher redness color and lower lightness than FO-1 and FO-2 respectively due to the astaxanthin pigments in the FOCA and FOSA. However, the FO-1 and FO-2 were more yellow than FOCA and FOSA. A significant decrease of chroma and hue angle value was obtained for FOCA and FOSA as compared to those of FO-1 and FO-2 (Tables 2.2 and 2.3).

Table 2.3 Astaxanthin, color, PV, and FFA of FO-2 and FOSA

	FO-2	FOSA
Astaxanthin(mg/100 g wet waste)	—	4.83±0.01
Astaxanthin (mg/100 g FOSA)	—	6.23±0.22
Color L*	47.7±0.28[a]	34.58±0.50[b]
Color a*	6.0±0.55[b]	36.45±1.27[a]
Color b*	77.77±0.35[a]	58.93±1.03[b]
Chroma	78.00±0.31[a]	69.30±0.94[b]
Hue angle	85.59±0.42[a]	58.26±1.11[b]
PV(mequiv /kg oil)	0.87±0.18[a]	1.02±0.13[a]
FFA(%)	0.30±0.00[a]	0.30±0.00[a]

Values are means and SD of three determinations. [ab]means with different letters in each row are significantly different ($p < 0.05$). FO-2 = Flaxseed oil; FOSA = Flaxseed oil containing shrimp astaxanthin; FFA= Free fatty acids; PV= Peroxide value.

In the crawfish astaxanthin extraction process, the PV of FO-1 was 3.97 mequiv/kg oil (Table 2.2), lower than the PV value of 5.2 mequiv/kg oil for FO extraction reported by a previous study (Bera and others 2006). After extraction, a slight increase was observed in PV value between FO-1 and FOCA (Table 2.2). The PV of FO-2 was 0.87 mequiv/kg oil (Table 2.3) which was different from FO-1 due to the difference between different batches of oils. However, the PV of FOSA was 1.02 mequiv/kg oil, which was similar to that of FO-2 statistically. Similarly, FO-2 and FOSA had similar FFA values (Table 2.3).

2.3.3 Fatty Acid Methyl Esters Profile of FO, FOCA, and FOSA

The fatty acids methyl esters profiles for FO, FOCA, and FOSA obtained from both laboratories were similar and they were summarized and reported in Tables 2.4 and 2.5. The fatty acid methyl esters compositions of FO-1 and FOCA are given in Table 2.4. Alpha-linolenic acid (ALA) was the predominant fatty acid accounting for 55.51 % and 55.47 % for FO-1 and FOCA, respectively, and similar ALA content in FO was reported by previous research (53.5 %) (Tzang and others 2009). Table 2.5 shows the fatty acid methyl

ester compositions of FO-2 and FOSA. Both FO-2 (73.03 %) and FOSA (71.03 %) had high percentages of polyunsaturated fatty acids (Table 2.5). The ALA content in FO-2 and FOSA were 58.2 % and 55.91 %, respectively. However, ALA content in FO-1, FO-2, FOCA and FOSA was slightly higher than a previously reported value (50.4%) (Bera and others 2006). No significant difference in ALA content was observed either between FO-1 and FOCA or between FO-2 and FOSA, demonstrating that the extraction procedure that was used had no effect on ALA content. Degradation of fatty acid has been reported to be related to fatty acid oxidation and acidification (Pereda and others 2008). Thus the extraction process did not cause ALA oxidation and acidification.

Table 2.4 Profile of fatty acid methyl esters for FO-1 and FOCA

Fatty acids (%)	FO-1	FOCA
C16:0 Palmitic	5.92±0.29[a]	6.06±0.31[a]
C18:0 Stearic	4.02±0.91[a]	4.07±0.75[a]
C18:1n9c Oleic	16.02±0.81[a]	17.00±0.81[a]
C18:2n6c Linoleic	15.02±0.11[a]	12.50±1.43[b]
C18:3n3 Alpha-Linolenic	55.51±1.58[a]	55.47±1.33[a]
Total omega 3	55.51±1.58[a]	55.48±1.33[a]
Total omega 6	15.08±0.15[a]	12.54±1.49[b]
Saturates	11.67±2.88[a]	12.31±2.43[a]
Monounsaturates	16.77±1.49[a]	17.00±0.28[a]
Polyunsaturates	70.61±1.71[a]	68.04±2.49[a]
Omega 3/Omega 6	3.68±0.08[b]	4.47±0.48[a]
Polyunsaturates/Saturates	6.36±1.56[a]	5.75±1.41[a]
Total fatty acids	99.05±0.9[a]	97.89±1.47[a]

Values are means and SD of three determinations. [ab]means with different letters in each row are significantly different ($p < 0.05$). FO-1 = Flaxseed oil; FOCA = Flaxseed oil containing crawfish astaxanthin. Only major fatty acids were reported.

Table 2.5 Profile of fatty acid methyl esters for FO-2 and FOSA

Fatty acids (%)	FO-2	FOSA
C16:0 Palmitic	5.22±0.4[a]	5.39±0.35[a]
C18:0 Stearic	3.47±0.88[a]	4.23±0.99[a]
C18:1n9c Oleic	17.05±0.97[a]	16.07±1.14[a]
C18:2n6c Linoleic	14.65±0.14[a]	14.99±0.47[a]
C18:3n3 Alpha-Linolenic	58.20±2.28[a]	55.91±2.79[a]
Total omega 3	58.38±2.37[a]	56.04±2.92[a]
Total omega 6	14.65±0.14[a]	14.99±0.47[a]
Saturates	8.69±3.26[a]	11.59±3.37[a]
Monounsaturates	19.96±1.37[a]	16.51±1.60[a]
Polyunsaturates	73.03±2.24[a]	71.03±2.56[a]
Omega 3/Omega 6	3.98±0.19[a]	3.74±0.29[a]
Polyunsaturates/Saturates	4.07±1.47[a]	4.40±0.37[a]
Total fatty acids	99.69±1.44[a]	99.13±1.24[a]

Values are means and SD of three determinations. [a]means with same letter in each row are not significantly different ($p > 0.05$). FO-2 = Flaxseed oil; FOSA = Flaxseed oil containing shrimp astaxanthin. Only major fatty acids were reported.

2.3.4 Lipid Oxidation of FO, FOCA, and FOSA

The peroxide value is used to measure peroxides formed in fats and oils as a result of autoxidation and oxidation processes, especially at the beginning of lipid oxidation (Choe and Min 2005). Figures 2.2 and 2.3 show the changes in PV of FO-1 and FOCA as a function of time at different temperatures. Lipid oxidation, as indicated by the PV, increased with increasing time and temperature. The FO-1 and FOCA heated at 30 ^{o}C exhibited minimal lipid oxidation with increasing time, whereas FO-1 heated at 40-60 ^{o}C showed higher lipid oxidation than FOCA with increasing time from 0 to 4 hr (Table 2.6). Lipid oxidation in edible oils occurs very slowly but it is accelerated when subjected to heat, air and light (Naz and others 2004). Similarly, the oxidation results for FO-2 and FOSA were shown in Figures 2.4 and 2.5. The lowest lipid oxidation was observed at 30 ^{o}C for both FO-2 and FOSA with increasing time. Higher temperature accelerates the lipid oxidation of FO-2 and FOSA (Table

2.7). However, FOCA and FOSA showed lower oxidation rates than those of FO-1 and FO-2 respectively, when oil samples were heated from 40-60 ^{o}C.

The use of antioxidants is an effective way to minimize or prevent lipid oxidation. Erkan and others (2009) reported that addition of the natural antioxidants (carnosic acid or sesamol) significantly decreased hydroperoxide formation during microwave heating. Also, Shyamala and others (2005) reported that sunflower oil containing leafy vegetable extracts minimized peroxide formation during heating and storage processes. Our study was in accordance with reports of reduced lipid oxidation of FO by the addition of antioxidants (Bera and others 2006; Erkan and others 2009), which indicated that the presence of the astaxanthin in the FO minimized the oxidation of the FO. Oxidation was significantly higher for FO-1 and FO-2 than that of FOCA and FOSA respectively regardless of different heating temperatures used. The oxidation rate (mequiv·kg oil^{-1}·h^{-1}) increased from 0.098 to 0.698 for FO-1 while it increased from 0.027 to 0.305 for FOCA when the oils were heated from 30 to 60^{o}C for 4 hr (Table 2.6). Similarly, the oxidation rate (mequiv·kg oil^{-1}·h^{-1}) increased from 0.018 to 0.229 for FO-2 when heated from 30 to 60 ^{o}C for 4 hr. However, the oxidation rate (mequiv·kg oil^{-1}·h^{-1}) for FOSA only increased from 0.003 to 0.094 for the same conditions (Table 2.7). The oxidation rates for the oil samples were well described by the Arrhenius equation (Figures 2.6 and 2.7) and the high R^2 values indicated that peroxide formation rates of these oils could be modeled by the Arrhenius equation. The activation energy for lipid oxidation of FO, FOCA and FOSA were calculated using the Arrhenius equation (Figures 2.6 and 2.7). The activation energies for lipid oxidation of FO-1 and FOCA were 51.07 kJ / mol and 65.84 kJ /

mol, respectively (Table 2.6). Similarly, the activation energies for FO-2 and FOSA oxidation were 68.97 kJ/mol and 93.37 kJ/mol, respectively (Table 2.7). Lower activation energy and higher oxidation rate indicated that FO-1 and FO-2 had a higher heat sensitive lipid oxidation rate than did FOCA and FOSA during heating. Adegoke and others (1998) reported that antioxidants such as tocopherols and propyl-gallate either delay or inhibit the initiation and propagation stages of oxidation by reacting with lipid-free radicals and peroxy or alkoxy radicals, respectively. Carotenoids have been reported to be the most efficient molecules for $^1O_2$ quenching (Laguerre and others 2007). Astaxanthin as a member of carotenoids family has conjugated double bonds and phenolic hydroxyl groups, which may have actively prevented oxidation of the glycerides in the FO during heating. Our results show that astaxanthin exhibited an effective antioxidant activity both in FOCA and FOSA when it was heated from 30 to 60 ^oC.

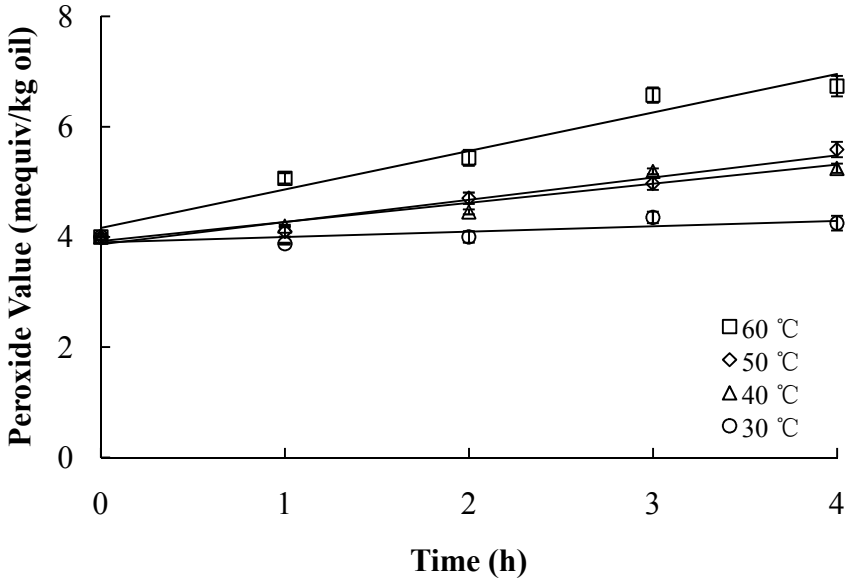

Figure 2.2 Effect of time on peroxide formation in the FO-1 at different temperatures. FO-1 = Flaxseed oil. Data are the average of three replicates.

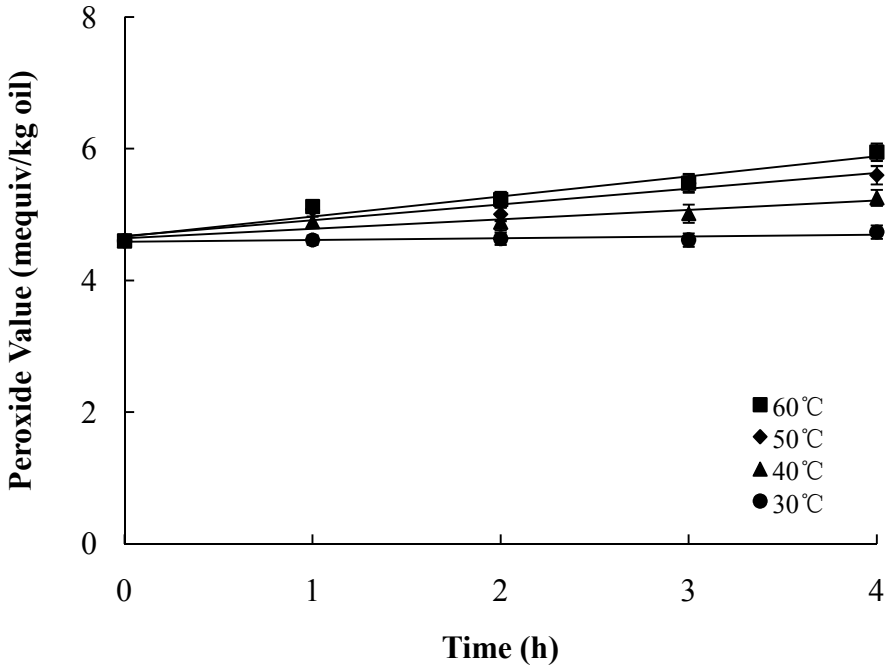

Figure 2.3 Effect of time on peroxide formation in the FOCA at different temperatures. FOCA = Flaxseed oil containing crawfish astaxanthin. Data are the average of three replicates.

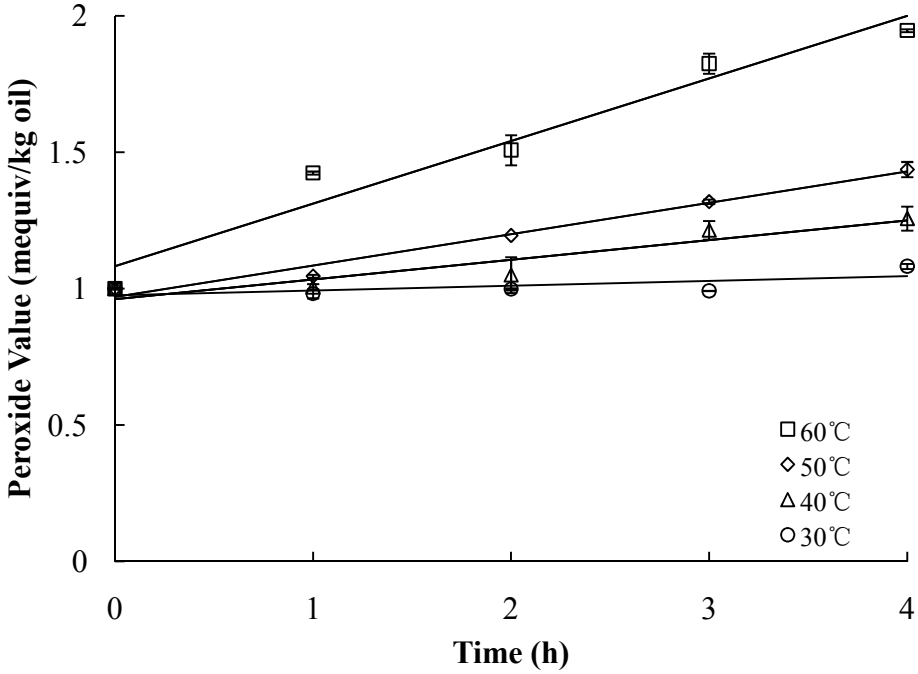

Figure 2.4 Effect of time on peroxide formation in the FO-2 at different temperatures. FO-2 = Flaxseed oil. Data are the average of three replicates.

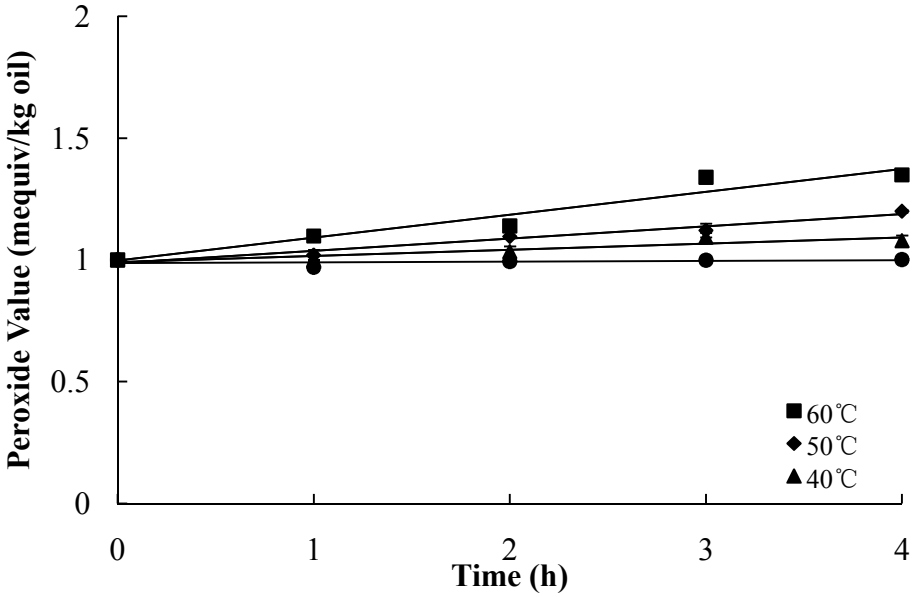

Figure 2.5 Effect of time on peroxide formation in the FOSA at different temperatures. FOSA = Flaxseed oil containing shrimp astaxanthin. Data are the average of three replicates

Table 2.6 Oxidation rates of FO-1 and FOCA

Temperature (^{o}C)	Oxidation rate (mequiv·kg oil^{-1}·h^{-1})	
	FO-1	FOCA
30	0.098±0.01^{aD}	0.027±0.02^{bD}
40	0.348±0.01^{aC}	0.144±0.01^{bC}
50	0.404±0.04^{aB}	0.24±0.03^{bB}
60	0.698±0.05^{aA}	0.305±0.04^{bA}
E_a (kJ/mol)	51.07±1.62^{b}	65.84±0.89^{a}

Values are means and SD of three determinations. ^{ab}means with different letters in each row are significantly different ($p < 0.05$). ^{ABCD}means with different letters in each column are significantly different ($p < 0.05$). E_a = Activation energy; FO-1 = Flaxseed oil; FOCA = Flaxseed oil containing crawfish astaxanthin.

Table 2.7 Oxidation rates of FO-2 and FOSA

Temperature (^{o}C)	Oxidation rate (mequiv·kg oil^{-1}·h^{-1})	
	FO-2	FOSA
30	0.018±0.00^{aD}	0.003±0.00^{bC}
40	0.072±0.01^{aC}	0.025±0.01^{bBC}
50	0.115±0.01^{aB}	0.051±0.01^{bB}
60	0.229±0.01^{aA}	0.094±0.00^{bA}
Ea (kJ/mol)	68.97±0.46^{b}	93.37±3.47^{a}

Values are means and SD of three determinations. ^{ab}means with different letters in each row are significantly different ($p < 0.05$). ^{ABCD}Means with the same letters in each column are not significantly different ($p > 0.05$). *Ea* = Activation energy; FO-2 = Flaxseed oil; FOSA = Flaxseed oil containing shrimp astaxanthin.

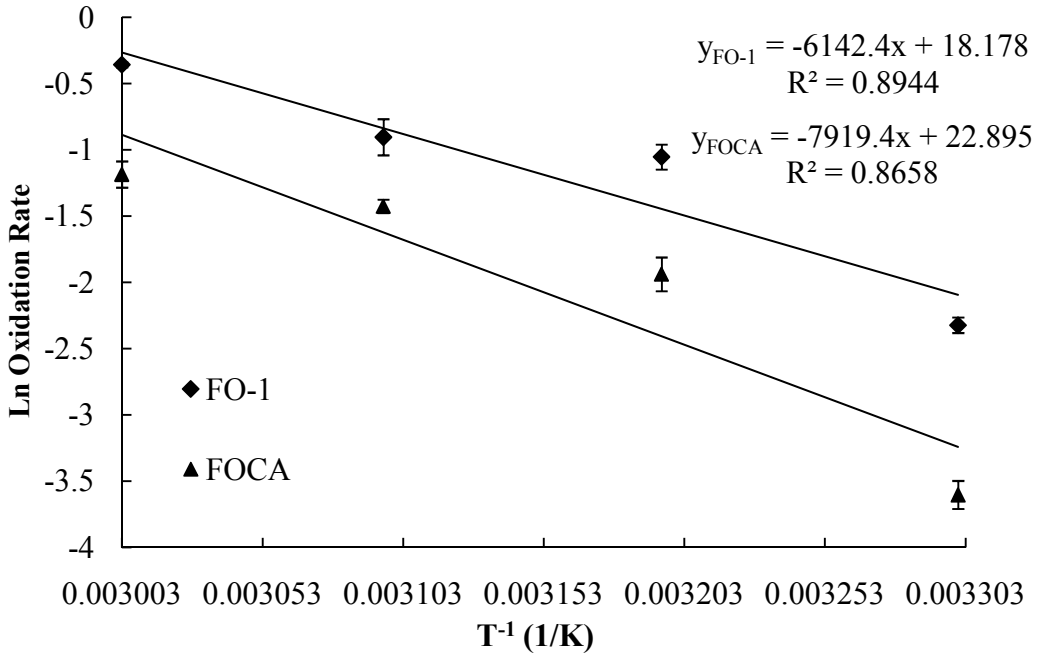

Figure 2.6 The Arrhenius plot for the peroxide values of the FO-1 and FOCA. FO-1 = Flaxseed oil; FOCA = Flaxseed oil containing crawfish astaxanthin

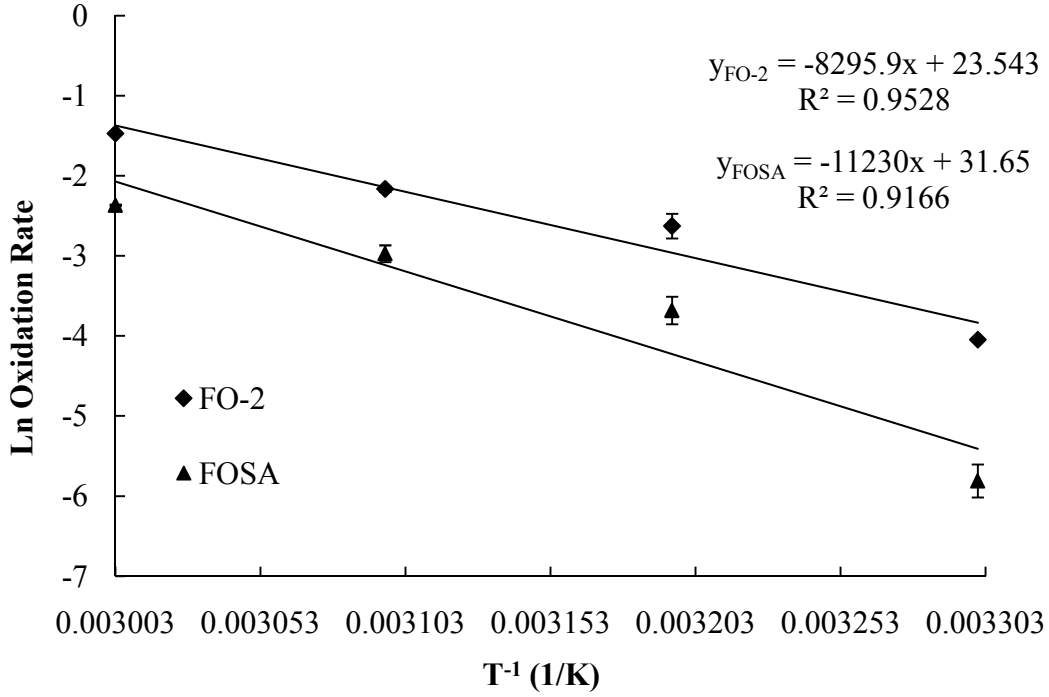

Figure 2.7 The Arrhenius plot for the peroxide values of the FO-2 and FOSA. FO-2 = Flaxseed oil; FOSA = Flaxseed oil containing shrimp astaxanthin

2.3.5 Astaxanthin Degradation Kinetics of FOCA and FOSA

Astaxanthin is sensitive to heat, oxidation, and light because of its highly unsaturated structure (Ribeiro and others 2005). Figures 2.8-2.11 show the results of astaxanthin degradation in the FOCA and FOSA during heating. The rate of degradation of astaxanthin was determined by linear regression of both (C-C') and *ln* (C/C') against heating time. The astaxanthin degradation was fitted by both zero (Figures 2.8 and 2.10) and first order (Figures 2.9 and 2.11) kinetics models. Both models showed that rate constant (*k)* for astaxanthin degradation of FOCA and FOSA increased with increased temperature. For astaxanthin degradation of FOCA, the R^2 for the zero order kinetics model was 0.7, 0.88, 0.89, and 0.94 for 30, 40, 50, and 60 ^{o}C, respectively (Table 2.8), while R^2 ranged from 0.85 to 0.97 (Table 2.10) for the first order kinetics model. For astaxanthin degradation of FOSA, the R^2 for the zero order kinetics model was 0.61, 0.83, 0.88, and 0.91 for 30, 40, 50, and 60 ^{o}C, respectively (Table 2.9), while R^2 ranged from 0.85 to 0.98 (Table 2.11) for the first order kinetics model. This indicated that first order kinetics could be used to describe the degradation of astaxanthin in FOCA and FOSA between 30 to 60 ^{o}C while zero order might describe the astaxanthin degradation in FOCA and FOSA at 60 ^{o}C. Niamnuy and others (2008) have also reported that the first order model can be used to describe the degradation of dried shrimp astaxanthin. Tachaprutinun and others (2009) have reported that most astaxanthin molecules degraded when astaxanthin solution (in ethanol) was heated to 70 ^{o}C for two hours. Levenspiel (1999) and Niamnuy and others (2008) have reported a higher *k* for a higher rate of reaction, which indicated astaxanthin degraded faster at a higher temperatures. Rao and others (2007) have

also reported reductions in astaxanthin concentrations at elevated heat processing temperatures. Astaxanthin degradation of FOCA was well described by the Arrhenius equation (Figures 2.12) and a high R^2 value of 0.98 and 0.99 was determined from zero and first order models, respectively. Similarly, astaxanthin degradation of FOSA was well described by the Arrhenius equation (Figures 2.13) and a high R^2 value of 0.97 and 0.99 was determined from zero and first order models, respectively. The E_a value obtained from zero and first order models for astaxanthin degradation of FOCA was 104.65 and 96.79 kJ/mol, respectively (Tables 2.8 and 2.10). The E_a value obtained from zero and first order models for astaxanthin degradation of FOSA was 84.53 and 88.44 kJ/mol, respectively (Tables 2.9 and 2.11). These values were lower than the reported E_a value of 110 kJ/mol for carotenoids degradation during heat treatment (Dhuique-Mayer and others 2007).

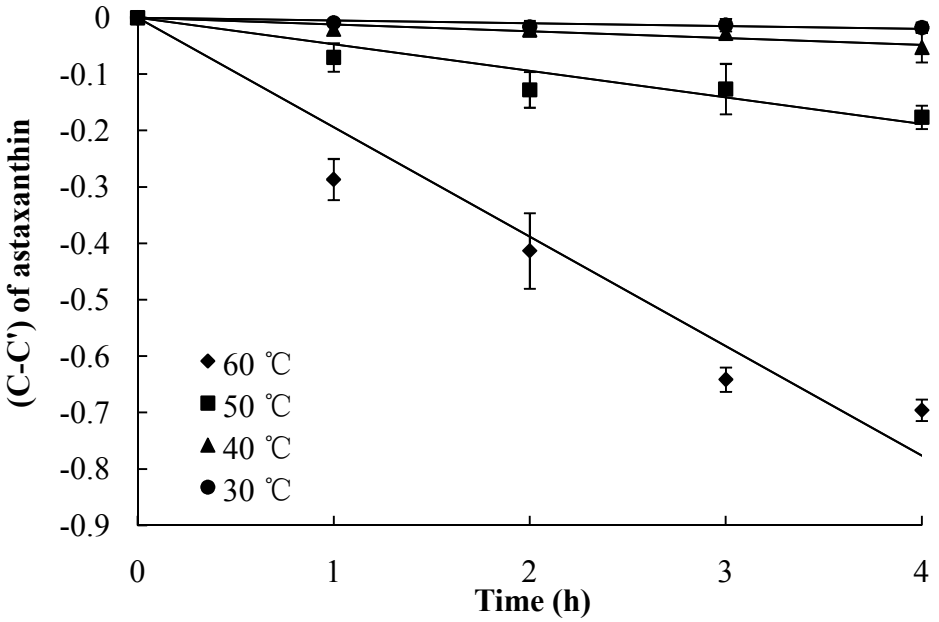

Figure 2.8 Zero order kinetics plots of astaxanthin degradation in FOCA at various temperatures. FOCA = Flaxseed oil containing crawfish astaxanthin. *C'* is the initial concentration of astaxanthin; *C* is the concentration of astaxanthin at time *t*.

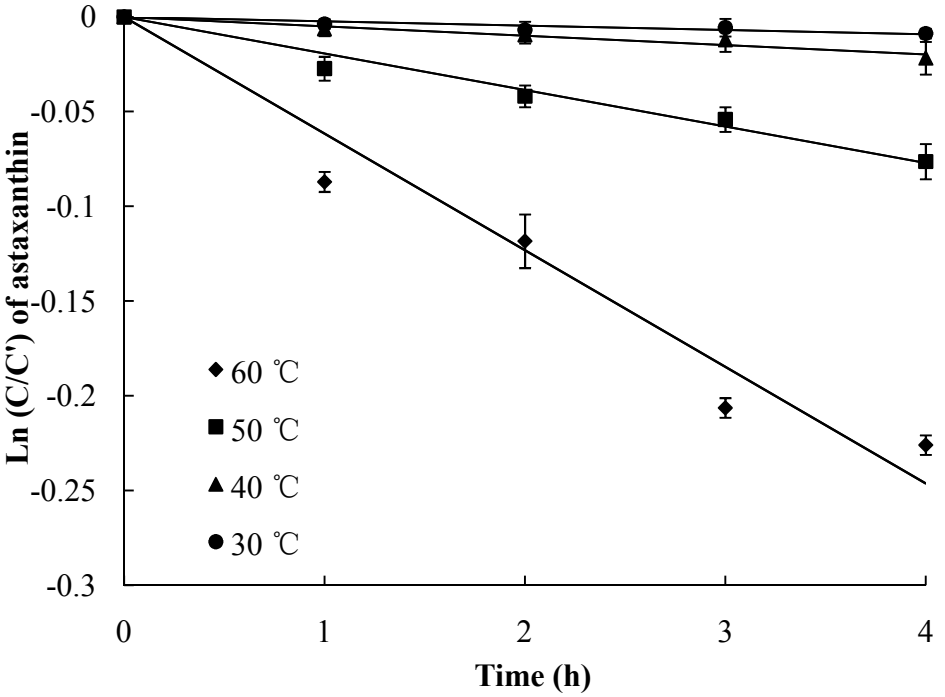

Figure 2.9 First order kinetics plots of astaxanthin degradation in FOCA at various temperatures. FOCA = Flaxseed oil containing crawfish astaxanthin. *C'* is the initial concentration of astaxanthin; *C* is the concentration of astaxanthin at time *t*.

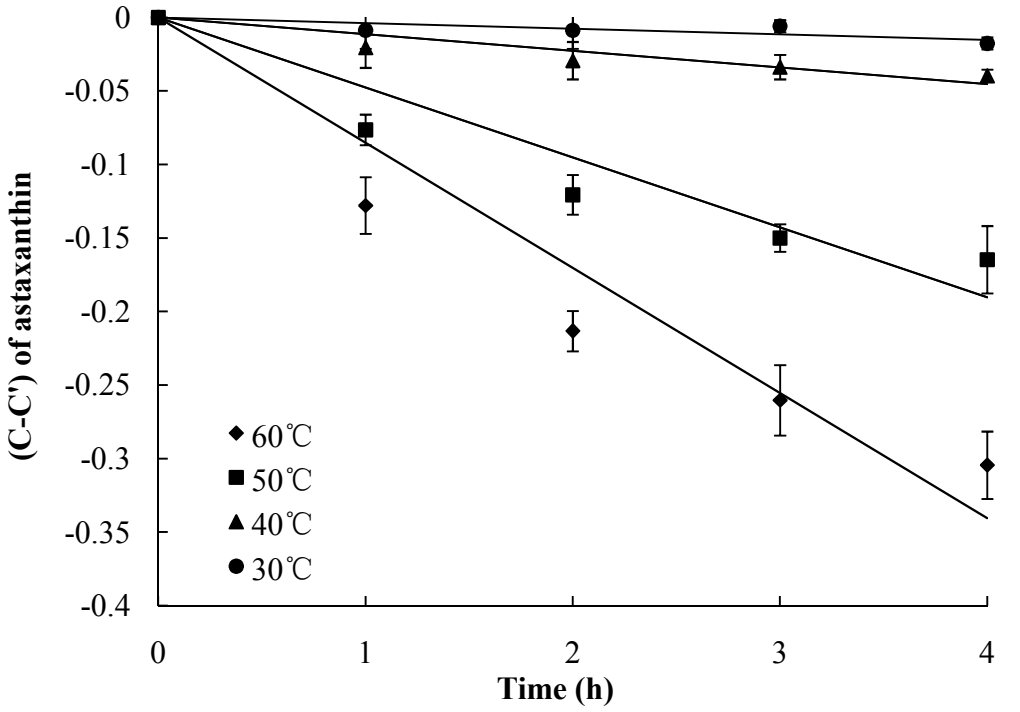

Figure 2.10 Zero order kinetic plots of astaxanthin degradation in FOSA at various temperatures. FOSA = Flaxseed oil containing shrimp astaxanthin. *C'* is the initial concentration of astaxanthin; *C* is the concentration of astaxanthin at time *t*.

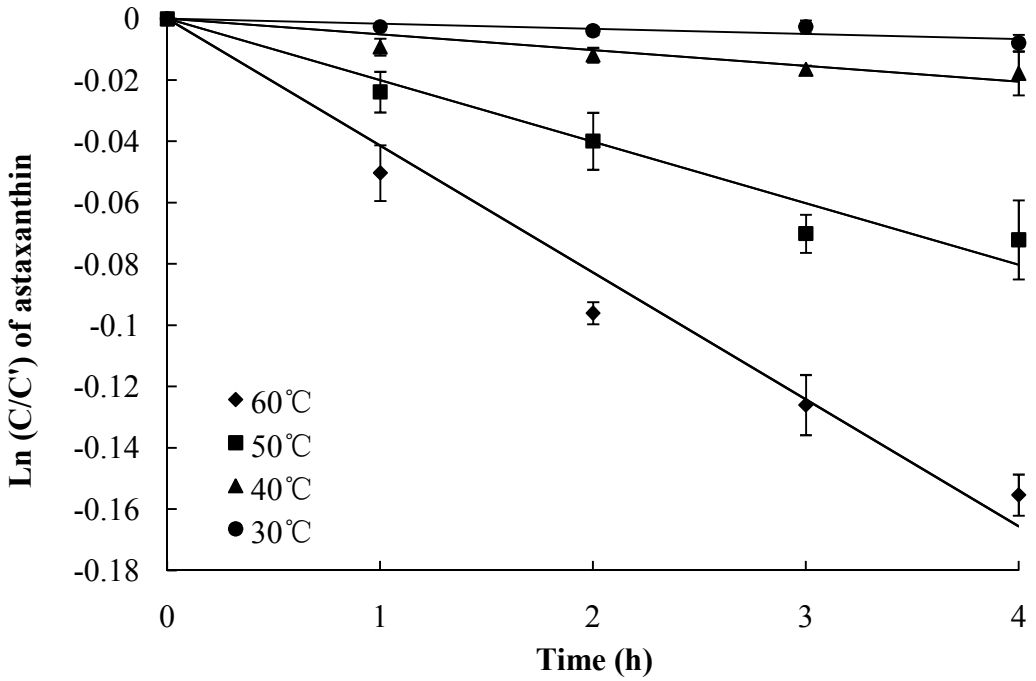

Figure 2.11 First order kinetic plots of astaxanthin degradation in FOSA at various temperatures. FOSA = Flaxseed oil containing shrimp astaxanthin. *C'* is the initial concentration of astaxanthin; *C* is the concentration of astaxanthin at time *t*.

Table 2.8 Zero order kinetics of astaxanthin degradation in FOCA

Temperature (^{o}C)	$k \times 10^2$ (mg·100 g FOA^{-1}·h^{-1})	R^2	*Ea* (kJ/mol)
30	0.49±0.03^{c}	0.70	
40	1.16±0.25^{c}	0.88	104.65±2.33
50	4.56±0.48^{b}	0.89	
60	20.22±0.76^{a}	0.94	

Values are means and SD of three determinations. ^{abc}Means with different letters in each column are significantly different ($p < 0.05$). *k* = Degradation rate constant; *Ea* = Activation energy. FOCA = Flaxseed oil containing crawfish astaxanthin.

Table 2.9 Zero order kinetics of astaxanthin degradation in FOSA

Temperature (^{o}C)	$k \times 10^2$ (mg·100 g FOA^{-1}·h^{-1})	R^2	*Ea* (kJ/mol)
30	0.46±0.11^{c}	0.61	
40	1.13±0.21^{c}	0.83	84.53±4.08
50	4.93±0.45^{b}	0.88	
60	7.79±0.00^{a}	0.91	

Values are means and SD of three determinations. ^{abc}Means with different letters in each column are significantly different ($p < 0.05$). *k* = Degradation rate constant; *Ea* = Activation energy. FOSA = Flaxseed oil containing shrimp astaxanthin.

Table 2.10 First order kinetics of astaxanthin degradation in FOCA

Temperature (°C)	$k \times 10^2$ (h^{-1})	R^2	*Ea* (kJ/mol)
30	0.22±0.02[c]	0.85	
40	0.50±0.11[c]	0.95	96.79±1.37
50	1.93±0.21[bc]	0.97	
60	6.49±0.30[a]	0.95	

Values are means and SD of three determinations. [abc]Means with different letters in each column are significantly different ($p < 0.05$). *k* = Degradation rate constant; *Ea* = Activation energy. FOCA = Flaxseed oil containing crawfish astaxanthin.

Table 2.11 First order kinetics of astaxanthin degradation in FOSA

Temperature (°C)	$k \times 10^2$ (h^{-1})	R^2	*Ea* (kJ/mol)
30	0.21±0.05[d]	0.85	
40	0.58±0.19[cd]	0.91	88.44±5.00
50	2.16±0.21[bc]	0.95	
60	4.14±0.97[a]	0.98	

Values are means and SD of three determinations. [abcd]Means with different letters in each column are significantly different ($p < 0.05$). *k* = Degradation rate constant; *Ea* = Activation energy. FOSA = Flaxseed oil containing shrimp astaxanthin.

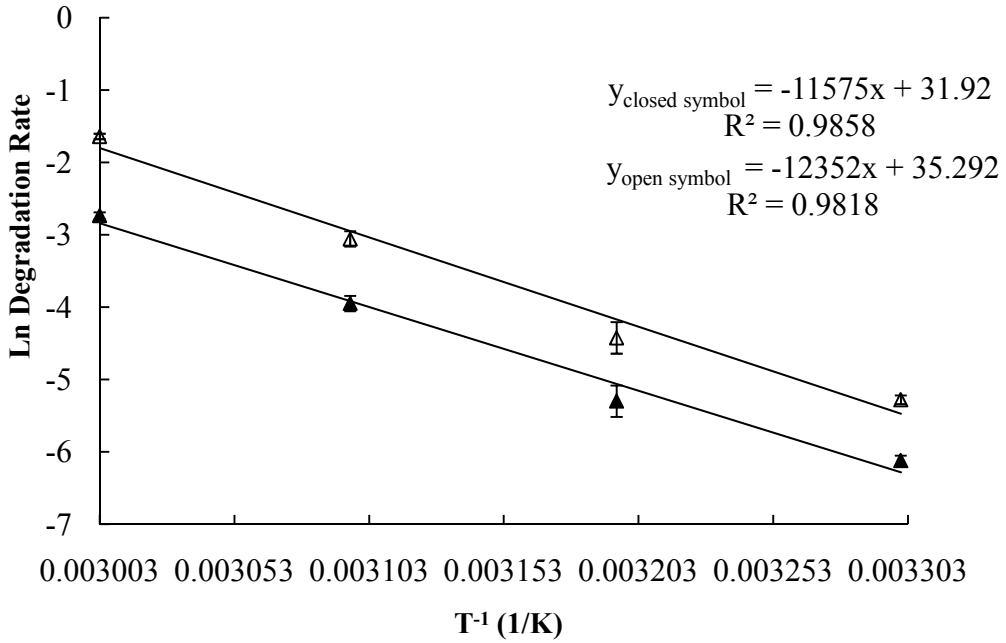

Figure 2.12 The Arrhenius plot for the astaxanthin degradation of FOCA. FOCA = Flaxseed oil containing crawfish astaxanthin. Open symbols represent degradation rates calculated from zero order kinetics; closed symbols represent degradation rates calculated from first order kinetics. Data are the average of three replicates.

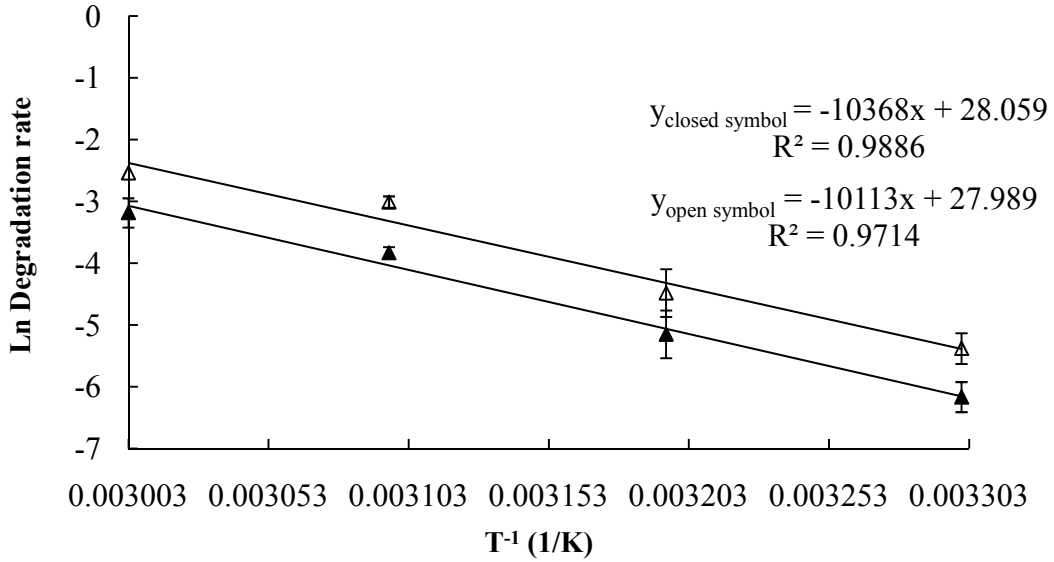

Figure 2.13 The Arrhenius plot for the astaxanthin degradation of FOSA. FOSA = Flaxseed oil containing shrimp astaxanthin. Open symbols represent degradation rates calculated from zero order kinetics; closed symbols represent degradation rates calculated from first order kinetics. Data are the average of three replicates.

2.4 Conclusions

The amount of extractable astaxanthin in crawfish and shrimp waste using FO was 3.02 mg / 100 g of crawfish waste and 4.83 mg/100 g of shrimp waste, respectively. The FOCA and FOSA had higher redness and lower lightness than FO. FOCA and FOSA showed minimal lipid oxidation at 30 ^{o}C with increasing time, whereas FO had a higher oxidation at 30-60 ^{o}C than FOCA and FOSA with increasing heating time from 0 to 4 hr. Collectively, the latter results demonstrated that astaxanthin could effectively reduce lipid oxidation in FO when it is heated from 30 to 60 ^{o}C. The degradation of astaxanthin during heating could be described by first order reaction kinetics. Astaxanthin was stable in FOCA and FOSA at 30 and 40 ^{o}C, but had substantial degradation at 50 and 60 ^{o}C. Byproducts generated from crawfish and shrimp peeling operations are a good source of high quality astaxanthin, which can be used as a natural colorant and antioxidant ingredient in human food and industrial applications.

CHAPTER 3 DEVELOPING MICROENCAPSULATED FLAXSEED OIL CONTAINING CRAWFISH AND SHRIMP ASTAXANTHIN

3.1 Introduction

Microencapsulation is an effective method to protect the stability of bioactive compounds from environmental factors by shielding the compounds from the environment with thin edible coating materials (Bustos and others 2003; Higuera-Ciapara and others 2004; Kagami and others 2003; Kolanowski and others 2006; Tan and others 2009; Sathivel and Kramer 2010). Several techniques, including spray drying, spray cooling, fluidized bed drying, extrusion, and centrifugal extrusion, can be used to produce microcapsules (Krishnan and others 2005). Spray drying is the most commonly used microencapsulation technology in food industries (Kagami and others 2003).

Astaxanthin has desirable bioactive properties for use in fortifying foods. However it is a highly unsaturated molecule which can degrade and lose its bioactive properties during processing and storage of the food product. Therefore, attempting to fortify foods with astaxanthin may lead to only limited success. Microencapsulation may make it possible to transform extracted astaxanthin in oil into a powdered form, wherein small droplets of oil containing astaxathin are surrounded and protected by a shell coating of proteins and/or carbohydrates. Astaxanthin in the microencapsulated form should allow fortification of foods without excessive degradation of the astaxanthin.

Astaxanthin is the main natural ketocarotenoid pigment responsible for the red orange color in crustacean and salmon flesh (Shahidi and Synowiecki 1991). This natural pigment

serves as a biological antioxidant with an antioxidant activity 10 times higher than other carotenoids such as zeaxanthin, lutein, canthaxantin, and β-carotene (Miki 1991). Examples of its effectiveness include: the supplementation of astaxanthin effectively suppressed carcinogenesis in mice urinary bladder tissue (Tanaka and others, 1994), it inhibited tumor growth in breast cancer (Jyonouchi and others 2000), and prevented oxidative stress (Tanaka and others 1995) and cardiovascular diseases (Snodderly 1995). Byproducts generated from shrimp and crawfish peeling operations are a good source of high quality astaxanthin which can be used as an antioxidant agent in flaxseed oil. Microencapsulated flaxseed oil containing astaxanthin powder has not been produced. There is a potential market for natural carotenoid-fortified foods. Natural carotenoids could be added to soft drinks, ice cream, desserts, candies, meat products and pet and aquaculture feeds (Delgado-Vargas and Paredes-Lopez 2003).

The objectives of this study were to: (1) develop microencapsulated flaxseed oil containing crawfish and shrimp astaxanthin powders using spray drying, (2) evaluate their oxidative stability, and (3) estimate the microencapsulated powder production efficiency and the energy required to produce microencapsulated flaxseed oil containing astaxanthin by spray drying.

3.2 Materials and Methods

3.2.1 Materials

Fresh crawfish and shrimp peeling byproducts containing cephalothoraxs, abdominal exoskeletons, and viscera were obtained from a local Louisiana seafood processor. Flaxseed

oil was purchased from iHerb Inc. (iHerb, Irwindale, CA). Lactose was purchased from Sigma-Aldrich, Co. (Sigma-Aldrich, Co, St. Louis, MO). Sodium caseinate was donated by American Casein Company (American Casein Company, Burlington, NJ). All other chemicals were purchased from Sigma Chemical Co. (Sigma Chemical Co., St. Louis, MO).

3.2.2 Extraction of Astaxanthin

Flaxseed oil (FO) containing crawfish astaxanthin (FOCA) or shrimp astaxanthin (FOSA) was prepared using a modified method of Sachindra and Mahendrakar (2005) as described in Figure 2.1. The thawed crawfish and shrimp byproducts were separately ground in a Hobart grinder (K5SS, Hobart Corporation, Troy, OH). One hundred grams of either the ground crawfish or shrimp byproducts was mixed with an equal volume of FO (iHerb, Irwindale, CA), stirred for 60 min at 60 ^{o}C, and then the mixture was centrifuged (Beckman J2-HC centrifuge, GMI, Inc., Ramsey, MN) at 8630 × *g* for 15 min at 4 ^{o}C. FOCA or FOSA and the water phase was separated from the solid phase and recovered. Then the FOCA or FOSA was separated from the water phase using a separatory funnel.

3.2.3 Preparation of Emulsions

Oil-in-water emulsions containing crawfish astaxanthin (ECA) or shrimp astaxanthin (ESA) were prepared for producing microencapsulated FOCA (MCA) and FOSA (MSA) powders using the modified method of Keogh and others (2001). The ratio (w/w) of the components used to prepare emulsions was 10 FOCA or FOSA: 10 sodium caseinate: 10 lactose: 70 water. The aqueous solution of the wall materials was prepared by dissolving sodium caseinate and lactose in distilled water at room temperature to allow complete

dissolution. The FOCA or FOSA was added into the aqueous phase, mixed and stirred for 5 min using a high-speed blender (IKA® Works, Inc., RW20, Wilmington, NC). The emulsions were then homogenized for 10 min using an ultrasonic processor. A Vibra cell Ultrasonic Processor, converter model CV33 equipped with a 13 mm probe (Sonics, Newtown, CT) was used at 80% amplitude with 2×1 s pulses (with 1 s delay between pulses). Samples were held in an ice bath during the procedure.

3.2.4 Characterization of Emulsions

3.2.4.1 Microstructure and Color of Emulsions

The microstructure of ECA or ESA was determined using a light microscope (Nikon Microphot-FXA, Nikon Instrument Inc., Japan). A drop of emulsion was observed at an objective magnification of 80x. Images of the structure for all emulsions were acquired using image processing software with a CCD camera. Color of ECA or ESA was measured using the method as described in 2.2.3.2.

3.2.4.2 Flow Behavior and Viscoelastic Properties

Flow behavior and viscoelastic properties of the emulsions were measured in triplicate using an AR 2000 Rheometer (TA Instrument, New Castle, DE) fitted with plate geometry. A steel plate with a 40-mm diameter was used and a 400 μm gap was set between the two plates. The shear stress was measured at 0, 15, and 25 ^{o}C at varying shear rates from 1 to 200 s^{-1}. The power law (Equation 3.1) was used to analyze the flow behavior index of emulsion samples.

$$\sigma = K\gamma^{n} \tag{3.1}$$

where σ = shear stress (Pa), γ = shear rate (s^{-1}), K = consistency index (Pa.s), and n = flow behavior index. The logarithms were taken on both sides of Equation 3.1, and a plot of log σ

versus log γ was constructed. The resulting straight line yielded the magnitude of log K (i.e., intercept) and n (i.e., slope).

Frequency sweep tests were conducted between 0.1 to10 Hz at a constant temperature of 25 ^{o}C. The storage modulus and loss modulus of emulsion samples were obtained using Universal Analysis (TA instrument) software and were calculated using Equations 3.2 and 3.3.

$$G' = \left[\frac{\sigma_0}{\gamma_0}\right]\cos\delta \tag{3.2}$$

$$G'' = \left[\frac{\sigma_0}{\gamma_0}\right]\sin\delta \tag{3.3}$$

where G' (Pa) is the storage modulus, G'' (Pa) is the loss modulus, σ is generated stress, and γ is oscillating strain.

3.2.5 Spray Drying

ECA or ESA was spray-dried under co-current drying conditions to produce microencapsulated flaxseed oil containing astaxanthin powders by a pilot plant scale spray dryer (FT 80 Tall Form Spray Dryer, Armfiled Inc., Jackson, NJ). The FT80 spray dryer includes inlet and outlet air fans, an electrical air heating chamber, a tall drying chamber, and a cyclone separator. The temperature, relative humidity, and air velocity of ambient air were measured using an Omega 4-in-1 multifunctional anemometer (Omega Engineering, Stamford, CT). The ambient air was blown into the air heating chamber by the inlet fan where the ambient air was heated by an electric resistance heater. The heated air (inlet air) was blown into the top of the drying chamber. The emulsion's temperature was measured and the emulsion was fed through the hygienic progressing cavity pump to a spray nozzle where it was

atomized and sprayed into the drying chamber. The emulsion droplets were dried in the drying chamber yielding dried powder (the microcapsules) and dust. The dried powder, dust, and air were pulled to the bottom of the drying chamber and then to the cyclone separator by the exhaust fan. The powder and dust were separated in the cyclone separator. The powder separated by the cyclone separator was collected in the cyclone collection vessel and the exhaust air was expelled through filter bag to the atmosphere. The internal diameter of ambient air intake pipe and exhaust air pipe, exhaust (outlet) air temperature, and outlet air velocity were measured. The relative humidity and exhaust air temperature that passed through exhaust fan were recorded. The emulsion, powder, and dust were analyzed for moisture content. The powder production rate was estimated and compared with the actual powder production rate. The mass flow rate for water entering and leaving the spray dryer and the energy required to dry the emulsion in the production of microencapsulated powder were determined.

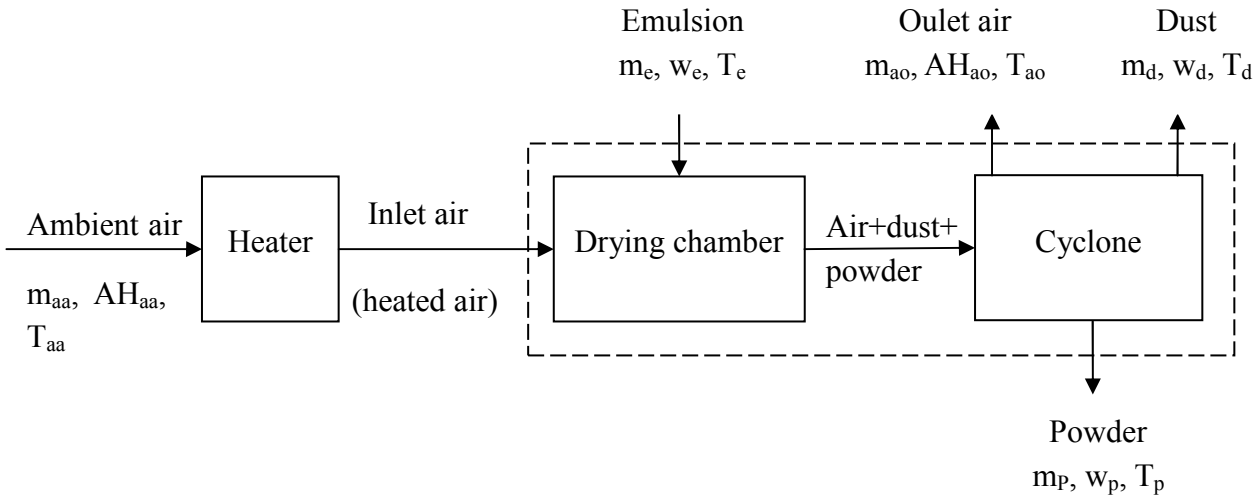

Figure 3.1 Mass balance for a spray drying process

3.2.5.1 Estimation of Production Rate of Microencapsulated Astaxanthin Powders

The overall mass flow rate on dry solids entering and leaving the spray dryer (Figure 3.1) was expressed by Equation 3.4.

$$m_e = mP + m_d \tag{3.4}$$

mP is the estimated powder production rate which included both the actual production flow rate (m_p) for the powder collected through cyclone vessel and product retained in the spray dryer. Physical properties of product retained in the spray dryer were assumed to be the same as the powder product collected in cyclone collection vessel.

The estimated production rate was obtained by the Equation 3.5.

$$mP = m_e - m_d \tag{3.5}$$

where m_e is emulsion flow rate (kg dry solids/h); m_d is dust flow rate (kg dry solids/h); mP is the estimated production rate (m_p) for the powder collected through cyclone vessel and product stored on the chambers, pipes, and joints and chambers walls.

3.2.5.2 Estimation of Evaporation Rate

An overall balance on water entering and leaving the spray dryer was expressed as Equation 3.6.

$$m_{aa}AH_{aa} + m_e w_e = m_{ao}AH_{ao} + m_d w_d + mPw_p \tag{3.6}$$

where m_{aa} is the dry air mass flow rate of inlet ambient air (kg dry air/h); m_{ao} is the dry air mass flow rate of outlet air (kg dry air/h); m_e is the mass flow rate of emulsion (kg dry solids/h); m_d is the mass flow rate of dust (kg dry solids/h); mP included both the product flow rate (m_p) for the powder collected through cyclone vessel and product retained in the spray dryer; AH_{aa} is the absolute humidity of inlet ambient air (kg water/kg dry air); AH_{ao} is the absolute humidity

of outlet air (kg water/kg dry air); w_e is the moisture content of dry basis of emulsion (kg water/kg dry solids); w_d is the moisture content of dry basis of dust (kg water/kg dry solids); w_p is the moisture content of dry basis of product (kg water/kg dry solids).

The evaporation rate (E_{va}) was calculated from the moisture uptake by the dry air as described by Equation 3.7.

$$E_{va} = m_{ao}AH_{ao} - m_{aa}AH_{aa} \tag{3.7}$$

The evaporation rate (E_{vp}) was also calculated based on the moisture content of the emulsion, powder collected through cyclone vessel and dust using Equation 3.8.

$$E_{vp} = m_e w_e - m_d w_d - mPw_p \tag{3.8}$$

The dry air mass flow rate of inlet ambient air and dry air mass flow rate of outlet air were calculated using Equation 3.9 as described by the AIChE Equipment Testing Procedure (2003).

$$m = \frac{V}{V'} \tag{3.9}$$

where m is the dry air mass flow rate (kg dry air/h); V is the volumetric flow rate of inlet or outlet air (m^3/s); V' is the specific volume of inlet or outlet air (m^3/kg dry air).

The volumetric flow rate of inlet ambient air and outlet air was calculated as described by Equation 3.10.

$$V = v \times A \tag{3.10}$$

where v is the average velocity of the inlet or outlet air (m/s); A is the cross sectional area of the inlet or outlet air pipe (m^2).

The specific volume of inlet ambient air and outlet air were calculated using Equation 3.11 as described by Singh and Heldman (2001).

$$V' = (0.082T + 22.4)(\frac{1}{29} + \frac{AH}{18}) \quad (3.11)$$

where T is the temperature of inlet ambient or outlet air (^{o}C); AH is the absolute humidity of inlet ambient or outlet air (kg water/kg dry air).

The absolute humidity of inlet ambient and outlet air were calculated as Equation 3.12 as described by AIChE Equipment Testing Procedure (2003).

$$AH = 0.622 \times \frac{p_w}{101.325 - p_w} \quad (3.12)$$

where AH is the absolute humidity of the inlet ambient or outlet air (kg water/kg dry air); p_w is the partial pressure exerted by water vapor (kPa).

The partial pressure exerted by water vapor pressure is calculated with Equation 3.13 as described by Singh and Heldman (2001).

$$p_w = p_v \times RH \quad (3.13)$$

where p_w is the partial pressure exerted by water vapor (kPa); p_v is the saturation pressure of water vapor (kPa); RH is the relative humidity (%).

3.2.5.3 Estimation of Energy Required to Dry the Emulsions

The energy required to heat the inlet ambient air was calculated using Equation 3.14 as described by Singh and Heldman (2001).

$$Q = m_{aa} c_p \Delta T = m_{aa} (c_{aa} + c_v AH_{aa})(T_{ad} - T_{aa}) \quad (3.14)$$

where m_{aa} is dry air mass flow rate of inlet ambient air (kg dry air/h); c_p is specific heat of inlet ambient air (kJ/[kg K]); c_{aa} is specific heat of inlet ambient dry air; c_v is the specific heat of water vapor (kJ/[kg K]); AH_{aa} is the absolute humidity of inlet ambient air (kg water/kg dry air); ΔT is the temperature difference between inlet ambient air and heated air (K); T_{ad} is temperature of inlet drying air (K); and T_{aa} is temperature of inlet ambient air (K).

3.2.6 Determination of Microencapsulation Efficiency of Microencapsulated Astaxanthin Powders

The amounts of surface and total oil were determined to calculate the microencapsulation efficiency (ME) as described by Tan and others (2005) with a slight modification. Hexane (50 ml) was added to 5 g of powder followed by stirring for 10 min. The suspension was then filtered and the residue rinsed thrice by passing 20 ml of hexane through each time. The residual powder was then air dried for 30 min and weighed. The amount of surface oil (OS) was calculated by the difference in weights of the microspheres.

OS = Original weight - Final weight of microspheres (3.15)

The total oil (OT), which included both the encapsulated oil (OE) and OS, was determined using the method described by Shahidi and Wanasundara (1995). Five gram of powder was dispersed in 25 ml of a 0.88% (w/v) KCl solution. Then 50 ml of chloroform, 25 ml of methanol and a few crystals of tert-butylhydroquinone (TBHQ) were added. The mixture was then homogenized using a high speed mixer for 5 min at 8000 rpm. The mixture was transferred to a separatory funnel and the chloroform layer was separated and then evaporated using a rotary evaporator at 60 ^{o}C to recover the oil.

The OE and the ME was calculated as described Equations 3.16 and 3.17, respectively.

OE = OT – OS (3.16)

$$ME = OE/OT \times 100\% \quad (3.17)$$

3.2.7 Determination of Astaxanthin Content of Microencapsulated Astaxanthin Powders

Astaxanthin content in microencapsulated astaxanthin powders was determined using the method described by Rodriguez-Huezo and others (2004) with slight modification. A 0.5 g sample of powder was dissolved in 5 mL of NaCl-methanol solution (prepared by mixing equal volumes of 10% NaCl and methanol) followed by vortexing for 5 min, after which 30 mL of hexane-acetone solution (prepared by mixing equal volumes of 100% hexane and 100% acetone) were added. Then the mixture was centrifuged at 3840 × *g* for 10 min at 10 °C. Absorbance of the supernatant was measured at 460 nm in quartz cuvette. The amount of astaxanthin in the powder sample was calculated using the following equation (Britton and others 1995):

$$\text{Astaxanthin (g)} = Av/A_{1\,cm}^{1\%} \cdot 100 \quad (3.18)$$

where *v* is the volume of solution, A is the absorbance value, $A_{1cm}^{1\%}$ is the specific absorption coefficient (2500) (Britton and others 1995).

3.2.8 Color of Microencapsulated Astaxanthin Powders

Color of microencapsulated astaxanthin powders was measured in triplicate using a LabScan® XE spectrophotometer (Hunter Associates Laboratory, INC. Resbon, VA) and was reported in CIELAB color scales (L*, a* and b* values). The instrument was standardized using the calibrated black and white standards that come with the instrument. Chroma and hue angle values were calculated using Equations 3.19 and 3.20, respectively.

$$\text{Chroma} = [a^{*2} + b^{*2}]^{1/2} \quad (3.19)$$

Hue angle = $\tan^{-1}$ (b*/a*) (3. 20)

3.2.9 Hydroperoxide of Microencapsulated Astaxanthin Powders

The hydroperoxide value of microencapsulated astaxanthin powders was measured according to the method of Boon and others (2008). A 0.5 g sample of microencapsulated powder was dispersed in 5 mL of distilled water. Then the dispersion was vortexed for 5 min to allow complete dispersion. A 0.3 mL aliquot of this dispersion was added into 1.5 mL of isooctane-2-propanal (3:1 v:v) solution and vortexed for 30 s. The organic phase was separated by centrifugation at 3400 × *g* for 2 min. Then, 100 μL of organic phase was mixed with 2.8 mL of methanol-1-butanol (2:1 v:v) followed by adding 15 μL of 3.94 M thiocyanate solution and 15μL of ferrous iron solution (prepared by mixing equal volumes of 0.144 M $FeSO_4 \cdot H_2O$ and 0.132 M $BaCl_2$, centrifuged and collected the clear supernatant). The mixture was vortexed and allowed to react for 20 min at room temperature. The absorbance was measured at 510 nm using a spectrophotometer (Thermo Fisher Scientific, Vernon Hills, IL). Hydroperoxide content was determined using a cumene hydroperoxide standard curve.

3.2.10 TBA of Microencapsulated Astaxanthin Powders

TBA of microencapsulated astaxanthin powders was measured using a method of Klinkesorn and others (2005). TBA solution was prepared by mixing 15 g of trichloroacetic acid, 0.375 g of TBA, 1.76 mL of 12 N HCl, and 82.9 mL of H_2O. Every 100 mL of TBA solution was mixed with 3 mL of 2% butylated hydroxytoluene in ethanol. A 0.5 g sample of microencapsulated astaxanthin powder was dispersed in 5 mL of distilled water. Then 1 mL of this mixture was mixed with 2 mL of TBA solution and vortexed and placed in boiling water

for 15 min. After cooling to room temperature, the mixture was centrifuged at 3400 × g for 25 min and absorbance was measured at 532 nm. TBA content was determined using a standard curve of 1,1,3,3-tetraethoxypropane.

3.2.11 Fatty Acid Methyl Esters Profiles of Microencapsulated Astaxanthin Powders

Fatty acid methyl esters profiles of FOCA, and FOSA were determined by two laboratories as described below. FOCA and FOSA were extracted from MCA and MSA at the USDA-ARS Laboratory, University of Alaska Fairbanks, AK using the method as described in section 3.2.6. Fatty acid methyl esters (FAMEs) were prepared using a modified method of Maxwell and Marmer (1983). A 20 mg sample of FO or FOA was dissolved in 4.5 mL isooctane and 500 µL of internal standard (10 mg methyl tricosanoate (23:0)/mL isooctane and 500 µL 2 N KOH (1.12 g/10mL MeOH) was added to the mixture. The mixture was vortexed for 1 min and centrifuged to the separate upper layer. The separated upper layer was mixed with 1 mL of saturated ammonium acetate solution and aqueous layer was removed and discarded. The mixture was centrifuged and the upper layer of the mixture was separated. Then 1 mL of distilled water was added to the separated upper layer and centrifuged, then 2-3 g anhydrous sodium sulfate was added, vortexed, and kept for 20-30 min. The mixture was centrifuged and the liquid containing methyl ester was separated. A 0.5 mL of isooctane containing methyl ester and 0.5 mL of isooctane were added to the amber GC vial. Gas chromatographic (GC) analysis was used with a GC model 7890A (Agilent) fitted with a HP-88 (100m x 0.25 mm ID x 0.25µm film) column. The oven program used was 90 °C for 8 min, followed by 10 °C/min to 175 °C for 10 min, 4 °C/min to

190 °C for 10 min, 5 °C/min to 210 °C for 5 min and then 20 °C/min to 250 °C for 8 min. ChemStation software was used to integrate peaks. Peaks were identified by comparing to reference standards obtained from Sigma: Supelco 37 mix. Data are expressed as percent of total integrated area.

Fatty acid methyl esters (FAMEs) were prepared at the laboratory of the W. A. Callegari Environmental Center, Louisiana State University, LA using the method described by Paquot and others (1987) with slight modification. A 25 mg sample of FO, FOCA or FOSA was dissolved in 10 mL of hexane. Then 10 µL of 2 N KOH (1.12 g/10 mL MeOH) was added to the mixture followed by vortexing for 1 min and this step was repeated for four times. Then 10 µL of 1 N H_2SO_4 was added to the mixture followed by vortexing for 1 min and centrifuging for 2 min at 3400 rpm to separate the upper layer. Then 5 µL of clear supernatant containing methyl esters was transferred to an auto sampler vial. Then 5 µL of internal standard (Hexadecanoic acid, 2-hydroxy-methyles dissolved in palmitate at 4 ppm concentration) and 1 mL of hexane was added to vial. The gas chromatographic (GC) analysis was used with a GC model 450-GC (Varian, Inc., Palo Alto, CA) fitted with a MF-28-12-1 (30 m x 0.25 mm ID x 0.25 µm film) column. The oven program used was 100 °C for 2 min, followed by 12 °C/min ramp to 255 °C and hold for 8 min. MS WorkStation software was used to integrate peaks. Data are expressed as percent of total integrated area. The fatty acid methyl esters profiles obtained for FO, FOCA, and FOSA were averaged and reported.

3.2.12 Scanning Electronic Microscopy of Microencapsulated Astaxanthin Powders

The morphology of the microencapsulated astaxanthin powders were evaluated by scanning electronic microscopy (SEM) (JSM-6610LV, JEOL Ltd., Japan) using an acceleration voltage of 5 kV. The samples were mounted on aluminum SEM stubs, coated with gold: palladium (60:40) in an Edwards S150 sputter coater (Edwards High Vacuum International, Wilmington, MA) and imaged with SEM.

3.2.13 Storage Stability of Microencapsulated Astaxanthin Powders

Amber bottles containing spray-dried microencapsulated astaxanthin powders were stored in a refrigerator at 5 ^{o}C and environment chambers at 25 ^{o}C and 40 ^{o}C. The powder samples were withdrawn periodically and analyzed for color, hydroperoxide, TBA, and astaxanthin content.

A first order (Equation 3.21) kinetics model was used to describe the astaxanthin degradation according to Niamnuy and others (2008).

$$C = C'\exp(-kt) \tag{3.21}$$

where *C'* is the initial concentration (μg·g powder^{-1}) of astaxanthin; *C* is the concentration (μg·g powder^{-1}) of astaxanthin at time *t*; *k* is the degradation rate constant (day^{-1}); *t* is the storage time (day).

The logarithms were taken on both sides of Equation 3.21.

$$\ln C = \ln C' - kt \tag{3.22}$$

The Equation (3.22) was rearranged as Equation 3.23.

$$\ln\left(\frac{C}{C'}\right) = -kt \tag{3.23}$$

A plot of $\ln\left(\frac{C}{C'}\right)$ versus time t was constructed for 5, 25, and 40 ^{o}C to determine k values and correlation coefficients. The slope of the straight line and the correlation coefficient were obtained from the trend line of the plot. The k values for the powder stored at 5, 25, and 40 ^{o}C were obtained from the resulted slope of the plot.

The effect of temperature on the degradation rate was described using the Arrhenius relationship as shown in Equation 3.24.

$$k = k_{\infty} \exp(-E_a / RT) \tag{3.24}$$

The logarithms were taken on both sides of Equation 3.24.

$$\ln k = \frac{-E_a}{RT} + \ln k_{\infty} \tag{3.25}$$

where k is the reaction rate constant; k_{∞} is the frequency factor; R is the universal gas constant (8.3145 J/mol K); T is the absolute temperature (K); and Ea is activation energy (J/mol). The resulting k values from first order models ($ln\ k$) versus $1/T$ were plotted and obtained activation energy for astaxanthin degradation using the Arrhenius model (Equation 3.24). The magnitude of Ea was calculated as the slope of the plot multiplied by the gas constant.

The color value a^* was correlated with astaxanthin concentration in microcapsules during storage time at different temperatures. A linear equation was used to describe the relation between a^* value and astaxanthin concentration:

$$a = k_1 c + k_2 \tag{3.26}$$

where a is the a^* value of microcapsules; c is the astaxanthin concentration (μg·g powder^{-1}); and k_1, k_2 are the regression coefficients.

3.2.14 Statistical Analysis

Mean values and standard deviations of triplicate determinations were reported. Analysis of variance (ANOVA) was carried out to determine the difference among treatments means (SAS Version 8.2, SAS Institute Inc., Cary, NC) using the *post hoc* Tukey's studentized range test.

3.3 Results and Discussion

3.3.1 Microstructure and Color of Emulsions

Microstructure of the ECA and ESA showed that both emulsions had a spherical shape (Figures 3.2 and 3.3), which ranged from 5 to 25 μm in size. L^* value is a measure of the lightness of ECA and ESA and a^* and b^* values are the measurement of redness and yellowness color of emulsions, respectively. Both ECA and ESA were light orange in color (Table 3.1). The color values of L^*, a^* and b^* values of ECA were 82.76±0.56, 10.89±0.20, and 21.15±0.33, respectively (Table 3.1), while L^*, a^*, and b^* values of ESA were 80.59±0.50, 12.8±0.17, and 22.28±0.37, respectively. Chroma is a measurement of the vividness of color (higher values indicate a more vivid color). Hue angle is defined as a color wheel with red at an angle 0^o and yellow at 90^o (Ergunes and Tarhan 2006). The chroma and hue angle values of ECA were 23.79±0.35 and 62.76±0.39, respectively (Table 3.1), while chroma and hue angle values of ESA were 25.9±0.4 and 70.37±0.1, respectively.

Table 3.1 Color values of ECA and ESA

	ECA	ESA
Color *L**	82.76±0.56	80.59±0.50
Color *a**	10.89±0.20	12.80±0.17
Color *b**	21.15±0.33	22.28±0.37
Chroma	23.79±0.35	25.90±0.40
Hue angle	62.76±0.39	70.37±0.10

Values are means and SD of triplicate determinations. ECA = emulsion containing crawfish astaxanthin; ESA = emulsion containing shrimp astaxanthin.

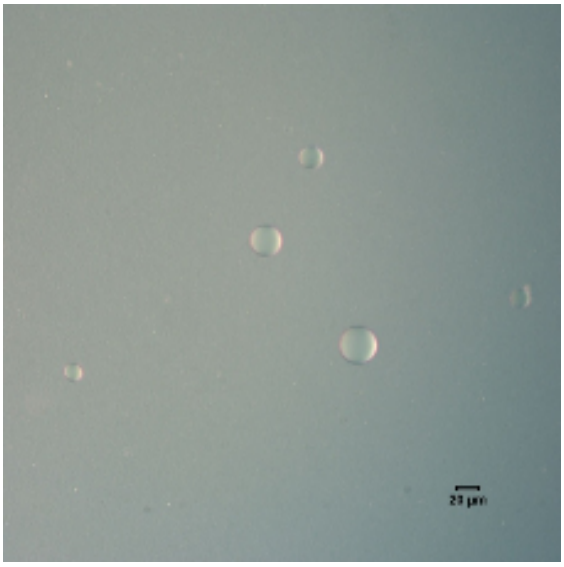

Figure 3.2 Light microscope of ECA
ECA = emulsion containing crawfish astaxanthin

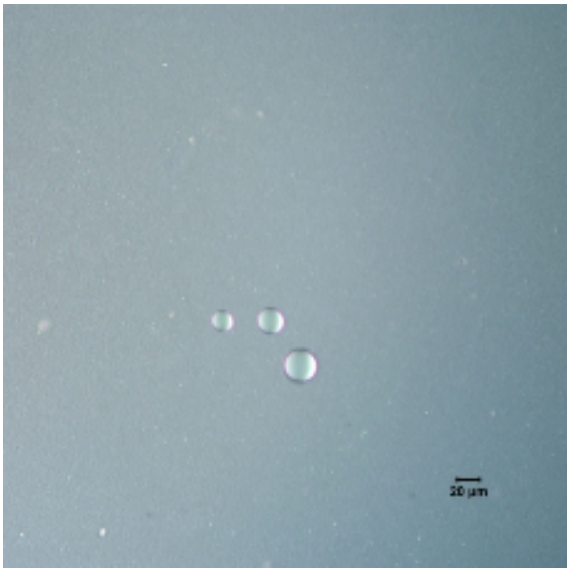

Figure 3.3 Light microscope of ESA
ESA = emulsion containing shrimp astaxanthin

3.3.2 Flow Behavior and Viscoelastic Properties of Emulsions

The flow index (*n*) for ECA and ESA were both less than 1.0 regardless of different temperatures (Tables 3.2 and 3.3) indicating that both the emulsions were pseudoplastic fluids (Batista and others 2006). The *n* values of ECA and ESA significantly increased with increased temperature. The *n* values ranged from 0.87±0.02 to 0.98±0.00 and 0.84±0.00 to 0.99±0.00 for ECA and ESA, respectively. The *K* values of ECA and ESA significantly increased with increased temperature. A higher *K* value of an emulsion indicates a more viscous consistency (Batista and others 2006). The apparent viscosities of ECA and ESA emulsions at 0, 15 and 25 ^{o}C are shown in Figures 3.4 and 3.5. Both ECA and ESA exhibited shear-thinning behavior at low shear rates at 0 ^{o}C, while shear-thinning behavior was not significant at 15 and 25 ^{o}C. Viscosity is modified by the feed temperature (Zakarian and King 1982; Zbicinski and others 2002; AIChE Equipment Testing Procedure 2003). It is important to know the changes of the viscosity because they alter the drying rate of the spray dryer.

Table 3.2 Flow behavior properties of ECA

Temperature (^{o}C)	ECA		
	n	*K (Pa.^{n})*	Apparent viscosity (Pa.s)
0	0.87±0.02^{c}	0.82±0.09^{a}	0.40±0.01^{a}
15	0.96±0.00^{b}	0.29±0.01^{b}	0.23±0.01^{b}
25	0.98±0.00^{a}	0.17±0.01^{c}	0.16±0.01^{c}

Values are means and SD of triplicate determinations. ^{abc}means with different letters in each column are significantly different ($p < 0.05$). ECA = emulsion containing crawfish astaxanthin; *n* = flow index; *K*= consistency index.

Table 3.3 Flow behavior properties of ESA

Temperature (°C)	ESA		
	n	*K (Pa.^{n})*	Apparent viscosity (Pa.s)
0	0.84±0.00^c	1.12±0.04^a	0.47±0.01^a
15	0.91±0.02^b	0.45±0.06^b	0.28±0.01^b
25	0.99±0.00^a	0.23±0.01^c	0.19±0.02^c

Values are means and SD of triplicate determinations. ^{abc}means with different letters in each column are significantly different ($p < 0.05$). ESA = emulsion containing shrimp astaxanthin; *n* = flow index; *K*= consistency index.

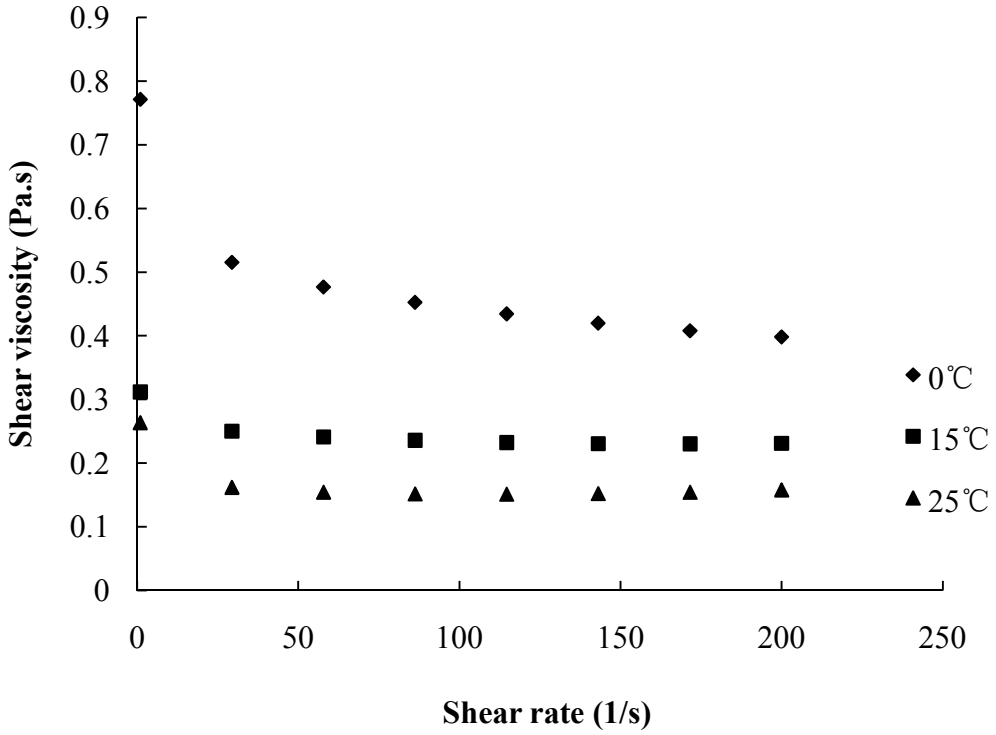

Figure 3.4 Apparent viscosity of ECA as a function of shear rate.
ECA = emulsion containing crawfish astaxanthin

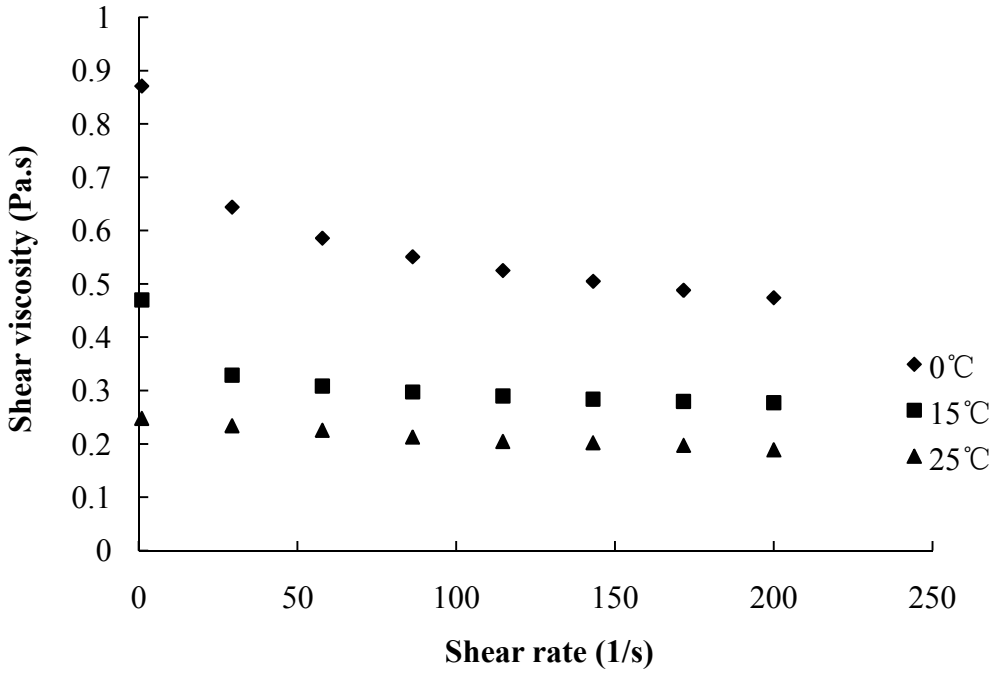

Figure 3.5 Apparent viscosity of ESA as a function of shear rate.
ESA = emulsion containing shrimp astaxanthin

Dynamic rheological tests can be used to characterize viscoelastic properties of emulsions. The G' (an elastic or storage modulus) and G" (a viscous or loss modulus) of the emulsions were determined as a function of frequency at a fixed temperature of 25 ^{o}C. G' is a measure of energy recovered per cycle of sinusoidal shear deformation and G" is an estimate of energy dissipated as heat per cycle (Rao 1999). The results of the frequency test are shown in Figures 3.6 and 3.7. Both G' and G" showed an increasing trend with the increase of angular frequency over the ranges examined in this study for ECA and ESA samples. G' was always larger than G" throughout the tested range of frequency for both ECA and ESA. Both emulsions behaved more like a viscoelastic material because it had a higher G' than G" which indicated that the they were stable (Moschakis and others 2005) and therefore stable microencapsulated flaxseed oil containing astaxanthin powders could be produced after spray drying the emulsions (Sathivel and Kramer 2010).

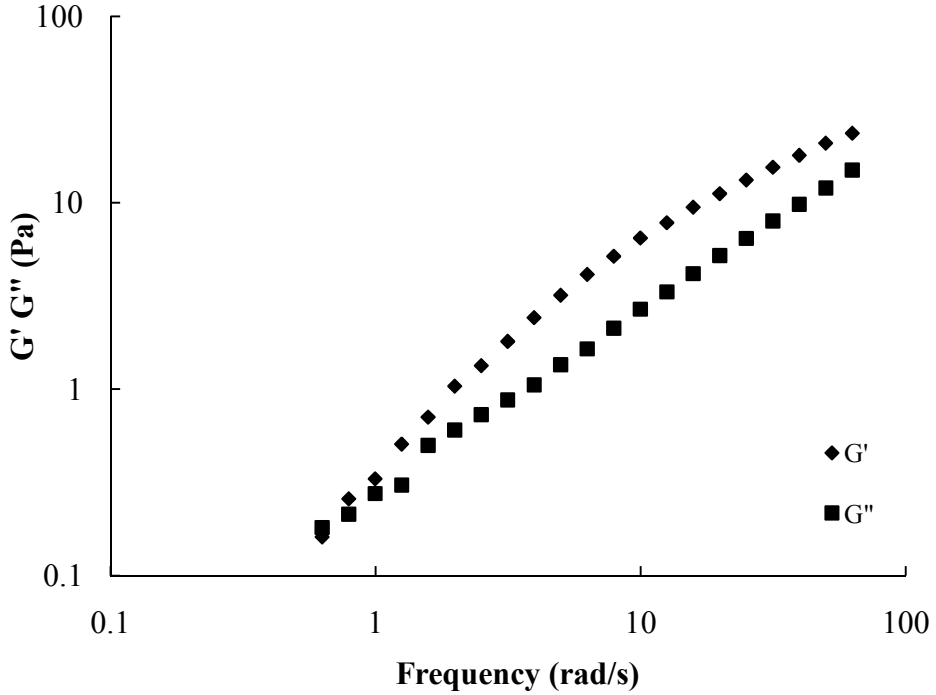

Figure 3.6 Viscoelastic properties of ECA.
ECA = Emulsion containing crawfish astaxanthin; G' = storage modulus; G" = loss modulus.

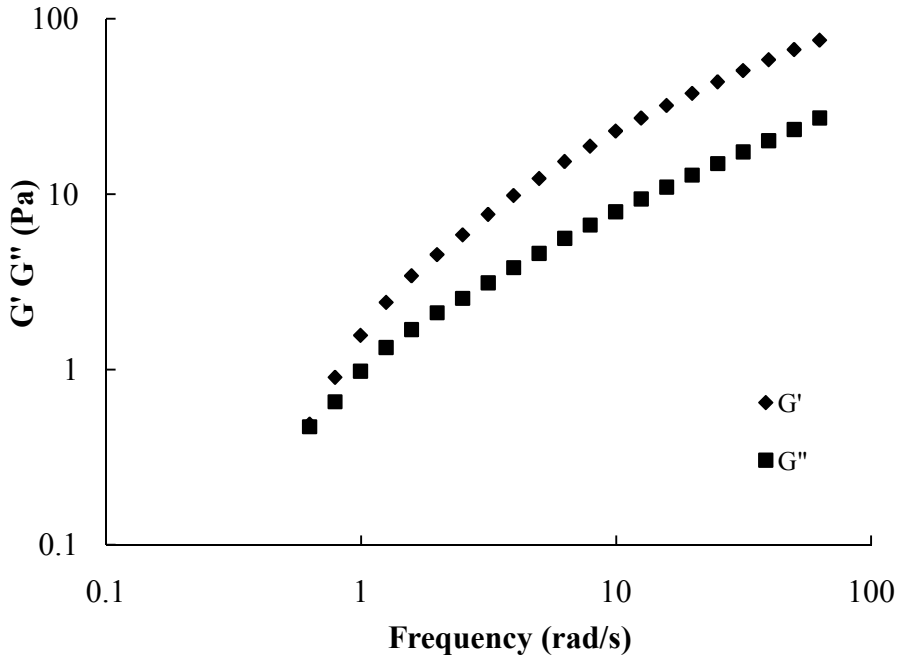

Figure 3.7 Viscoelastic properties of ESA.
ESA = Emulsion containing shrimp astaxanthin; G' = storage modulus; G" = loss modulus.

3.3.3 Spray Drying

Table 3.4 Summary calculation of the evaporation rate and energy required to spray dry ECA

	Inlet ambient air	Outlet air
Temperature (^oC)	26.27±1.63	82.93±0.92
Velocity (km/h)	61.12±2.40	14.78±2.38
Internal pipe diameter (m)	0.034	0.075
Volumetric flow rate inlet or outlet air (m^3/h)	55.47±2.17	65.28±10.58
Relative humidity (%)	58.44±3.11	5.2±0.20
Partial pressure exerted by water vapor (kPa)	2.00±0.11	2.79±0.11
Saturation pressure of water vapor (kPa)*	3.425	53.654
Absolute humidity × 10^3 (kg water/kg dry air)	12.54±0.68	17.61±0.70
Specific volume of inlet or outlet air (m^3/kg dry air)	0.864±0.01	1.035±0.01
Mass flow rate (kg dry air/h)	64.21±2.1	63.03±10.01
Specific heat of dry air at 26.27 ^oC (kJ/kg K)*	1.0126	—
Specific heat of water vapor at 26.27 ^oC (kJ/kg K)**	1.88	—
Evaporation rate (kg water/h)[1]	0.303±0.10[a]	
Evaporation rate (kg water/h)[2]	0.294±0.01[a]	
Energy required to spray dry ECA (kJ)	$1.022\times10^4 \pm 0.011\times10^4$	

*Obtained from appendix A 4.2 and A 4.4, respectively (Singh and Heldman 2001). **Selected as 1.88 kJ/(kg K) according to Singh and Heldman (2001). [1]Calculated based on moisture uptake by the dry air (kg water/h). [2]Calculated based on the moisture content of the emulsion, powder collected through cyclone vessel, and dust (kg water/h). [a]Means with same letter in each column are not significantly different ($p > 0.05$). ECA = emulsion containing flaxseed oil with crawfish astaxanthin.

Table 3.5 Mass and production flow rates for spray drying ECA

	ECA	MCA	Dust
Moisture content (wet basis, %)	70±1.79	6.24±0.36	6.60±0.44
Moisture content (dry basis, kg water/kg dry solids)	2.34±0.20	0.067±0.01	0.07±0.01
Mass flow rate × 10^3 (wet basis, kg/h)	433.33±15.28	104.33±9.71	3.23±0.91
Mass flow rate × 10^3 (dry basis, kg dry solids/h)	130.1±11.8	97.80±8.80	3.02±0.86
Estimated powder production rate × 10^3 (kg dry solids/h)		127.08±12.64	

Estimated powder production rate included both powder collected through cyclone vessel and product stored on the chambers, pipes, and joints and chambers walls. ECA = emulsion containing flaxseed oil with crawfish astaxanthin; MCA = microencapsulated flaxseed oil containing crawfish astaxanthin powder.

Table 3.6 Summary calculation of the evaporation rate and energy required to spray dry ESA

	Inlet ambient air	Outlet air
Temperature (^oC)	25.73±1.10	81.81±0.80
Velocity (km/h)	59.77±1.86	14.97±1.31
Internal pipe diameter (m)	0.034	0.075
Volumetric flow rate inlet or outlet air (m^3/h)	55.45±2.09	66.09±5.76
Relative humidity (%)	57.78±1.42	5.07±0.25
Partial pressure exerted by water vapor (kPa)	1.92±0.05	2.61±0.13
Saturation pressure of water vapor (kPa)*	3.32	51.566
Absolute humidity × 10^3 (kg water/kg dry air)	12.00±0.30	16.46±0.84
Specific volume of inlet or outlet air (m^3/kg dry air)	0.862±0.01	1.03±0.01
Mass flow rate (kg dry air/h)	64.36±2.37	64.14±5.68
Specific heat of dry air at 25.73 ^oC (kJ/kg K)*	1.0126	—
Specific heat of water vapor at 25.73 ^oC (kJ/kg K)**	1.88	—
Evaporation rate (kg water/h)[1]	0.286±0.12[a]	
Evaporation rate (kg water/h)[2]	0.29±0.01[a]	
Energy required to spray dry ESA (kJ)	$1.028\times10^4 \pm 0.048 \times10^4$	

*Obtained from appendix A 4.2 and A 4.4, respectively (Singh and Heldman 2001). **Selected as 1.88 kJ/(kg K) according to Singh and Heldman (2001). [1]Calculated based on moisture uptake by the dry air (kg water/h). [2]Calculated based on the moisture content of the emulsion, powder collected through cyclone vessel, and dust (kg water/h). [a]Means with same letter in each column are not significantly different ($p > 0.05$). ESA = emulsion containing flaxseed oil with shrimp astaxanthin.

Table 3.7 Mass and production flow rates for spray drying ESA

	ESA	MSA	Dust
Moisture content (wet basis, %)	69.66±1.25	6.04±0.41	6.43±0.34
Moisture content (dry basis, kg water/kg dry solids)	2.3±0.14	0.064±0.01	0.07±0.01
Mass flow rate × 10^3 (wet basis, kg/h)	428±12.53	100.67±8.5	4.17±0.25
Mass flow rate × 10^3 (dry basis, kg dry solids/h)	130.08±8.33	94.57±7.78	3.90±0.22
Estimated powder production rate × 10^3 (kg dry solids/h)		126.18±8.13	

Estimated powder production rate included both powder collected through cyclone vessel and product stored on the chambers, pipes, and joints and chambers walls. ESA = emulsion containing flaxseed oil with shrimp astaxanthin; MSA = microencapsulated flaxseed oil containing shrimp astaxanthin powder.

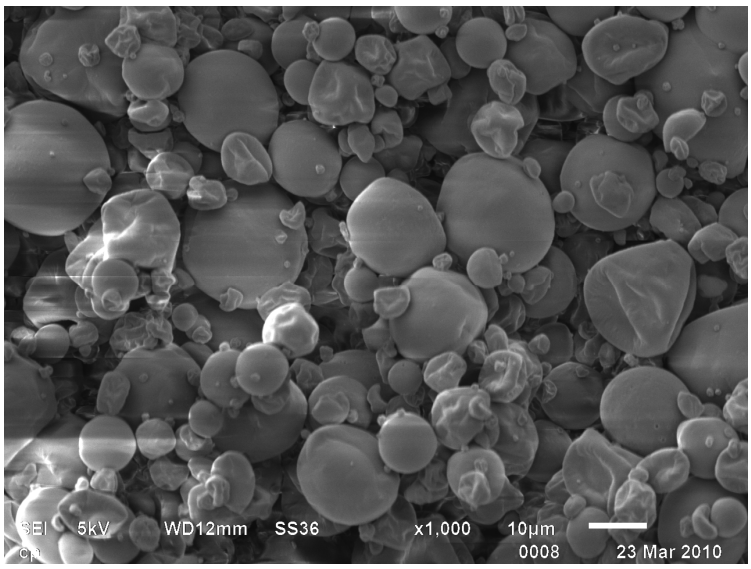

Figure 3.8 Scanning electronic microscopy of MCA. MCA = microencapsulated flaxseed oil containing crawfish astaxanthin.

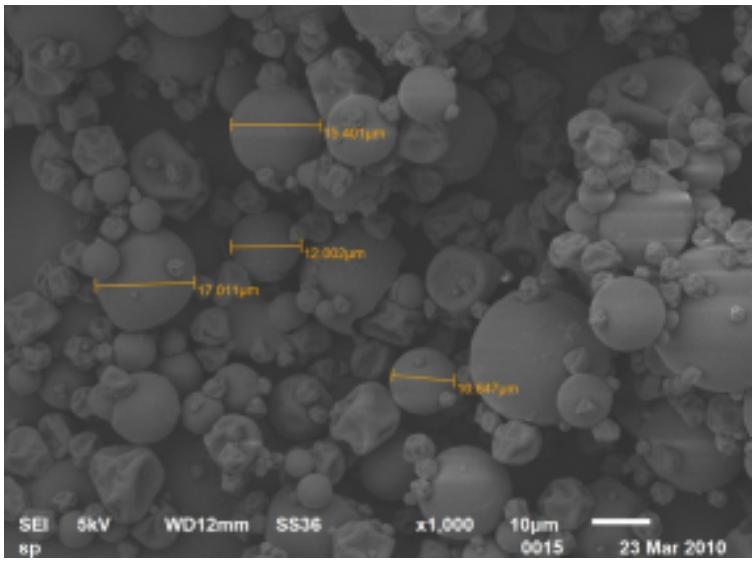

Figure 3.9 Scanning electronic microscopy of MSA. MSA = microencapsulated flaxseed oil containing shrimp astaxanthin.

The estimated production rates were 0.127 and 0.126 kg dry solids/h for MCA and MSA, respectively, while the actual production rates were 0.0978 and 0.0946 kg dry solids/h for MCA and MSA, respectively (Tables 3.5 and 3.7). As expected, the actual powder production rates were lower than estimated production rates, which might be due to powder particles were retained in chamber wall, pipes, and joints and chambers walls. Huang and

others (2006) reported that a large amount of powder can be deposited on the outlet pipe and chamber wall during spray drying. The evaporation rates calculated from moisture uptake by the dry air were 0.303 and 0.286 kg water/h for MCA and MSA, respectively (Tables 3.4 and 3.6), while the calculated evaporation rates based on the moisture content of the emulsion, product, and dust were 0.294 and 0.29 kg water/h, respectively (Tables 3.4 and 3.6). Temperature and humidity of the inlet dry air and feed rate directly affects the water evaporation from the powder during spray drying (Garg and others 2009; Gharsallaoui and others 2007). Low inlet air temperatures cause low evaporation rates and produce powder with high moisture contents, and agglomerated powder particles, while a high air inlet temperature causes excessive evaporation and produces low quality powders. A higher evaporation rate can result when the feed droplets pass through a lower humidity and/or higher temperature drying chamber (Huang and others 2006) and affect the particle size and produce smaller particles during spray drying. In this study, 2 μm to 20 μm particles of the MCA and MSA were produced at the evaporation rate of 0.303 and 0.286 kg water/h for MCA and MSA (Figures 3.8 and 3.9). Separated microencapsulated particles produced from the drying process indicated that the air inlet temperature used for the spray dryer and evaporation rates had not caused powder agglomeration.

A Similar shape of MCA and MSA morphology was reported for microencapsulated sunflower oil (Ahn and others 2008; Katona and others 2010). The shape and size of microcapsules depends on evaporation rate and several other factors including viscosity of emulsion, atomization, feed rate (Sathivel and Kramer 2010; Walton 2000; Kagami and others

2003); therefore, it is important to determine the factors such as evaporation rate, feed rate, viscosity of emulsion, and atomization pattern

Both inlet and outlet air flow had similar dry air mass flow rate, which evidenced that the technique, instrumentation and measurements used to measure air flow rates were accurate. The energy required to spray dry ECA and ESA were 1.022×10^4 and 1.028×10^4 kJ, respectively (Tables 3.4 and 3.6). The required power was determined as 2.84 and 2.86 kW for spray drying ECA and ESA, respectively, which were well within the available power of the electric heater (4.5 kW) of the FT80/81 Tall Form spray dryer (Spray dryer manual, Armfield, Ringwood, UK).

3.3.4 Surface Oil and Total Oil Content, Microencapsulation Efficiency, Lipid Oxidation, Astaxanthin, and Color of Microencapsulated Astaxanthin Powders

The OS for MCA and MSA were 0.04±0.00 and 0.05±0.00 g/g powder, respectively (Table 3.8). The surface oil expresses the amount of oil that is non-encapsulated and it is an important parameter determining the product quality because the non-encapsulated oil is prone to oxidize thus may lead to the development of off-flavors and affect the acceptability of the product (Drusch and Berg 2008). The OT indicates the total extractable oil of microcapsules which includes both surface oil and encapsulated oil. The OT for MCA and MSA were 0.32±0.00 and 0.33±0.01 g/g powder, respectively (Table 3.8). The ME for MCA and MSA were 86.06±1.44 % and 84.84±0.55 %, respectively, which indicated that most of the oil was encapsulated and less oil was on the surface of the microcapsules. Therefore, as expected, both microencapsulated astaxanthin powders had less hydroperoxides and TBA values (Table 3.8). The hydroperoxide values of MCA and MSA were 3.13±0.61

and 2.64±0.30 mmol/kg oil, respectively. The hydroperoxide values of MCA and MSA were lower than the reported value (15.2 meq/kg oil) for encapsulation of sunflower oil by Ahn and others (2008) and (8.2 mmol/kg oil) for encapsulated fish oil by Serfert and others (2009). The TBA values for MCA and MSA were 0.09±0.00 and 0.07±0.00 mmol/kg oil, respectively.

The astaxanthin concentration in MCA and MSA was 13.76±0.37 and 16.08±0.24 μg/g powder, respectively (Table 3.8). The MCA and MSA were light orange in color. The color values of *L*, a** and *b** values of MCA were 91.20±0.45, 5.37±0.25, 15.11±0.66, respectively (Table 3.8), while *L**, *a**, and *b** values of MSA were 92.71±0.44, 5.71±0.34, and 14.55±0.81, respectively. The chroma and hue angle values of MCA were 16.04±0.70 and 70.43±0.21, respectively (Table 3.8), while chroma and hue angle values of MSA were 15.63±0.87 and 68.57±0.20, respectively.

Table 3.8 Surface oil and total oil content, microencapsulation efficiency, hydroperoxide, TBA, astaxanthin, and color of MCA and MSA

	MCA	MSA
OS (g/g powder)	0.04±0.00	0.05±0.00
OT (g/g powder)	0.32±0.00	0.33±0.01
ME (%)	86.06±1.44	84.84±0.55
Hydroperoxide (mmol/kg oil)	3.13±0.61	2.64±0.30
TBA (mmol/kg oil)	0.09±0.00	0.07± 0.00
Astaxanthin (μg/g powder)	13.76±0.37	16.08±0.24
Color L*	91.20±0.45	92.71±0.44
Color a*	5.37±0.25	5.71±0.34
Color b*	15.11±0.66	14.55±0.81
Chroma	16.04±0.70	15.63±0.87
Hue angle	70.43±0.21	68.57±0.20

Values are means and SD of three determinations. MCA = microencapsulated flaxseed oil containing crawfish astaxanthin; MSA = microcapsulated flaxseed oil containing shrimp astaxanthin; OS = surface oil content; OT = total oil content; ME = microencapsulation efficiency.

3.3.5 Fatty Acid Methyl Esters Profile of Microencapsulated Astaxanthin Powders

Table 3.9 Fatty acid methyl esters profile of FOCA and MCA

Fatty acids (%)	FOCA	MCA
C16:0 Palmitic	5.66±0.39[a]	5.83±0.64[a]
C18:0 Stearic	4.00±0.68[a]	3.84±0.70[a]
C18:1n9c Oleic	17.36±0.25[a]	16.97±0.49[a]
C18:2n6c Linoleic	13.01±1.69[a]	13.73±1.05[a]
C18:3n3 Alpha-Linolenic	56.71±2.06[a]	56.32±2.88[a]
Total omega 3	56.71±2.06[a]	56.32±2.88[a]
Total omega 6	13.01±1.69[a]	13.73±1.05[a]
Saturates	11.42±2.92[a]	11.40±3.71[a]
Monounsaturates	17.9±0.38[a]	17.70±0.37[a]
Polyunsaturates	69.72±3.65[a]	70.04±3.93[a]
Omega 3/Omega 6	4.41±0.45[a]	4.11±0.11[a]
Polyunsaturates/Saturates	4.37±0.41[a]	4.15±0.10[a]
Total fatty acids	99.03±1.11[a]	99.14±0.60[a]

Values are means and SD of three determinations. [a]Means with same letter in each row are not significantly different ($p > 0.05$). FOCA = flaxseed oil containing crawfish astaxanthin; MCA = MCA = microencapsulated flaxseed oil containing crawfish astaxanthin. Only major fatty acids were reported.

Table 3.10 Fatty acid methyl esters profile of FOSA and MSA

Fatty acids (%)	FOSA	MSA
C16:0 Palmitic	5.32±0.40[a]	5.47±0.47[a]
C18:0 Stearic	4.27±0.94[a]	4.03±0.67[a]
C18:1n9c Oleic	16.06±1.13[a]	16.66±0.11[a]
C18:2n6c Linoleic	14.88±0.57[a]	13.72±0.92[b]
C18:3n3 Alpha-Linolenic	56.31±3.22[a]	55.47±2.84[a]
Total omega 3	56.31±3.22[a]	55.56±2.92[a]
Total omega 6	14.88±0.57[a]	13.72±0.92[b]
Saturates	11.55±3.41[a]	11.87±3.51[a]
Monounsaturates	16.47±1.56[a]	17.23±0.62[a]
Polyunsaturates	71.19±2.73[a]	69.28±3.68[a]
Omega 3/Omega 6	3.80±0.35[a]	4.06±0.18[a]
Polyunsaturates/Saturates	4.42±0.36[a]	4.23±0.17[a]
Total fatty acids	99.22±1.30[a]	98.37±0.78[a]

Values are means and SD of three determinations. [ab]Means with different letters in each row are significantly different ($p < 0.05$). FOSA = flaxseed oil containing shrimp astaxanthin; MSA = microencapsulated flaxseed oil containing shrimp astaxanthin. Only major fatty acids were reported.

The fatty acids methyl esters for FOCA, MCA, FOSA, and MSA obtained from both laboratories had similar fatty acids methyl esters profiles and they were summarized and reported in Tables 3.9 and 3.10. Alpha-linolenic acid (ALA) was the predominant fatty acid accounting for 56.71±2.06 % and 56.32±2.88 % for FOCA and MCA (Table 3.9), respectively. The ALA content in FOSA and MSA were 56.31±3.22 % and 55.56±2.92 %, respectively (Table 3.10). Both FOCA (69.72±3.65 %) and MCA (70.04±3.93 %) had high percentages of polyunsaturated fatty acids (Table 3.9). Similarly, both FOSA (71.19±2.73 %) and MSA (69.28±3.68 %) had high percentages of polyunsaturated fatty acids (Table 3.10). No significant difference in ALA content was observed either between FOCA and MCA or between FOSA and MSA, demonstrating that the spray drying had no significant effect on ALA content of FOCA and FOSA.

3.3.6 Storage Stability of Microencapsulated Astaxanthin Powders

The hydroperoxide values of MCA and MSA increased during storage regardless of storage temperatures (Figures 3.10 and 3.11). A more rapid increased in hydroperoxide content was observed for MCA and MSA during storage at 40 ^{o}C than those at 5 and 25 ^{o}C. The initial hydroperoxide value of MCA was 3.13±0.61 mmol/ kg oil and after storage at 40 ^{o}C for 26 days increased to 15.72±1.03 mmol/ kg oil. MCA and MSA samples stored at 5 ^{o}C had lower hydroperoxide values but they had the tendency to significantly increase with time (Figures 3.10 and 3.11). The hydroperoxide value of MSA increased from 2.64±0.3 to 14.84±0.61 mmol/ kg oil at 40 ^{o}C after 26 days, while it only increased from 2.64±0.3 to 10.50±0.59 mmol/ kg oil at 5 ^{o}C. A similar trend was observed for MCA. The

hydroperoxide value of MCA increased from 3.13±0.61 to 15.72±1.03 mmol/ kg oil at 40 ^{o}C and increased from 3.13±0.61 to 10.25±1.06 mmol/ kg oil at 5 ^{o}C. Kolanowski and others reported that the hydroperoxides of microencapsulated fish oil increased from 4.06 to 30 mmol/kg oil after 32 days storage at room temperature, while Serfert and others (2009) reported that the hydroperoxides value of microencapsulated fish oil increased from 20 to 80 mmol/kg oil after 56 days storage at 20 ^{o}C. Other previous studies have also reported similar lipid oxidation trends for microencapsulated oil powders during storage (Baik and others 2004; Klinkesorn and others 2005; Kagami and others 2003). Naz and others (2004) reported that lipid oxidation in edible oils occurs very slowly but it is accelerated when subjected to heat, air and light.

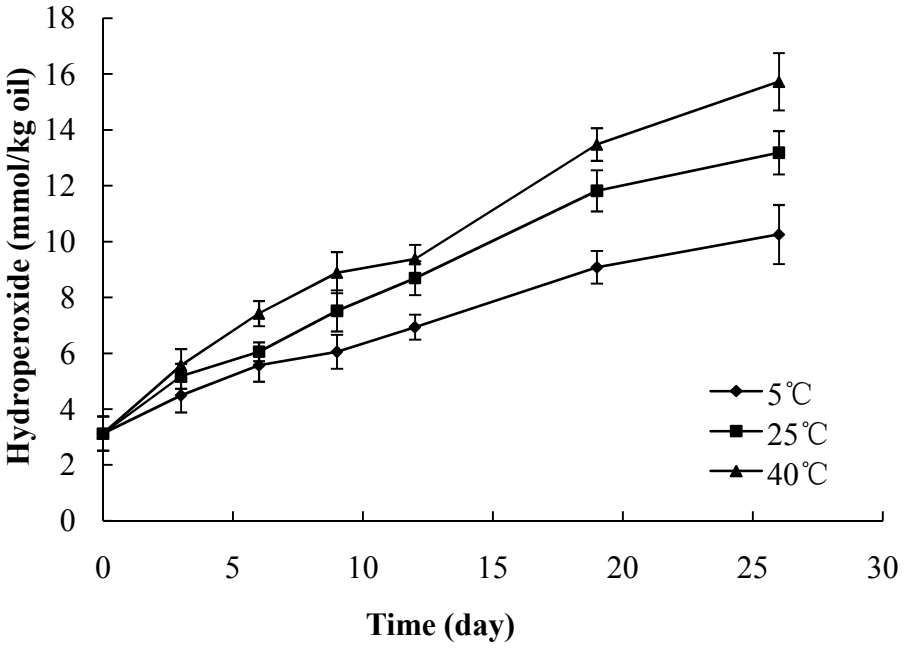

Figure 3.10 Formation of lipid hydroperoxides in MCA
MCA = microencapsulated flaxseed oil containing crawfish astaxanthin

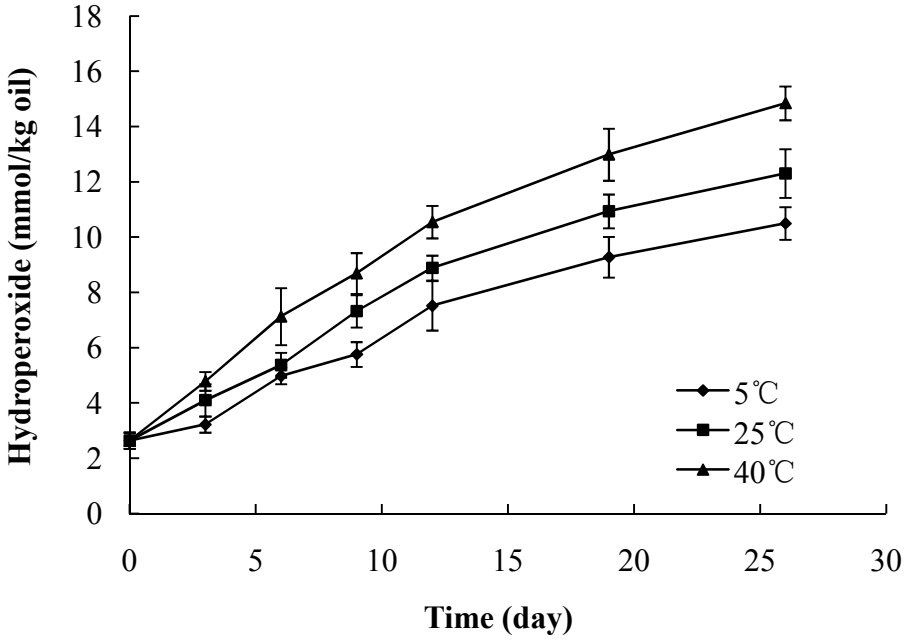

Figure 3.11 Formation of lipid hydroperoxides in MSA
MSA = microencapsulated flaxseed oil containing shrimp astaxanthin

The formation of TBA as a function of storage time and temperature in MCA and MSA are shown in Figures 3.12 and 3.13. TBA significantly increased during the storage period regardless of storage temperature. Several previous studies also reported that the formation of TBA in microencapsulated oil powders increased with increasing time and temperature (Baik and others 2004; Boon and others 2008; Klinkesorn and others 2005). The initial TBA of MCA and MSA were 0.087±0.00 and 0.074±0.00 mmol/kg oil, respectively. After 26-day storage at 5 ^{o}C, TBA of MCA and MSA increased to 0.16±0.01 and 0.14±0.01 mmol/kg oil, respectively. The TBA value increased to 0.27±0.01 and 0.22±0.01 mmol/kg oil for MCA and MSA respectively during storage at 40 ^{o}C. The microencapsulated astaxanthin powders stored at 40^{o}C had a higher TBA value than that stored at 5 ^{o}C.

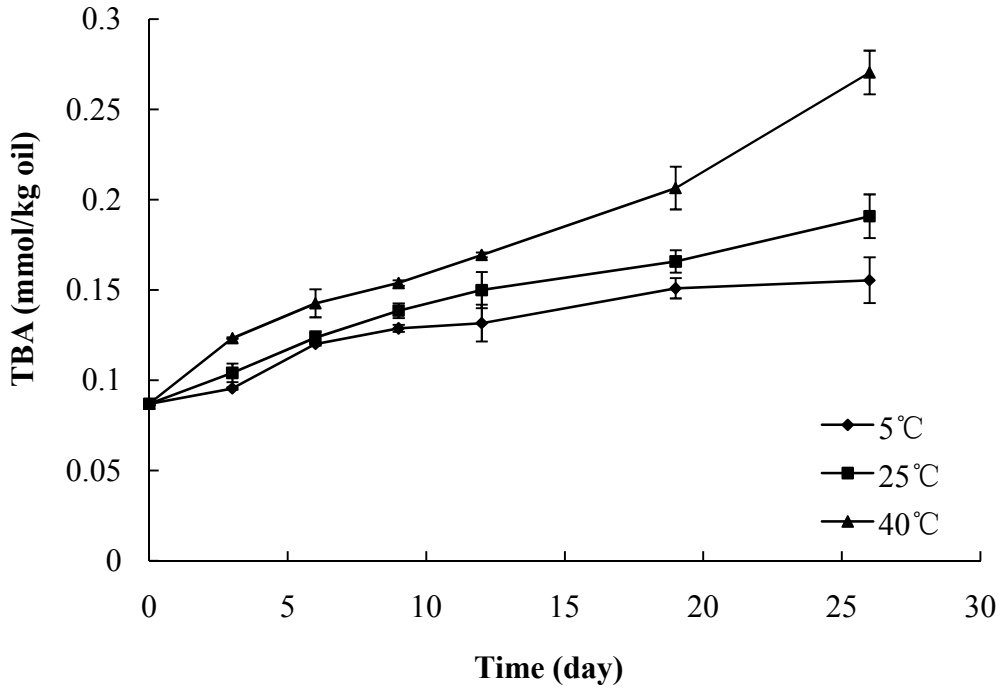

Figure 3.12 Formation of TBA in MCA
MCA = microencapsulated flaxseed oil containing crawfish astaxanthin

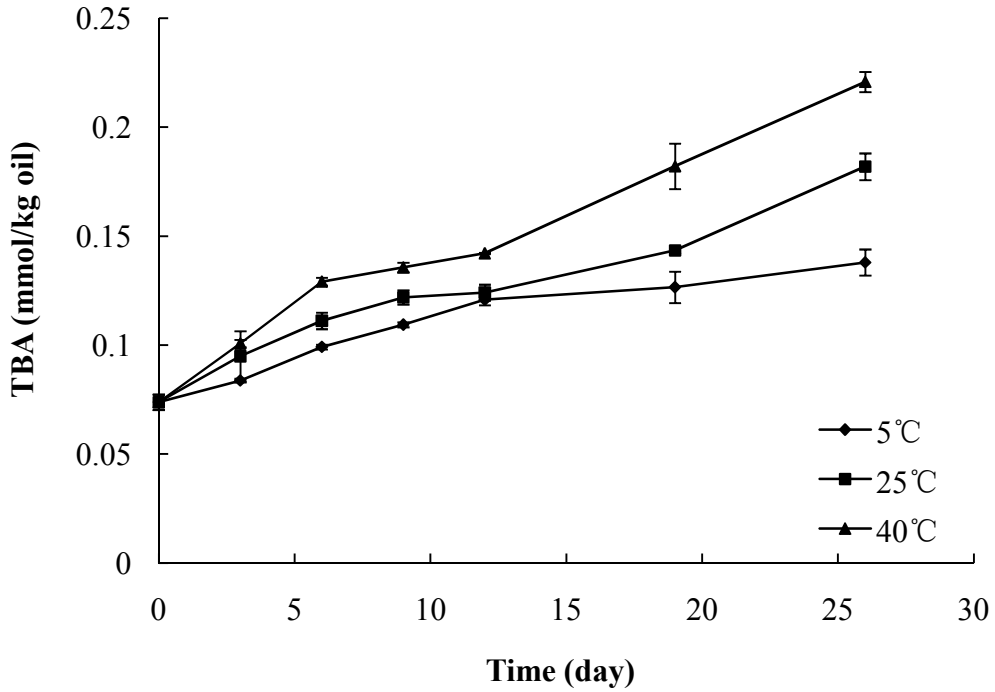

Figure 3.13 Formation of TBA in MSA
MSA = microencapsulated flaxseed oil containing shrimp astaxanthin

Astaxanthin is sensitive to heat, oxidation, and light because of its unsaturated structure thereby it gradually degrades during storage (Ribeiro and others 2005). Astaxanthin stability was evaluated on the basis of retained astaxanthin content in MCA and MSA during storage at 5, 25, and 40 ^{o}C. Figures 3.14 and 3.15 show the astaxanthin stability in MCA and MSA over storage at different temperatures. Astaxanthin concentration in MCA and MSA decreased with increased storage time and temperature. The initial astaxanthin concentration for MCA and MSA was 13.76±0.37 and 16.08±0.24 μg/g powder, respectively. After storage at 5, 25, and 40 ^{o}C for 26 days, the astaxanthin concentration in MCA decreased to 10.16±0.28, 8.28±0.55, and 6.48±0.24 μg/g powder, respectively. Similarly, the astaxanthin content in MSA decreased to 12.24±0.24, 10.88±0.60, and 9±0.36 μg/g powder at 5, 25, and 40 ^{o}C, respectively. Rodriguez-Huezo and others (2004) also reported a total carotenoids content in microcapsules degraded 50% after 25 days storage at 35 ^{o}C. Ribeiro and others (2005) reported that the astaxanthin degradation was approximately 60% of its initial concentration in an emulsion after 3 weeks of storage at 4 ^{o}C.

Astaxanthin degradation in MCA and MSA was modeled by first-order reaction kinetics. Table 3.11 shows the degradation rate constants (day^{-1}), and activation energy of MCA and MSA during storage. The high R^2 (Table 3.11) indicated that astaxanthin degradation in MCA and MSA could be well described by first-order reaction kinetics. Previous studies have reported that the degradation of astaxanthin follows a first-order kinetics reaction (Ahmed and others 2002; Niamnuy and others 2008; Rodriguez-Huezo and others 2004). The degradation rate constants (k) for MCA and MSA increased with increased storage temperature,

which indicated that astaxanthin degraded faster at a higher temperature than that of a lower temperature. The degradation rate constants (k) for MCA that was stored at 5, 25, and 40 ^{o}C were 1.33×10^{-2}, 2.16×10^{-2}, and 3.19×10^{-2} day^{-1}, respectively, whereas for MSA it was 1.18×10^{-2}, 1.71×10^{-2}, and 2.5×10^{-2} day^{-1}, respectively. Figure 3.16 shows the Arrhenius plot of ln (k) versus 1/T for astaxanthin degradation during storage. The astaxanthin degradation rate constants (k) in MCA and MSA were well described by the Arrhenius equation (Figure 3.16) with high R^2 (0.9716 and 0.9879 respectively) obtained. The activation energies of astaxanthin degradation in MCA and MSA were 15.65 and 13.73 kJ/mol respectively, which were lower than the previously reported activation energy (20.56 kJ/mol) for carotenoids degradation during heat treatment (Ahmed and others 2002).

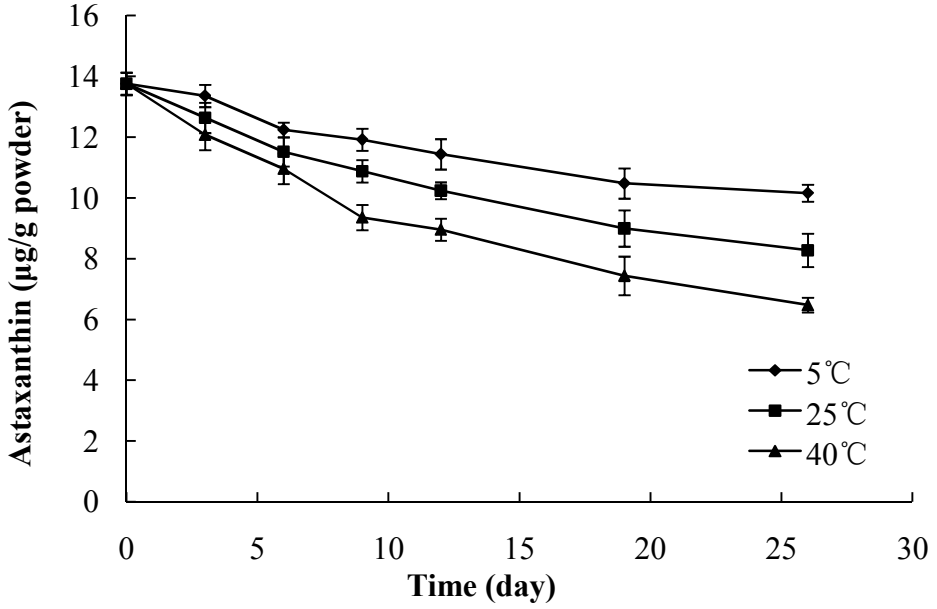

Figure 3.14 Degradation of astaxanthin in MCA during storage at 5, 25, and 40 ^{o}C
MCA = microencapsulated flaxseed oil containing crawfish astaxanthin

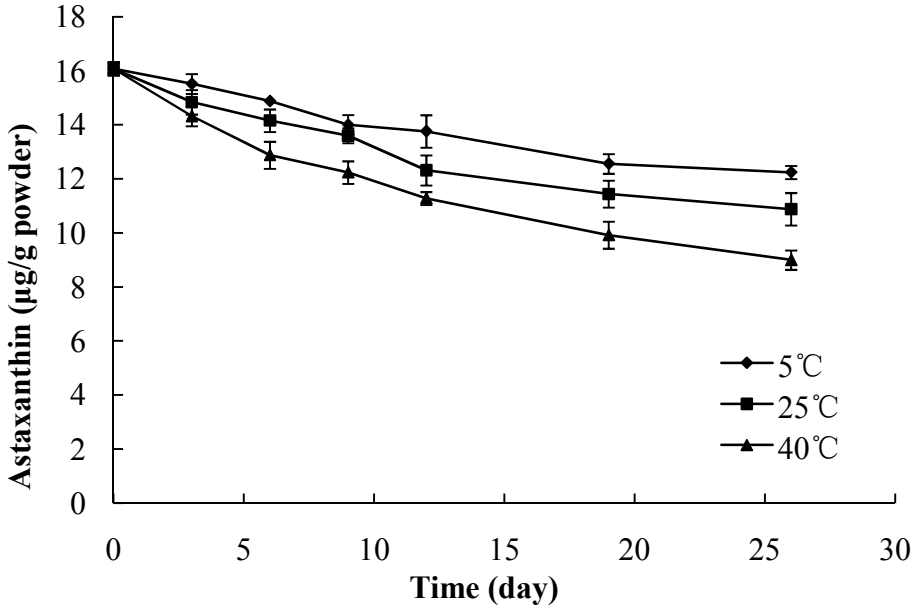

Figure 3.15 Degradation of astaxanthin in MSA during storage at 5, 25, and 40 ^{o}C
MSA = microencapsulated flaxseed oil containing shrimp astaxanthin

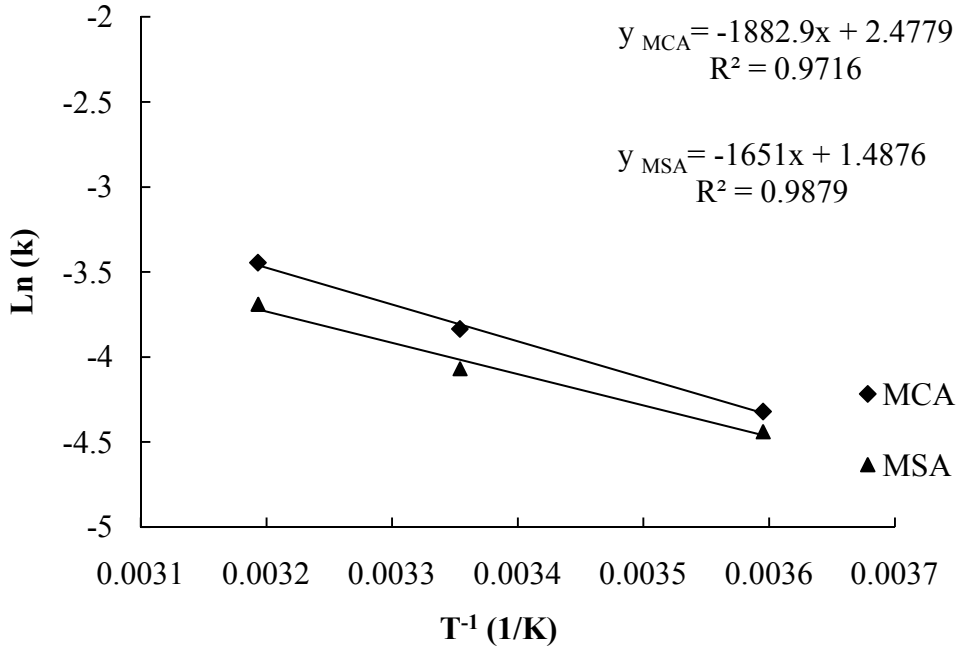

Figure 3.16 The Arrhenius plot for the astaxanthin degradation of MCA and MSA. MCA = microencapsulated flaxseed oil containing crawfish astaxanthin; MSA = microencapsulated flaxseed oil containing shrimp astaxanthin.

Table 3.11 Degradation rate equations, rate constants (day^{-1}), and activation energy of MCA and MSA

	Temperature (^oC)	First-order degradation	k (day^{-1})	R^2	Activation energy (kJ/mol)
MCA	5	C=13.76[-exp(0.0133)t]	1.33×10^{-2}	0.9373	
	25	C=13.76[-exp(0.0216)t]	2.16×10^{-2}	0.955	15.65
	40	C=13.76[-exp(0.0319)t]	3.19×10^{-2}	0.9525	
MSA	5	C=16.08[-exp(0.0118)t]	1.18×10^{-2}	0.9533	
	25	C=16.08[-exp(0.0171)t]	1.71×10^{-2}	0.9296	13.73
	40	C=16.08[-exp(0.025)t]	2.50×10^{-2}	0.9305	

k = Degradation rate constants; R^2 = Square of correlation coefficient; C = Astaxanthin concentration; MCA = Microencapsulated flaxseed oil containing crawfish astaxanthin; MSA = Microencapsulated flaxseed oil containing crawfish astaxanthin.

Figures 3.17 and 3.18 show the change of a* values of MCA and MSA during storage. Generally, a* value of MCA and MSA decreased with increased temperature and storage time. The initial a* values of MCA and MSA were 5.37±0.25 and 5.71±0.34, respectively. After 26 days storage, the a* value of MCA decreased to 4.98±0.08, 4.78±0.05, and 3.96±0.02 at 5, 25, and 40 ^oC, respectively. Similarly, it decreased to 5.33±0.08, 5.15±0.03, and 4.62±0.05 for MSA at 5, 25, and 40 ^oC, respectively. The red color of MCA and MSA are mainly attributed to the reddish-orange colored astaxanthin. The loss of astaxanthin in salmon muscle was highly correlated with the reduction in redness of the muscle and the loss of a* value in salmon muscle was very likely due to the loss of astaxanthin which is sensitive to photo-oxidation (Yagiz and others 2010). Ahmed and others (2002) reported that the Hunter (a*×b*) values correlated with pigment concentration in papaya puree during heat treatment. Similar results were also reported by McKenna and others (2003) that the decrease of a* and b* values of salmon fillets during irradiation was attributed to the degradation of carotenoids pigment. The

square of correlation coefficient (R^2) between astaxanthin concentration and a* value for MCA at 5, 25, and 40 ^oC were 0.92, 0.91, and 0.94, respectively, while it was 0.90, 0.92, and 0.96 for MSA. The high R^2 indicated that the relation between a* value and astaxanthin concentration could be well described by linear equations. Thus, the a* color value could be used to predict the astaxanthin concentration during processing or storage. Ahmed and others (2002) used visual color to correlate the carotenoid content during thermal processing of papaya puree.

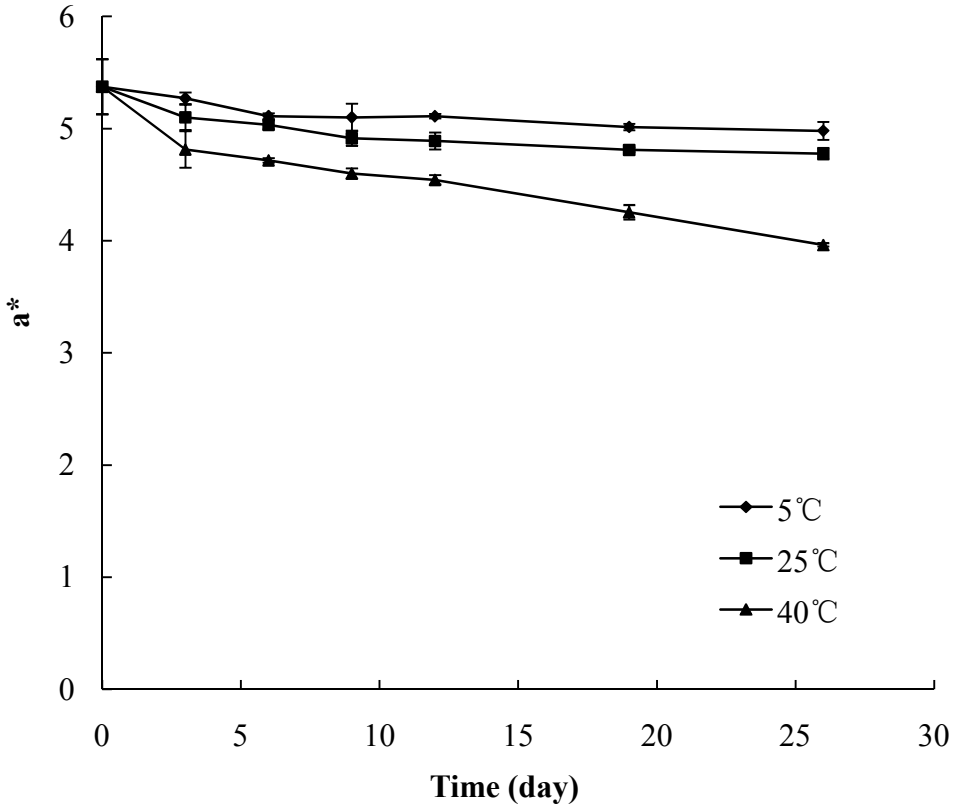

Figure 3.17 Changes in a* value of MCA during storage at 5, 25, and 40 ^oC
MCA = microencapsulated flaxseed oil containing crawfish astaxanthin

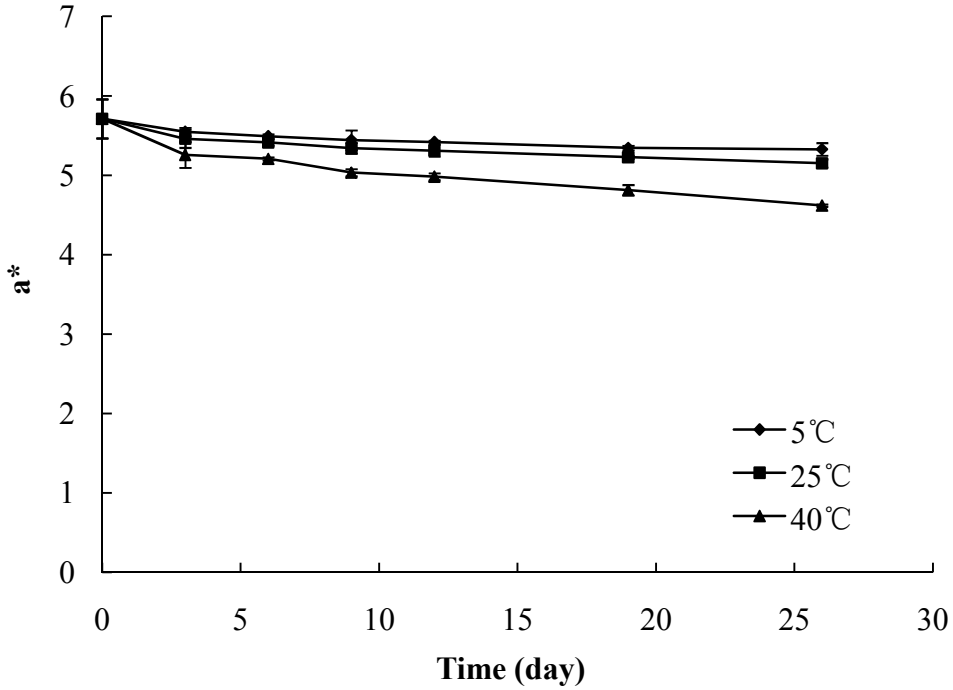

Figure 3.18 Changes in a* value of MSA during storage at 5, 25, and 40 °C
MSA = microencapsulated flaxseed oil containing shrimp astaxanthin

Table 3.12 Linear equation coefficients between a* value and astaxanthin concentration

	Temperature (°C)	Linear equation	k_1	k_2	R^2
MCA	5	a=0.099c+3.9579	0.099	3.9579	0.9234
	25	a=0.1015c+3.879	0.1015	3.879	0.9101
	40	a=0.1678c+2.9541	0.1678	2.9541	0.9427
MSA	5	a=0.099c+3.9579	0.0118	0.9533	0.9029
	25	a=0.0929c+4.1345	0.0929	4.1345	0.9194
	40	a=0.1397c+3.3782	0.1397	3.3782	0.9599

a = *a** value; c = Astaxanthin concentration; k_1, k_2 = Regression coefficients; r^2 = Square of correlation coefficient; MCA = Microencapsulated flaxseed oil containing crawfish astaxanthin; MSA = Microencapsulated flaxseed oil containing shrimp astaxanthin.

3.4 Conclusions

Homogeneous emulsions were prepared using FOCA and FOSA and the droplet size of the emulsions ranged from 5 to 25 μm. The emulsions made with FOCA and FOSA had viscoelastic properties with G' > G", which means that they exhibited solid behavior. Both

ECA and ESA showed pseudoplastic characteristics ($n < 1$). The energy required to spray dry ECA and ESA was 1.022×10^4 and 1.028×10^4 kJ, respectively. The MCA and MSA microcapsules were light red in color. Microencapsulation process did not affect the ALA content of flaxseed oil. The astaxanthin in MCA and MSA was more stable when powders were stored at 5 ^{o}C than when they were stored at 25^{o}C and 40^{o}C. Degradation of astaxanthin in MCA and MSA followed first-order reaction kinetics and could be well described by the Arrhenius equation. This study provided a method to prepare microencapsulated flaxseed oil containing astaxanthin, which facilitates the potential use of astaxanthin for food fortification and other functional properties.

CHAPTER 4 SUMMARY AND CONCLUSIONS

The seafood industry in Gulf of Mexico coastal and other seafood States in the United States of America discards millions of tons of seafood byproducts yearly. On average, 100 million pounds of waste generated from crawfish and shrimp peeling operations in Louisiana annually are discarded or used as aquaculture feed but with low economic value. Thus, disposal of these seafood byproducts are a growing environmental problem. The question is what to do with the crawfish and shrimp byproducts? Methods of utilizing crawfish and shrimp byproducts are needed to convert these byproducts into more marketable forms. Crawfish and shrimp waste are an excellent source of astaxanthin, which has high antioxidant and other functional properties. The recovery of astaxanthin components from the crawfish and shrimp byproducts waste will add new dollar value to the crawfish and shrimp industries. The goal of this study was to extract astaxanthin from crawfish and shrimp byproducts and to develop astaxanthin dry powders using microencapsulation technology. The specific objectives of this study were to: (1) extract astaxanthin from crawfish (*Procambarus clarkii*) and shrimp (*Litopenaeus setiferus*) byproducts using flaxseed oil, (2) study the oxidation rates and the astaxanthin degradation rates in the flaxseed oil, (3) develop microencapsulated flaxseed oil containing crawfish and shrimp astaxanthin powders using spray drying, (4) estimate the microencapsulated powder production efficiency and the energy required to produce microencapsulated flaxseed oil containing astaxanthin by spray drying.

The second chapter was devoted to extract astaxanthin from crawfish and shrimp byproducts using flaxseed oil and evaluate the lipid oxidation and astaxanthin degradation

rates. The total astaxanthin content in crawfish and shrimp byproducts was 8.84 mg/100 g wet crawfish waste and 6.47 mg/100 g wet shrimp byproducts, respectively. The amount of astaxanthin extracted from crawfish and shrimp byproducts using flaxseed oil was 3.02 mg / 100 g wet crawfish waste and 4.83 mg/100 g wet shrimp waste, respectively. When FOCA, and FOSA were heated to 30 ^{o}C, the both oils exhibited minimal lipid oxidation with increasing heating time, whereas FO, when heated to 40, 50, 60 ^{o}C, had a higher lipid oxidation rate than FOCA and FOSA with increasing heating time from 0 to 4 hr. This indicated that astaxanthin was an effective antioxidant agent in FO when it was heated from 30 to 60 ^{o}C. The rates of lipid oxidation for FO, FOCA, and FOSA could be well described by Arrhenius equation. The degradation of astaxanthin in FOCA and FOSA followed first order reaction kinetics. Astaxanthin was stable in FOCA and FOSA at 30 and 40 ^{o}C, but had substantial degradation at 50 and 60 ^{o}C. The degradation of astaxanthin during the heating could be described by first order reaction kinetics. This study demonstrated that extracted astaxanthin with FO from crawfish and shrimp byproducts can effectively reduce lipid oxidation in FO when it is heated from 30 to 60 ^{o}C.

In chapter three, microencapsulated flaxseed oil containing crawfish and shrimp astaxanthin powders were developed and analyzed for the storage stability of the powders. The microencapsulated powders production efficiency and the energy required to produce microencapsulated flaxseed oil containing astaxanthin powders by spray drying were determined. The energy required to spray dry 0.433 kg ECA and 0.428 kg ESA was 1.022×10^{4} and 1.028×10^{4} kJ, respectively. The actual product rate of MCA and MSA was

lower than the estimated production rate of MCA and MSA. The astaxanthin concentration of microencapsulated powders containing FOCA and FOSA was 13.76±0.37 and 16.08±0.24 μg/g powder, respectively. Alpha-linolenic acid (ALA) was the predominant fatty acid in MCA and MSA, which accounted for 56.32 and 55.47 %, respectively. The microencapsulation process did not affect the ALA content of flaxseed oil. The lipid oxidation of MCA and MSA was lower at 5 ^{o}C storage than those at 25 ^{o}C and 40 ^{o}C during 26 days storage. The astaxanthin in MCA and MSA was more stable when powders were stored at 5 ^{o}C than they stored at 25 ^{o}C and 40 ^{o}C. Degradation of astaxanthin in MCA and MSA fitted with first-order reaction kinetics model showed that the degradation rate constants for MCA and MSA increased with increased storage temperature, which indicated that astaxanthin degraded faster at a higher temperature than that at lower temperature. This study demonstrated that astaxanthin extracted from crawfish and shrimp byproducts using flaxseed oil can be microencapsulated using spray drying technology. Microencapsulation reduced the lipid oxidation and astaxanthin degradation. This study provided a method to extract astaxanthin from crawfish and shrimp byproducts using flaxseed oil and provided a method to prepare microencapsulated flaxseed oil containing astaxanthin. The research findings will help utilize crawfish and shrimp byproducts.

REFERENCES

Adegoke GO, Kumar MV, Krishna AGG, Varadaraj MC, Sambaiah K, Lokesh BR. 1998. Antioxidants and lipid oxidation in foods - A critical appraisal. Journal of Food Science and Technology-Mysore 35(4):283-298.

Ahmed J, Shivhare US, Sandhu KS. 2002. Thermal degradation kinetics of carotenoids and visual color of papaya puree. J Food Sci 67(7):2692-2695.

Ahn JH, Kim YP, Lee YM, Seo EM, Lee KW, Kim HS. 2008. Optimization of microencapsulation of seed oil by response surface methodology. Food Chem 107(1):98-105.

AIChE Equipment Testing Procedure. 2003. Spray dryers: A guide to performance evaluation. NY: American Institute of Chemical Engineers.

Aidos I, Lourenco S, Van der Padt A, Luten JB, Boom RM. 2002. Stability of crude herring oil produced from fresh byproducts: Influence of temperature during storage. J Food Sci 67(9):3314-3320.

AOAC. 1995. Official methods of analysis of AOAC International. Arlington, VA: AOAC International.

Armenta RE, Guerrero-Legarreta I. 2009. Stability Studies on Astaxanthin Extracted from Fermented Shrimp Byproducts. J Agr Food Chem 57(14):6095-6100.

Augustin MA, Hemar Y. 2009. Nano- and micro-structured assemblies for encapsulation of food ingredients. Chem Soc Rev 38(4):902-912.

Avila IMLB, Silva CLM. 1999. Modelling kinetics of thermal degradation of colour in peach puree. J Food Eng 39(2):161-166.

Baik MY, Suhendro EL, Nawar WW, McClements DJ, Decker EA, Chinachoti P. 2004. Effects of antioxidants and humidity on the oxidative stability of microencapsulated fish oil. J Am Oil Chem Soc 81(4):355-360.

Batista AP, Raymundo A, Sousa I, Empis J. 2006. Rheological characterization of coloured oil-in-water food emulsions with lutein and phycocyanin added to the oil and aqueous phases. Food Hydrocolloid 20(1):44-52.

Bayrarn OA, Bayram M, Tekin AR. 2005. Spray drying of sumac flavour using sodium chloride, sucrose, glucose and starch as carriers. J Food Eng 69(2):253-260.

Bera D, Lahiri D, Nag A. 2006. Studies on a natural antioxidant for stabilization of edible oil and comparison with synthetic antioxidants. J Food Eng 74(4):542-545.

Bloedon LT, Szapary PO. 2004. Flaxseed and cardiovascular risk. Nutr Rev 62(1):18-27.

Boon CS, Xu Z, Yue X, McClements DJ, Weiss J, Decker EA. 2008. Factors affecting lycopene oxidation in oil-in-water emulsions. J Agr Food Chem 56(4):1408-1414.

Britton G, Liaaen-Jensen S, Pfander H. 1995. Carotenoids. Basel ; Boston: Birkhäuser Verlag.

Bruschi ML, Cardoso MLC, Lucchesi MB, Gremiao MPD. 2003. Gelatin microparticles containing propolis obtained by spray-drying technique: preparation and characterization. Int J Pharm 264(1-2):45-55.

Burton GW, Ingold KU. 1984. Beta-Carotene - an Unusual Type of Lipid Antioxidant. Science 224(4649):569-573.

Bustos R, Romo L, Yanez K, Diaz G, Romo C. 2003. Oxidative stability of carotenoid pigments and polyunsaturated fatty acids in microparticulate diets containing krill oil for nutrition of marine fish larvae. J Food Eng 56(2-3):289-293.

Calo P, Velazquez JB, Sieiro C, Blanco P, Longo E, Villa TG. 1995. Analysis of Astaxanthin and Other Carotenoids from Several Phaffia-Rhodozyma Mutants. J Agr Food Chem 43(5):1396-1399.

Carolina BC, Carolina S, Zamora MC, Jorge C. 2007. Glass transition temperatures and some physical and sensory changes in stored spray-dried encapsulated flavors. Lwt-Food Science and Technology 40(10):1792-1797.

Champagne CP, Fustier P. 2007. Microencapsulation for the improved delivery of bioactive compounds into foods. Curr Opin BioTech 18(2):184-190.

Chen DM, Han YB, Gu ZX. 2006. Application of statistical methodology to the optimization of fermentative medium for carotenoids production by Rhodobacter sphaeroides. Process Biochem 41(8):1773-1778.

Chen HM, Meyers SP. 1982. Extraction of Astaxanthin Pigment from Crawfish Waste Using a Soy Oil Process. J Food Sci 47(3):892-896.

Chen HM, Meyers SP. 1984. A Rapid Quantitative Method for Determination of Astaxanthin Pigment Concentration in Oil Extracts. J Am Oil Chem Soc 61(6):1045-1047.

Chew BP, Park JS, Wong MW, Wong TS. 1999. A comparison of the anticancer activities of dietary beta-carotene, canthaxanthin and astaxanthin in mice in vivo. Anticancer Research 19(3A):1849-1853.

Choe E, Min DB. 2005. Chemistry and reactions of reactive oxygen species in foods. J Food Sci 70(9):R142-R159.

Choi YE, Yun YS, Park JM. 2002. Evaluation of factors promoting astaxanthin production by a unicellular green alga, Haematococcus pluvialis, with fractional factorial design. Biotechnol Progr 18(6):1170-1175.

Cira LA, Huerta S, Hall GM, Shirai K. 2002. Pilot scale lactic acid fermentation of shrimp wastes for chitin recovery. Process Biochem 37(12):1359-1366.

Colakoglu AS. 2007. Oxidation kinetics of soybean oil in the presence of monoolein, stearic acid and iron. Food Chem 101(2):724-728.

Conn PF, Schalch W, Truscott TG. 1991. The Singlet Oxygen and Carotenoid Interaction. J Photoch Photobio B 11(1):41-47.

Cunnane SC, Ganguli S, Menard C, Liede AC, Hamadeh MJ, Chen ZY, Wolever TMS, Jenkins DJA. 1993. High Alpha-Linolenic Acid Flaxseed (Linum-Usitatissimum) - Some Nutritional Properties in Humans. Brit J Nutr 69(2):443-453.

Dai CY, Wang BC, Zhao HW. 2005. Microencapsulation peptide and protein drugs delivery system. Colloid Surface B 41(2-3):117-120.

De Holanda HD, Netto FM. 2006. Recovery of components from shrimp (Xiphopenaeus kroyeri) processing waste by enzymatic hydrolysis. J Food Sci 71(5):C298-C303.

Delgado-Vargas F, Jimenez AR, Paredes-Lopez O. 2000. Natural pigments: Carotenoids, anthocyanins, and betalains - Characteristics, biosynthesis, processing, and stability. Crit Rev Food Sci 40(3):173-289.

Delgado-Vargas F, Paredes-Lopez O. 2003. Natural colorants for food and nutraceutical uses. Boca Raton, FL: CRC Press.

Dhuique-Mayer C, Tbatou M, Carail M, Caris-Veyrat C, Dornier M, Amiot MJ. 2007. Thermal degradation of antioxidant micronutrients in Citrus juice: Kinetics and newly formed compounds. J Agr Food Chem 55(10):4209-4216.

Di Mascio P, Murphy ME, Sies H. 1991. Antioxidant Defense Systems - the Role of Carotenoids, Tocopherols, and Thiols. Am J Clin Nutr 53(1):S194-S200.

Drusch S. 2007. Sugar beet pectin: A novel emulsifying wall component for microencapsulation of lipophilic food ingredients by spray-drying. Food Hydrocolloid 21(7):1223-1228.

Drusch S, Berg S. 2008. Extractable oil in microcapsules prepared by spray-drying: Localisation, determination and impact on oxidative stability. Food Chem 109(1):17-24.

Dziezak JD. 1988. Microencapsulation and Encapsulated Ingredients. Food Technol-Chicago 42(4):136-151.

Edge R, McGarvey DJ, Truscott TG. 1997. The carotenoids as anti-oxidants - a review. J Photoch Photobio B 41(3):189-200.

Ergunes G, Tarhan S. 2006. Color retention of red peppers by chemical pretreatments during greenhouse and open sun drying. J Food Eng 76(3):446-452.

Erkan N, Ayranci G, Ayranci E. 2009. A kinetic study of oxidation development in sunflower oil under microwave heating: Effect of natural antioxidants. Food Res Int 42(8):1171-1177.

Fabregas J, Dominguez A, Regueiro M, Maseda A, Otero A. 2000. Optimization of culture medium for the continuous cultivation of the microalga Haematococcus pluvialis. Appl Microbiol Biot 53(5):530-535.

Fang TJ, Cheng YS. 1993. Improvement of Astaxanthin Production by Phaffia-Rhodozyma through Mutation and Optimization of Culture Conditions. J Ferment Bioeng 75(6):466-469.

Fang TJ, Chiou TY. 1996. Batch cultivation and astaxanthin production by a mutant of the red yeast, Phaffia rhodozyma NCHU-FS501. J Ind Microbiol 16(3):175-181.

Farmilo A, Wilkinso.F. 1973. Mechanism of Quenching of Singlet Oxygen in Solution. Photochem Photobiol 18(6):447-450.

Frankel EN. 1984. Lipid Oxidation - Mechanisms, Products and Biological Significance. J Am Oil Chem Soc 61(12):1908-1917.

Garg S, Sharma P, Jayaprakashan SG, Subramanian R. 2009. Spray evaporation of liquid foods. Lwt-Food Science and Technology 42(1):119-124.

Gentles A, Haard NF. 1991. Pigmentation of Rainbow-Trout with Enzyme-Treated and Spray-Dried Phaffia-Rhodozyma. Prog Fish Cult 53(1):1-6.

Gharsallaoui A, Roudaut G, Chambin O, Voilley A, Saurel R. 2007. Applications of spray-drying in microencapsulation of food ingredients: An overview. Food Res Int 40(9):1107-1121.

Girotti AW. 1990. Photodynamic Lipid-Peroxidation in Biological-Systems. Photochem Photobiol 51(4):497-509.

Gong XD, Chen F. 1998. Influence of medium components on astaxanthin content and production of Haematococcus pluvialis. Process Biochem 33(4):385-391.

Gu ZX, Chen DM, Han YB, Chen ZG, Gu FR. 2008. Optimization of carotenoids extraction from Rhodobacter sphaeroides. LWT-Food Sci Technol 41(6):1082-1088.

Guerin M, Huntley ME, Olaizola M. 2003. Haematococcus astaxanthin: applications for human health and nutrition. Trends Biotechnol 21(5):210-216.

Guillou A, Khalil M, Adambounou L. 1995. Effects of Silage Preservation on Astaxanthin Forms and Fatty-Acid Profiles of Processed Shrimp (Pandalus-Borealis) Waste. Aquaculture 130(4):351-360.

Halliwell B, Chirico S. 1993. Lipid-Peroxidation - Its Mechanism, Measurement, and Significance. Am J Clin Nutr 57(5):S715-S725.

Handayani AD, Sutrisno, Indraswati N, Ismadji S. 2008. Extraction of astaxanthin from giant tiger (Panaeus monodon) shrimp waste using palm oil: Studies of extraction kinetics and thermodynamic. Bioresource Technol 99(10):4414-4419.

Harper CR, Edwards ME, DeFilipis AP, Jacobson TA. 2007. Flaxseed oil increases the plasma concentrations of Cardioprotective (n-3) fatty acids in humans. (vol 136, pg 83, 2006). J Nutr 137(12):2816-2816.

Harper CR, Edwards MJ, DeFilipis AP, Jacobson TA. 2006. Flaxseed oil increases the plasma concentrations of cardioprotective (n-3) fatty acids in humans. J Nutr 136(1):83-87.

Higuera-Ciapara I, Felix-Valenzuela L, Goycoolea FM. 2006. Astaxanthin: A review of its chemistry and applications. Crit Rev Food Sci 46(2):185-196.

Higuera-Ciapara I, Felix-Valenzuela L, Goycoolea FM, Arguelles-Monal W. 2004. Microencapsulation of astaxanthin in a chitosan matrix. Carbohyd Polym 56(1):41-45.

Hogan SA, McNamee BF, O'Riordan ED, O'Sullivan M. 2001. Emulsification and microencapsulation properties of sodium caseinate/carbohydrate blends. Int Dairy J 11(3):137-144.

Homayouni A, Azizi A, Ehsani MR, Yarmand MS, Razavi SH. 2008. Effect of microencapsulation and resistant starch on the probiotic survival and sensory properties of synbiotic ice cream. Food Chem 111(1):50-55.

Huang L X, Kumar K, Mujumdar AS. 2006. A comparative study of a spray dryer with rotary disc atomizer and pressure nozzle using computational fluid dynamic simulations. Chem Eng Process 45: 461-70.

Ip PF, Chen F. 2005. Production of astaxanthin by the green microalga Chlorella zofingiensis in the dark. Process Biochem 40(2):733-738.

Jacques PF. 1999. The potential preventive effects of vitamins for cataract and age-related macular degeneration. Int J Vitam Nutr Res 69(3):198-205.

Johnson EA, Lewis MJ. 1979. Astaxanthin Formation by the Yeast Phaffia-Rhodozyma. J Gen Microbiol 115(Nov):173-183.

Jyonouchi H, Sun S, Iijima K, Gross MD. 2000. Antitumor activity of astaxanthin and its mode of action. Nutrition and Cancer-an International Journal 36(1):59-65.

Kagami Y, Sugimura S, Fujishima N, Matsuda K, Kometani T, Matsumura Y. 2003. Oxidative stability, structure, and physical characteristics of microcapsules formed by spray drying of fish oil with protein and dextrin wall materials. J Food Sci 68(7):2248-2255.

Katona JM, Sovilj VJ, Petrovic LB. 2010. Microencapsulation of oil by polymer mixture-ionic surfactant interaction induced coacervation. Carbohyd Polym 79(3):563-570.

Kenyon MM. 1995. Modified Starch, Maltodextrin, and Corn Syrup Solids as Wall Materials for Food Encapsulation. Acs Sym Ser 590:42-50.

Keogh MK, O'Kennedy BT, Kelly J, Auty MA, Kelly PM, Fureby A, Haahr AM. 2001. Stability to oxidation of spray-dried fish oil powder microencapsulated using milk ingredients. J Food Sci 66(2):217-224

Kesava SS, An GH, Kim CH, Rhee SK, Choi ES. 1998. An industrial medium for improved production of carotenoids from a mutant strain of Phaffia rhodozyma. Bioprocess Eng 19(3):165-170.

Kittikalwan P, Powthongsook S, Pavasant P, Shotipruk A. 2007. Encapsulation of Haematococcus pluvialis using chitosan for astaxanthin stability enhancement. Carbohyd Polym 70(4):378-385.

Klinkesorn U, Sophanodora P, Chinachoti P, McClements DJ, Decker EA. 2005. Stability of spray-dried tuna oil emulsions encapsulated with two-layered interfacial membranes. J Agr Food Chem 53(21):8365-8371.

Kolanowski W, Ziolkowski M, Weissbrodt J, Kunz B, Laufenberg G. 2006. Microencapsulation of fish oil by spray drying-impact on oxidative stability. Part 1. Eur Food Res Technol 222(3-4):336-342.

Krishnan S, Kshirsagar AC, Singhal RS. 2005. The use of gum arabic and modified starch in the microencapsulation of a food flavoring agent. Carbohyd Polym 62(4):309-315.

Kritchevsky SB. 1999. beta-carotene, carotenoids and the prevention of coronary heart disease. J Nutr 129(1):5-8.

Ladikos D, Lougovois V. 1990. Lipid Oxidation in Muscle Foods - a Review. Food Chem 35(4):295-314.

Laguerre M, Lecomte J, Villeneuve P. 2007. Evaluation of the ability of antioxidants to counteract lipid oxidation: Existing methods, new trends and challenges. Prog Lipid Res 46(5):244-282.

Landy P, Druaux C, Voilley A. 1995. Retention of Aroma Compounds by Proteins in Aqueous-Solution. Food Chem 54(4):387-392.

Laos K, Lugas T, Mdndmets A, Vokk R. 2007. Encapsulation of beta-carotene from sea buckthorn (Hippophai rhamnoides L.) juice in furcellaran beads. Innov Food Sci Emerg 8(3):395-398.

Levenspiel O. 1999. Chemical reaction engineering,3rd ed. New York: Wiley.

Liu YS, Wu JY. 2007. Optimization of cell growth and carotenoid production of Xanthophyllomyces dendrorhous through statistical experiment design. Biochem Eng J 36(2):182-189.

Lorenz RT, Cysewski GR. 2000. Commercial potential for Haematococcus microalgae as a natural source of astaxanthin. Trends Biotechnol 18(4):160-167.

Louisiana AgCenter Website: http://www.agctr.lsu.edu/en/crops_livestock/aquaculture

Magdassi S. 1997. Delivery systems in cosmetics. Colloid Surface A 123:671-679.

Maxwell RJ, Marmer WN. 1983. Systematic Protocol for the Accumulation of Fatty-Acid Data from Multiple Tissue Samples - Tissue Handling, Lipid Extraction and Class Separation, and Capillary Gas-Chromatographic Analysis. Lipids 18(7):453-459.

Mayne ST. 1996. Beta-carotene, carotenoids, and disease prevention in humans. Faseb Journal 10(7):690-701.

McClements DJ, Decker EA, Weiss J. 2007. Emulsion-based delivery systems for lipophilic bioactive components. J Food Sci 72(8):R109-124.

McDonald RE, Min DB. 1996. Food lipids and health. New York: Marcel Dekker.

McKenna DR, Nanke KE, Olson DG. 2003. The effects of irradiation, high hydrostatic pressure, and temperature during pressurization on the characteristics of cooked-reheated salmon and catfish fillets. J Food Sci 68(1):368-377.

Meyer PS, Dupreez JC, Kilian SG. 1993. Selection and Evaluation of Astaxanthin-Overproducing Mutants of Phaffia-Rhodozyma. World J Microb Biot 9(5):514-520.

Meyers SP, Bligh D. 1981. Characterization of Astaxanthin Pigments from Heat-Processed Crawfish Waste. J Agr Food Chem 29(3):505-508.

Miki W. 1991. Biological Functions and Activities of Animal Carotenoids. Pure Appl Chem 63(1):141-146.

Moschakis T, Murray BS, Dickinson E. 2005. Microstructural evolution of viscoelastic emulsions stabilised by sodium caseinate and xanthan gum. J Colloid Interf Sci 284(2):714-728.

Naz S, Sheikh H, Siddiqi R, Sayeed SA. 2004. Oxidative stability of olive, corn and soybean oil under different conditions. Food Chem 88(2):253-259.

Niamnuy C, Devahastin S, Soponronnarit S, Raghavan GSV. 2008. Kinetics of astaxanthin degradation and color changes of dried shrimp during storage. J Food Eng 87(4):591-600.

Nunes IL, Mercadante AZ. 2007. Encapsulation of lycopene using spray-drying and molecular inclusion processes. Bra Arch Biol Techn 50(5):893-900.

Orosa M, Valero JF, Herrero C, Abalde J. 2001. Comparison of the accumulation of astaxanthin in Haematococcus pluvialis and other green microalgae under N-starvation and high light conditions. Biotechnol Lett 23(13):1079-1085.

Palozza P, Krinsky NI. 1992. Astaxanthin and Canthaxanthin Are Potent Antioxidants in a Membrane Model. Arch Biochem Biophys 297(2):291-295.

Paquot C, Hautfenne A, IUPAC. 1987. Standard methods for the analysis of oils, fats, and derivatives.Boston, MA: Blackwell Scientific Publications.

Parajo JC, Santos V, Vazquez M. 1998. Optimization of carotenoid production by Phaffia rhodozyma cells grown on xylose. Process Biochem 33(2):181-187.

Pereda J, Ferragut V, Quevedo JM, Guamis B, Trujillo AJ. 2008. Effects of ultra-high-pressure homogenization treatment on the lipolysis and lipid oxidation of milk during refrigerated storage. J Agr Food Chem 56(16):7125-7130.

Perez-Alonso C, Baez-Gonzalez JG, Beristain CI, Vernon-Carter EJ, Vizcarra-Mendoza MG. 2003. Estimation of the activation energy of carbohydrate polymers blends as selection criteria for their use as wall material for spray-dried microcapsules. Carbohyd Polym 53(2):197-203.

Perez-Galvez A, Negro-Balmaseda JJ, Minguez-Mosquera MI, Cascajo-Almenara MV, Garrido-Fernandez J. 2008. Astaxanthin from crayfish (Procambarus clarkii) as a pigmentary ingredient in the feed of laying hens. Grasas Aceites 59(2):139-145.

Piette J. 1991. Biological Consequences Associated with DNA Oxidation Mediated by Singlet Oxygen. J Photoch Photobio B 11(3-4):241-260.

Ramirez J, Gutierrez H, Gschaedler A. 2001. Optimization of astaxanthin production by Phaffia rhodozyma through factorial design and response surface methodology. J Biotechnol 88(3):259-268.

Rao AR, Sarada R, Ravishankar GA. 2007. Stabilization of astaxanthin in edible oils and its use as an antioxidant. J Sci Food Agr 87(6):957-965.

Rao MA. 1999. Rheology of fluid and semisolid foods : principles and applications. Gaithersburg, MD: Aspen Publishers.

Rengel D, Diez-Navajas A, Serna-Rico A, Veiga P, Muga A, Milicua JCG. 2000. Exogenously incorporated ketocarotenoids in large unilamellar vesicles. Protective activity against peroxidation. Bba-Biomembranes 1463(1):179-187.

Ribeiro HS, Rico LG, Badolato GG, Schubert H. 2005. Production of O/W emulsions containing astaxanthin by repeated Premix membrane emulsification. J Food Sci 70(2):E117-E123.

Risch SJ. 1995a. Encapsulation - Overview of Uses and Techniques. Acs Sym Ser 590:2-7.

Risch SJ. 1995b. Review of Patents for Encapsulation and Controlled-Release of Food Ingredients. Acs Sym Ser 590:196-203.

Risch SJ, Reineccius G, American Chemical Society. Division of Agricultural and Food Chemistry. 1995. Encapsulation and controlled release of food ingredients. Washington, DC: American Chemical Society.

Rocha T, Lebert A, Martyaudouin C. 1993. Effect of Pretreatments and Drying Conditions on Drying Rate and Color Retention of Basil (Ocimum-Basilicum). Food Science and Technology-Lebensmittel-Wissenschaft & Technologie 26(5):456-463.

Rodriguez-Huezo ME, Pedroza-Islas R, Prado-Barragan LA, Beristain CI, Vernon-Carter EJ. 2004. Microencapsulation by spray drying of multiple emulsions containing carotenoids. J Food Sci 69(7):E351-E359.

Rosenberg M, Sheu TY. 1996. Microencapsulation of volatiles by spray-drying in whey protein-based wall systems. Int Dairy J 6(3):273-284.

Sachindra NM, Bhaskar N, Mahendrakar NS. 2005. Carotenoids in different body components of Indian shrimps. J Sci Food Agr 85(1):167-172.

Sachindra NM, Bhaskar N, Mahendrakar NS. 2006. Recovery of carotenoids from shrimp waste in organic solvents. Waste Management 26(10):1092-1098.

Sachindra NM, Bhaskar N, Siddegowda GS, Sathisha AD, Suresh PV. 2007. Recovery of carotenoids from ensilaged shrimp waste. Bioresource Technol 98(8):1642-1646.

Sachindra NM, Mahendrakar NS. 2005. Process optimization for extraction of carotenoids from shrimp waste with vegetable oils. Bioresource Technol 96(10):1195-1200.

Saito A, Regier LW. 1971. Pigmentation of Brook Trout (Salvelinus-Fontinalis) by Feeding Dried Crustacean Waste. J Fish Res Board Can 28(4):509-512.

Sathivel S, Kramer D. 2010. Microencapsulation, edible film and coatings applications in seafood processing. In Wanasundara U, Shahidi F, Alasalvar C, Miyashita K, editors. Handbook of Seafood Quality, Safety and Health Applications. Wiley-Blackwell Publishers.

Seddon JM, Ajani UA, Sperduto RD, Hiller R, Blair N, Burton TC, Farber MD, Gragoudas ES, Haller J, Miller DT, et al. 1994. Dietary carotenoids, vitamins A, C, and E, and advanced age-related macular degeneration. Eye Disease Case-Control Study Group. JAMA-J Am Med Assoc 272(18):1413-1420.

Serfert Y, Drusch S, Schwarz K. 2009. Chemical stabilisation of oils rich in long-chain polyunsaturated fatty acids during homogenisation, microencapsulation and storage. Food Chem 113(4):1106-1112.

Shahidi F, Han XQ. 1993. Encapsulation of Food Ingredients. Crit Rev Food Sci 33(6):501-547.

Shahidi F, Synowiecki J. 1991. Isolation and Characterization of Nutrients and Value-Added Products from Snow Crab (Chinoecetes-Opilio) and Shrimp (Pandalus-Borealis) Processing Discards. J Agr Food Chem 39(8):1527-1532.

Shahidi F, Wanasundara UN. 1995. Oxidative stability of encapsulated seal blubber oil. Flavor Technology 610:139-151.

Shahidi F, Metusalach, Brown JA. 1998. Carotenoid pigments in seafoods and aquaculture. Crit Rev Food Sci 38(1):1-67.

Shahidi F, Weenen H. 2006. Food lipids : chemistry, flavor, and texture. Washington, DC: American Chemical Society.

Shih CT, Hang YD. 1996. Production of carotenoids by Rhodotorula rubra from sauerkraut brine. LWT-Food Science and Technology 29(5-6):570-572.

Shyamala BN, Gupta S, Lakshmi AJ, Prakash J. 2005. Leafy vegetable extracts - antioxidant activity and effect on storage stability of heated oils. Innov Food Sci Emerg 6(2):239-245.

Sigurgisladottir S, Parrish CC, Lall SP, Ackman RG. 1994. Effects of Feeding Natural Tocopherols and Astaxanthin on Atlantic Salmon (Salmo-Salar) Fillet Quality. Food Res Int 27(1):23-32.

Singh RP, Heldman DR. 2001. Introduction to food engineering. San Diego, CA: Academic Press.

Sliwinski EL, Lavrijsen BWM, Vollenbroek JM, van der Stege HJ, van Boekel MAJS, Wouters JTM. 2003. Effects of spray drying on physicochemical properties of milk protein-stabilised emulsions. Colloid Surface B 31(1-4):219-229.

Snodderly DM. 1995. Evidence for Protection against Age-Related Macular Degeneration by Carotenoids and Antioxidant Vitamins. Am J Clin Nutr 62(6):S1448-S1461.

St. Angelo AJ, American Chemical Society. Division of Agricultural and Food Chemistry., American Chemical Society. Meeting. 1992. Lipid oxidation in food. Washington, DC: American Chemical Society.

Tachaprutinun A, Udomsup T, Luadthong C, Wanichwecharungruang S. 2009. Preventing the thermal degradation of astaxanthin through nanoencapsulation. Int J Pharm 374(1-2):119-124.

Tan CP, Man YBC, Selamat J, Yusoff MSA. 2001. Application of arrhenius kinetics to evaluate oxidative stability in vegetable oils by isothermal differential scanning calorimetry. J Am Oil Chem Soc 78(11):1133-1138.

Tan LH, Chan LW, Heng PWS. 2009. Alginate/starch composites as wall material to achieve microencapsulation with high oil loading. J Microencapsul 26(3):263-271.

Tanaka T, Kawamori T, Ohnishi M, Makita H, Mori H, Satoh K, Hara A. 1995a. Suppression of azoxymethane-induced rat colon carcinogenesis by dietary administration of naturally occurring xanthophylls astaxanthin and canthaxanthin during the postinitiation phase. Carcinogenesis 16(12):2957-2963.

Tanaka T, Makita H, Ohnishi M, Mori H, Satoh K, Hara A. 1995b. Chemoprevention of rat oral carcinogenesis by naturally occurring xanthophylls, astaxanthin and canthaxanthin. Cancer Res 55(18):4059-4064.

Tanaka T, Morishita Y, Suzui M, Kojima T, Okumura A, Mori H. 1994. Chemoprevention of Mouse Urinary-Bladder Carcinogenesis by the Naturally-Occurring Carotenoid Astaxanthin. Carcinogenesis 15(1):15-19.

Torrissen O, Tidemann E, Hansen F, Raa J. 1981. Ensiling in Acid - a Method to Stabilize Astaxanthin in Shrimp Processing by-Products and Improve Uptake of This Pigment by Rainbow-Trout (Salmo-Gairdneri). Aquaculture 26(1-2):77-83.

Tracy RP. 1999. Inflammation markers and coronary heart disease. Curr Opin Lipidol 10(5):435-441.

Tzang BS, Yang SF, Fu SG, Yang HC, Sun HL, Chen YC. 2009. Effects of dietary flaxseed oil on cholesterol metabolism of hamsters. Food Chem 114(4):1450-1455.

Vega C, Kim EHJ, Chen XD, Roos YH. 2005. Solid-state characterization of spray-dried ice cream mixes. Colloid Surface B 45(2):66-75.

Walton DE. 2000. The morphology of spray-dried particles a qualitative view. Dry Technol 18(9):1943-1986.

Yagiz Y, Kristinsson HG, Balaban MO, Welt BA, Raghavan S, Marshall MR. 2010. Correlation between astaxanthin amount and a* value in fresh Atlantic salmon (Salmo salar) muscle during different irradiation doses. Food Chem 120(1):121-127.

Zakarian AJ, and King CJ. 1982. Volatiles loss in the zone during spray drying of emulsions. Ind Eng Chem Proc DD 21: 107-13.

Zbicinski I., Delag A., Strumillo C., and Adamiec J. 2002. Advanced experimental analysis of drying kinetics in spray drying. Chem Eng J 86: 207-16.

Zhang BY, Geng YH, Li ZK, Hu HJ, Li YG. 2009. Production of astaxanthin from Haematococcus in open pond by two-stage growth one-step process. Aquaculture 295(3-4):275-281.

APPENDIX: SAMPLE CALCULATION FOR SPRAY DRYING

Estimation of production rate

The overall balance of dry solids entering and leaving the system under steady state conditions would be

$$m_e = mP + m_d$$

Based on this, the product flow rate was estimated as following

$$mP = m_e - m_d = 0.13 - 0.003 = 0.127 \text{ kg/h}$$

Air flow balance

1) Inlet air

From the velocity of inlet air and the diameter of the inlet air pipe, we obtained the volumetric flow rate

$$V_{ai} = v_{ai} \times A_{ai} = \frac{v_{ai}\pi d^2}{4} = \frac{16.97 \times 3.14 \times 0.034^2}{4} = 0.0154 \text{ m}^3/\text{s} = 55.47 \text{ m}^3/\text{h}$$

where V_{ai} is the volumetric flow rate of inlet air; v_{ai} is the velocity of the inlet air (m/s); A_{ai} is the cross sectional area of the inlet air pipe (m^2); d is the diameter of the inlet air pipe (m).

The partial pressure exerted by water vapor (p_w) was calculated

$$p_w = p_v \times RH = 3.425 \times 0.5844 = 2.00 \text{ kPa}$$

where p_w is the partial pressure exerted by water vapor (kPa); p_v is the saturation pressure of water vapor (kPa); RH is the relative humidity (%).

The absolute humidity of inlet air was calculated as

$$AH_{ai} = 0.622 \times \frac{p_w}{101.325 - p_w} = 0.622 \times \frac{2.00}{101.325 - 2.00} = 0.0125 \text{ kg water/kg dry air}$$

where AH_{ai} is the absolute humidity of the inlet air (kg water/kg dry air); p_w is the partial

pressure exerted by water vapor (kPa).

The specific volume of inlet air was calculated using following equation

$$V'_{ai} = (0.082T + 22.4)\left(\frac{1}{29} + \frac{AH}{18}\right)$$
$$= (0.082 \times 26.27 + 22.4)\left(\frac{1}{29} + \frac{0.0125}{18}\right) = 0.864\ m^3/kg\ \text{dry air}$$

where T is the temperature of inlet air (^oC); AH is the absolute humidity of inlet air (kg water/kg dry air); this equation is applicable at atmospheric pressure.

The dry air mass flow rate of inlet air was calculated as following

$$m_{ai} = \frac{V_{ai}}{V'_{ai}} = \frac{0.0154}{0.864} = 0.0178\ kg/s = 64.08\ kg/h$$

where m_{ai} is the dry air mass flow rate of inlet air; V_{ai} is the volumetric flow rate of inlet air (m^3/s); V_{ai}' is the specific volume of inlet air (m^3/kg dry air).

2) Outlet air

From the velocity of outlet air and the diameter of the outlet air pipe, we obtained the volumetric flow rate

$$V_{ao} = v_{ao} \times A_{ao} = \frac{v_{ao}\pi d^2}{4} = \frac{4.1 \times 3.14 \times 0.075^2}{4} = 0.0181\ m^3/s = 65.16\ m^3/h$$

where V_{ao} is the volumetric flow rate of outlet air; v_{ao} is the velocity of the outlet air (m/s); A_{ao} is the cross sectional area of the outlet air pipe (m^2); d is the diameter of the outlet air pipe (m).

The partial pressure exerted by water vapor (p_w) was calculated

$$p_w = p_v \times RH = 53.654 \times 0.052 = 2.79\ kPa$$

where p_w is the partial pressure exerted by water vapor (kPa); p_v is the saturation pressure of water vapor (kPa); RH is the relative humidity (%).

The absolute humidity of outlet air was calculated as

$$AH_{ao} = 0.622 \times \frac{p_w}{101.325 - p_w} = 0.622 \times \frac{2.79}{101.325 - 2.79}$$

$$= 0.0176 \text{ kg water/kg dry air}$$

where AH_{ao} is the absolute humidity of the outlet air (kg water/kg dry air); p_w is the partial pressure exerted by water vapor (kPa).

The specific volume of outlet air was calculated using following equation

$$V'_{ao} = (0.082T + 22.4)\left(\frac{1}{29} + \frac{AH}{18}\right)$$

$$= (0.082 \times 82.93 + 22.4)\left(\frac{1}{29} + \frac{0.0176}{18}\right) = 1.035 \text{ m}^3/\text{kg dry air}$$

where T is the temperature of outlet air (^oC); AH is the absolute humidity of outlet air (kg water/kg dry air); this equation is applicable at atmospheric pressure.

The dry air mass flow rate of outlet air was calculated as following

$$m_{ao} = \frac{V_{ao}}{V'_{ao}} = \frac{0.0181}{1.035} = 0.0175 \text{ kg/s} = 63 \text{ kg/h}$$

where m_{ao} is the dry air mass flow rate of outlet air; V_{ao} is the volumetric flow rate of outlet air (m^3/s); V_{ao}' is the specific volume of outlet air (m^3/kg dry air).

Estimation of evaporation rate

An overall balance on water entering and leaving the system gives

$$m_{aa}AH_{aa} + m_e w_e = m_{ao}AH_{ao} + m_d w_d + mPw_p \quad (3.6)$$

where m_{aa} is the dry air mass flow rate of inlet ambient air (kg dry air/h); m_{ao} is the dry air mass flow rate of outlet air (kg dry air/h); m_e is the mass flow rate of emulsion (kg dry solids/h); m_d is the mass flow rate of dust (kg dry solids/h); mP is including both the product flow rate (m_p) for the powder collected through cyclone vessel and product stored on the chambers, pipes, and joints and chambers walls; AH_{aa} is the absolute humidity of inlet ambient air (kg water/kg dry

air); AH_{ao} is the absolute humidity of outlet air (kg water/kg dry air); w_e is the moisture content of dry basis of emulsion (kg water/kg dry solids); w_d is the moisture content of dry basis of dust (kg water/kg dry solids); w_p is the moisture content of dry basis of product (kg water/kg dry solids).

The evaporation rate (E_{va}) that was calculated from the moisture uptake by air was

$$E_{va} = m_{ao}AH_{ao} - m_{ai}AH_{ai} = 63 \times 0.0176 - 64.08 \times 0.0125 = 0.308 \text{ kg water/h}$$

The evaporation rate (E_{vp}) that was calculated from product and dust moisture was

$$E_{vp} = m_e w_e - m_d w_d - mPw_p = 0.13 \times 2.34 - 0.003 \times 0.07 - 0.127 \times 0.066$$

$$= 0.296 \text{ kg water/h}$$

Estimation of energy required to dry the emulsions

The energy required to heat inlet air to drying air was calculated as following

$$Q = m_{ai}c_p\Delta T = m_{ai}(c_{ai} + c_v\, AH_{ai})(T_{ad} - T_{ai})$$

$$= 64.08 \times (1.0126 + 1.88 \times 0.0125) \times (453.15 - 299.42)$$

$$= 10206.64 \text{ kJ/h} = 2.84 \text{ kW}$$

where m_{ai} is dry air mass flow rate of inlet air (kg/h); c_p is specific heat of inlet air at constant pressure (kJ/[kg K]); c_{ai} is specific heat of inlet dry air at constant pressure; c_v is specific heat of water vapor at constant pressure; AH_{ai} is the absolute humidity of inlet air (kg water/kg dry air); ΔT is the temperature difference between inlet air and drying air (K); T_{ad} is temperature of drying air; T_{ai} is temperature of inlet air.

VITA

Jianing Pu was born in March 1986 in Shijiazhuang, China. He earned his bachelor of Engineering in biotechnology in Jiangnan University, Wuxi, China, in June 2008. He joined the Department of Food Science at Louisiana State University for his Master of Science in August 2008. Currently, he is a master's degree candidate and will receive his degree in December 2010.